Unified Large And Small Signal Discrete-space Modeling For Pwm Converters In Ccm

2005

Ehab Hamed Shoubaki
University of Central Florida

UNIFIED LARGE AND SMALL SIGNAL DISCRETE-SPACE MODELING FOR PWM CONVERTERS IN CCM

by

EHAB H. SHOUBAKI
B.S. Princess Sumaya University for Technology, 1996

A thesis submitted in partial fulfillment of the requirements
for the degree of Master of Science
in the School of Electrical Engineering and Computer Science
in the College of Engineering and Computer Science
at the University of Central Florida
Orlando, Florida

Summer Term
2005

ABSTRACT

In this Thesis a Unified Discrete State-Space Model for power converters in CCM is presented. Two main approaches to arriving at the discrete model are used. The first approach involves an impulse function approximation of the duty cycle modulations of the converter switches , and this approach results in a small signal discrete model. The Second approach is direct and does not involve any approximation of the modulations , this approach yields both a large signal nonlinear discrete model and a linear small signal model. Harmonic analysis of the converter states at steady-state is done for steady-state waveform acquisition , which increases the accuracy of the model especially for finding the control to inductor current frequency response. Finally the Discrete model is verified for the Half-Bridge DC/DC topology for its three main control schemes (Asymmetric , Symmetric , DCS). A GUI platform in MATLAB is presented as a wrapper that utilizes the models and analysis presented in this thesis.

ACKNOWLEDGMENTS

This author wishes to thanks his advisor , Dr. Issa Batarseh , for his help and support through the rough waters of academia. Also much thanks is directed towards Dr. Jaber Abuqahouq for his involved discussions and helpful advice. Much appreciations also for my friends and family. Last and most, I thank my beautiful wife Hiba for her patience and support ,without her assurance this work could never had seen the light of day.

TABLE OF CONTENTS

ABSTRACT iii

ACKNOWLEDGMENTS iv

TABLE OF CONTENTS v

LIST OF FIGURES vii

LIST OF CODES AND TABLES x

CHAPTER 1 : INTRODUCTION 1

1.1 Need for automatic control in PWM converters 1

1.2 Average Continuous Modeling of PWM converters 3

1.3 Introduction to Digital Control and Discrete modeling of PWM converters 12

1.4 Thesis Outline 14

CHAPTER 2 : OVERVIEW AND STEADY-STATE HARMONIC ANALYSIS 15

2.1 General State-Space Switched Model. 15

2.2 Small Signal perturbation. 18

2.3 Motivation for Harmonic Analysis: 19

2.4 Fourier Series: 20

2.5 Theoretical acquisition of Harmonics of steady-state waveforms: 23

2.6 Implementation in MATLAB 27

CHAPTER 3 : SMALL-SIGNAL DYNAMIC ANALYSIS USING IMPULSE APPROXIMATION 29

3.1 Motivation 29

3.2 Discrete small signal State-Space Model 29

CHAPTER 4 : LARGE AND SMALL SIGNAL STATE-SPACE DISCRETE MODEL WITHOUT IMPULSE APPROXIMATION 40

4.1 Motivation 40

4.2 Discrete Large signal State-Space Mode 41

4.3 Discrete Small signal State-Space Model without impulse approximation. 46

CHAPTER 5 : APPLICATION OF DISCRETE MODELING METHOD TO THE HALF-BRIDGE DC/DC TOPOLOGY WITH CURRENT DOUBLER 54

5.1 Overview of Half-Bridge topology with three main control method 54

5.2 State-Space representation of Modes of the Half-Bridge DC/DC topology with current doubler 55

5.3 Application of Chapter 3 small-signal model to the Half-Bridge DC/DC topology with current doubler 59

5.4 Application of Chapter 4 Large-signal model to the Half-Bridge DC/DC topology with current doubler 68

5.4 Comparison with an experimental prototype 70

CHAPTER 6 : IMPLEMENTATION OF DISCRETE MODEL IN A GUI FOR CONTROLLER DESIGN USING MATLAB 73

6.1 Overview of GUI platform 73

6.2 Design Example 81

CHAPTER 7 : CONCLUSION AND FUTURE WORK 84

7.1 Conclusion 84

7.2 Future Work 85

REFERENCES 86

LIST OF FIGURES

Number page

1-1 : Illustration of regulation through duty cycle control …….....2

1-2 : Switching Components Cell in each of the three main topologies:

(a) Buck (b) Boost(c) Buck Boost 6

1-3: Switching Cell Block ...…….…..7

1-4 : Cell Block Waveforms in the case of DCM ...……...…8

1-5: Cell Block continuous model for DCM .....…….…..…8

1-6 : Small-Signal equivalent circuit ……..…..10

1-7: Simulation of actual buck circuit and average model in PSPICE …….…....10

1-8 : Frequency response of Buck , (a) Magnitude , (b) Phase …….……11

1-9 : Comparison between Average Model vs. actual circuit simulation ……...…..12

2-1 : Switching functions $\overline{d}_1(t)$ and $\overline{d}_2(t)$ for two switches in steady-state ….....17

2-2 : Perturbation of Switching functions $\hat{d}_1(t)$ and $\hat{d}_2(t)$ for two switches …..…….....17

2-3: Magnitude of Fourier Coefficients of $\overline{d}_1(t)$ ……..…...22

2-4: Magnitude of Fourier Coefficients of $\overline{d}_2(t)$ …….....22

3-1 : Approximation of Duty cycle perturbations as impulse functions ……..…..30

4-1 : Switching Model Piecewise linear regions with varying switching instants …...…42

5-1: (a) Isolated Half-Bridge Converter, (b) Mode I (S1 on, S2 off),

(b) Mode II (S1 off,S2 on), (c) Mode III (S1 off, S2 off) .....…….....56

5-2 :HB DC/DC steady-state waveforms for symmetric control …….……60

5-3 :HB DC/DC steady-state waveforms for asymmetric control ……..…61

5-4 :HB DC/DC steady-state waveforms for DCS control ……...62

5-5 : Simplorer Simulation of the Asymmetric Control case 63

5-6 : Frequency Response for HB DC/DC example for Symmetric , Asymmetric and DCS control respectively 64

5-7 : Comparison between the Average Model and the Discrete Model for DCS control …….....…….....67

5-8 : Application of Large Signal model to HB DC/DC topology for Symmetric and DCS control respectively …….....…….....68

5-9 : Application of Large Signal model to HB DC/DC topology for Asymmetric control …….....…….....69

5-10 : Comparison of Closed loop frequency response between experiment and theory …….....71

6-1 : Digital Controller Designer main window 75

6-2 : Digital Controller Designer parameters window 76

6-3 : Digital Controller Designer Time response window 77

6-4 : Digital Controller Designer parameter sweep window 78

6-5 : Digital Controller Designer Root Locus window 79

6-6 : Digital Controller Designer Steady-State waveforms window 80

6-7 : Parameters for Lab Prototype Half-Bridge with current doubler and Symmetric control 81

6-8 : Desired Bandwidth and phase margin with required compensator poles and zeros 82

6-9 : Compensator realization in the analog domain 83

6-10 : Difference Equation coefficients for Digital Controller realization 83

LIST OF CODES AND TABLES

Number page

Code I : Harmonic Analysis implementation using MATLAB ……...…28

Table 3-1 : Model parameters substitution for various topologies with different control schemes …….....……..…...37

Table 5-1 : Model parameter sunstitution for each control scheme …….....55

Code II : Matlab Script to implement Discrete Model …….…....64

CHAPTER 1

INTRODUCTION

1.1 Need for automatic control in PWM converters

Since the inception of SMPS converters (Switched Mode Power Supply) it was known that operation without regulation is not adequate for cases where the load is variable, or the parameters of the converter change either intentionally or through aging. That is why automatic control is widely implemented in switching converters and open loop operation is nonexistent.

Depending on the topology used there are many different control schemes available. One of the earliest is to control the on and off times of the switches in a SMPS and to vary their values depending upon how far the system is off the desired operational range. Another technique is to control another parameter in the circuit and use that parameter to regulate the output , essentially having two control loops , an inner and an outer one. Current Mode Programming (whether peak or averaged) is the most famous example for this type of control , were there is an inner loop that controls the inductor current and then an outer loop controlling the reference to the previous loop , the output voltage being dependant on the inductor current. This control technique is popular since it simplifies the outer control loop because the power stage is essentially operating as a

voltage controlled current source. A third method of automatic control is achieved through varying the switching frequency , and this method is prevalent in soft switching topologies.

Due to this immense importance for automatic control in the switched power field the question arises as to how to close the loop on the converter, that is how to design an appropriate compensator to maintain stability at the required operating point. It is apparent that the powerful tools of Linear Control Theory (frequency domain theories) and Modern Control Theory (time domain theories) cannot be used directly for DC/DC converter since they are highly nonlinear systems. The rest of this chapter will describe the different approaches for solving this problem.

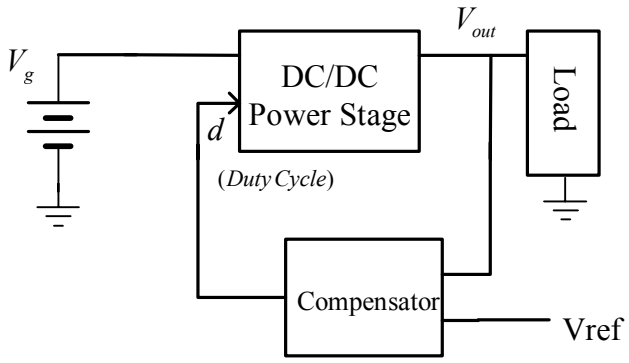

Figure 1-1 : Illustration of regulation through duty cycle control

1.2 Average Continuous Modeling of PWM converters

Since the power converter is not just nonlinear but also of piecwise switched nature, averaging techniques must be used to obtain a continuous model , which is then linearized using small signal perturbation. Middlebrook and cuk [1] pioneered this field in the late seventies using state space averaging , and later others[2,3] like Vorperien introduced circuit oriented average models. Both methods differ only in form , the second being more popular since circuit oriented analysis is ubiqituous in the electrical engineering community, and engineers prefer to deal normally with circuits rather than matrices. Another reason for the preference for circuit oriented methods is the ease by which they can be implemented in popular circuit simulation software like PSPICE.

Such so called small signal analysis of the system can yield for moderately complex systems very complex and tedious symbolic expressions of the transfer functions of intrerest. Those expressions are called “high entropy expressions” (a term coined by Middlebrook) . There are many ways of dealing with such complex systems, one is order reduction ; i.e. applying some simplifying assumptions to the system. Order reduction can be piecwise in frequency meaning that the simplifying assumptions can be different for different frequency ranges , this decreases reduction errors and as an example is used in [4]. Another is empirical , and is to simply bypass the analysis stage and use a frequency response analyzer to obtain the open loop transfer funtion. But the main disadvantage in this case is the lack of insight into the effect of the various components and parameters on the dynamics of the system

The State-Space Average Modeling is the most general method of the two , it requires translating the DC/DC converter into State-Space representation for each switching mode, that is for each piecewise linear region in time. Since this method involves matrix algebra Modern Control techniques can be easily exploited. Although even if this method is used most prefer to derive transfer functions from the resultant model so as to use traditional control techniques. To show how this works assume the topology of interest has two modes of operation , and each mode can be described with the following State-Space equations,

Mode I,

$$\frac{d\mathbf{x}}{dt} = \mathbf{A_1 x} + \mathbf{B_1 u} \tag{1.1}$$

$$y = \mathbf{C_1 x} + \mathbf{D_1 u} \tag{1.2}$$

and Mode II ,

$$\frac{d\mathbf{x}}{dt} = \mathbf{A_2 x} + \mathbf{B_2 u} \tag{1.3}$$

$$y = \mathbf{C_2 x} + \mathbf{D_2 u} \tag{1.4}$$

and the duration of Mode I is dT_s and of Mode II is $d`T_s$ when d is the Duty cycle at the particular operating point and d`=1-d . Then [1] proves that the power stage can be approximated be the following continuous State-Space model ,

$$\frac{d\mathbf{x}}{dt} = \mathbf{A_{avg} x} + \mathbf{B_{avg} u} \tag{1.5}$$

$$\vec{y} = \mathbf{C_{avg} x} + \mathbf{D_{avg} u} \tag{1.6}$$

where,

$$\mathbf{A}_{\mathbf{avg}} = d\mathbf{A}_{\mathbf{1}} + d'\mathbf{A}_{\mathbf{2}} \tag{1.7}$$

$$\mathbf{B}_{\mathbf{avg}} = d\mathbf{B}_{\mathbf{1}} + d'\mathbf{B}_{\mathbf{2}} \tag{1.8}$$

$$\mathbf{C}_{\mathbf{avg}} = d\mathbf{C}_{\mathbf{1}} + d'\mathbf{C}_{\mathbf{2}} \tag{1.9}$$

$$\mathbf{D}_{\mathbf{avg}} = d\mathbf{D}_{\mathbf{1}} + d'\mathbf{D}_{\mathbf{2}} \tag{1.10}$$

Equations (1.5) and (1.6) represent a continuous average model , but it is still not linear with respect to the duty cycle as input. The way to achieve the linear model which by nature is small-signal is to apply small signal perturbations to all the variables in (1.5)-(1.6) , and then to group the DC and small signal parts separately. Doing so gives,

$$\frac{d\hat{\mathbf{x}}}{dt} = \mathbf{A}_{\mathbf{avg}}\hat{\tilde{x}} + \mathbf{B}_{\mathbf{avg}}\hat{v}_g + \left[\left(\mathbf{A}_{\mathbf{1}} - \mathbf{A}_{\mathbf{2}}\right)\mathbf{X} + (\mathbf{B}_{\mathbf{1}} - \mathbf{B}_{\mathbf{2}})V_g\right]\hat{d} \tag{1.11}$$

$$\hat{y} = \mathbf{C}_{\mathbf{avg}}\hat{x} + \left(\mathbf{C}_{\mathbf{1}} - \mathbf{C}_{\mathbf{2}}\right)\mathbf{X}\hat{d} \tag{1.12}$$

where,

$$\mathbf{X} = -\mathbf{A}^{-1}\mathbf{B}V_g \tag{1.13}$$

$$Y = -\mathbf{C}\mathbf{A}^{-1}\mathbf{B}V_g \tag{1.14}$$

Equations (1.11)-(1.12) is the desired linear small signal model useful for designing an appropriate compensator. A transfer function can be extracted from it through applying the Laplace transform and it turns out being,

$$\frac{\hat{Y}(s)}{\hat{d}(s)} = (\mathbf{C_1} - \mathbf{C_2})\mathbf{X} + \mathbf{C_{avg}}\left(s\mathbf{I} - \mathbf{A_{avg}}\right)^{-1}\left[(\mathbf{A_1} - \mathbf{A_2})\mathbf{X} + (\mathbf{B_1} - \mathbf{B_2})V_g\right] \qquad (1.15)$$

The circuit oriented Average modeling methods are numerous but all depend on averaging all currents and voltages in the converter circuit over one switching period. Vorperian [2] introduced a methodology similar to the one used for analyzing transistor circuit were the block in the circuit containing the switching devices is examined and replaced by a closely equivalent average model consisting or dependent voltage and current sources. The blocks to be replaced are as shown in figure 1-2.

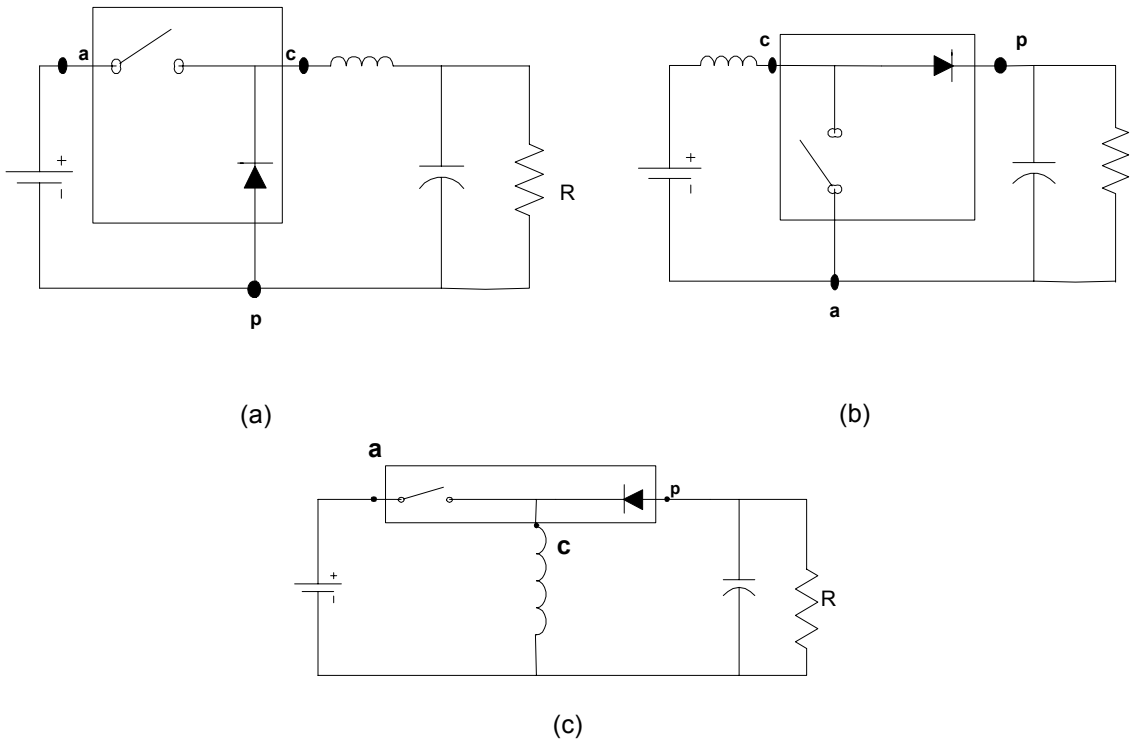

Figure 1-2 : Switching Components Cell in each of the three main topologies: (a) Buck (b) Boost (c) Buck-Boost

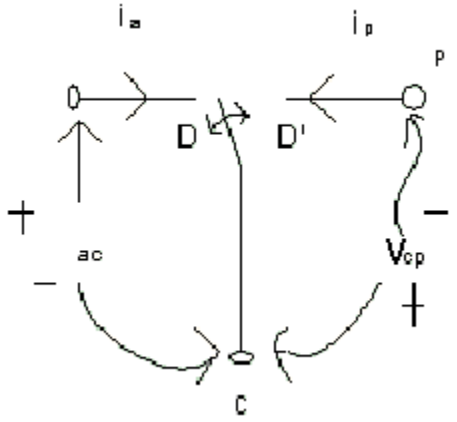

Figure 1-3: Switching Cell Block

Figure 1-3 shows a detail of the switching cell block , it is a three terminal block were the ‘c’ node represents where the inductor is connected and the ‘a’ node is at the terminal were the active switch is, likewise the ‘p’ node is were the passive diode is. The heart of this modeling method is to examine the waveforms in general across the terminals of the block and try to relate their average values together. For example for the special case were the topology is operating in DCM the currents $i_a(t)$ and $i_p(t)$ look as shown in figure 1-4, and the Continuous Model that can be deduced from the averaging of these waveforms that are shown in figure 1-5.[2] showed that this equivalent circuit of the block has ,

$$\mu = \frac{d^2}{2LF_s}\frac{v_{cp}}{i_a} = \frac{d^2}{2LF_s}\frac{v_{ac}}{i_p} \tag{1.16}$$

so it is still a nonlinear model and linearizing it requires applying small signal perturbation which yields,

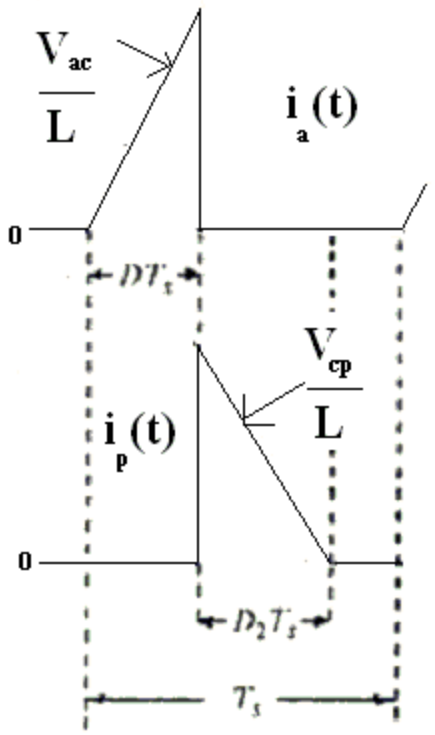

Figure 1-4 : Cell Block Waveforms in the case of DCM

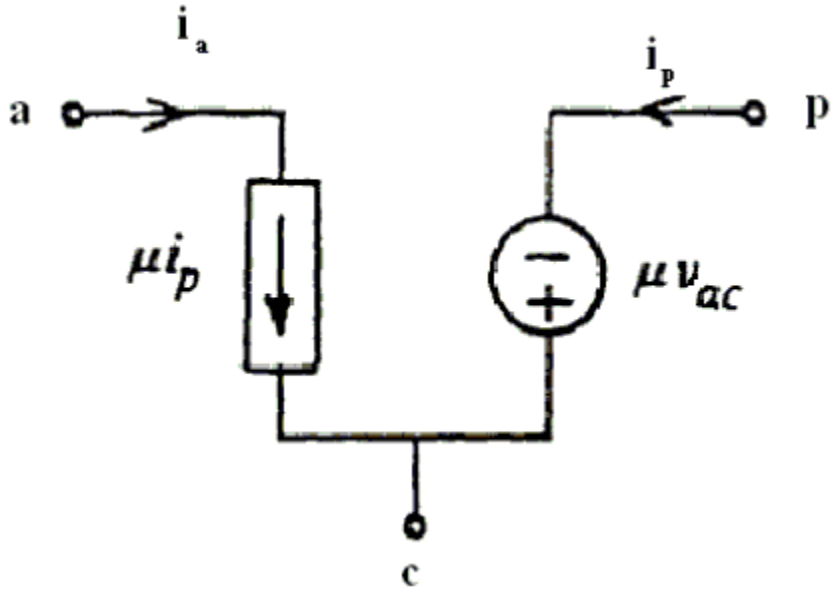

Figure 1-5: Cell Block continuous model for DCM

$$\hat{i}_p = g_f \hat{v}_{ac} + k_0 \hat{d} - g_0 \hat{v}_{cp} \tag{1.17}$$

where,

$$k_o = \frac{2I_p}{D} = \frac{2DV_{ac}{}^2}{2LF_sV_{cp}} \tag{1.18}$$

$$g_o = \frac{I_p}{V_{cp}} = \frac{D^2V_{ac}{}^2}{2LF_sV_{cp}{}^2} \tag{1.19}$$

$$g_f = \frac{2I_p}{V_{ac}} = \frac{2D^2V_{ac}}{2LF_sV_{cp}} \tag{1.20}$$

and,

$$\hat{i}_a = g_i \hat{v}_{ac} + k_i \hat{d} \tag{1.21}$$

where,

$$g_i = \frac{I_a}{V_{ac}} = \frac{D^2}{2LF_s} \tag{1.22}$$

$$k_i = \frac{2I_a}{D} = \frac{2DV_{ac}}{2LF_s} \tag{1.23}$$

And therefore the small signal equivalent circuit is as shown in figure 1-6 , see [2]. It was said that one advantage of a circuit oriented approach is the ease by which the model can be implemented in PSPICE, so for demonstration purpose the Buck circuit in figure 1-7 was simulated both in original switching form and with the average model. Figure 1-8 displays the control to output voltage frequency response obtained and figure 1-9 compares the average model vs actual responses.

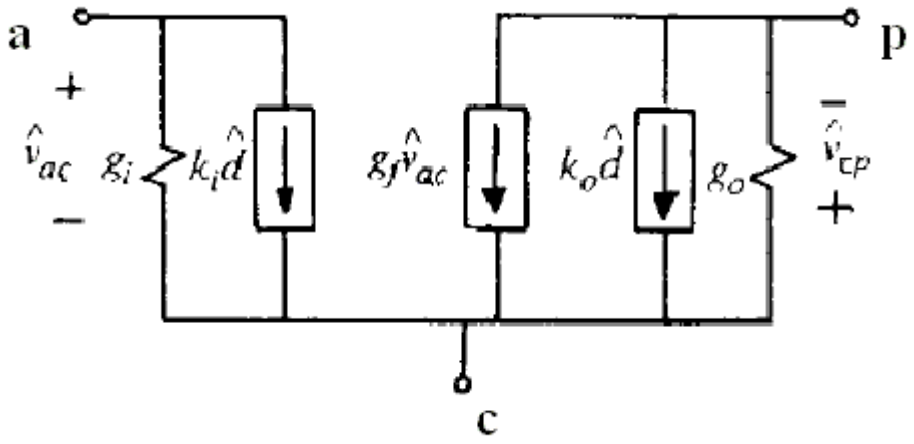

Figure 1-6 : Small-Signal equivalent circuit

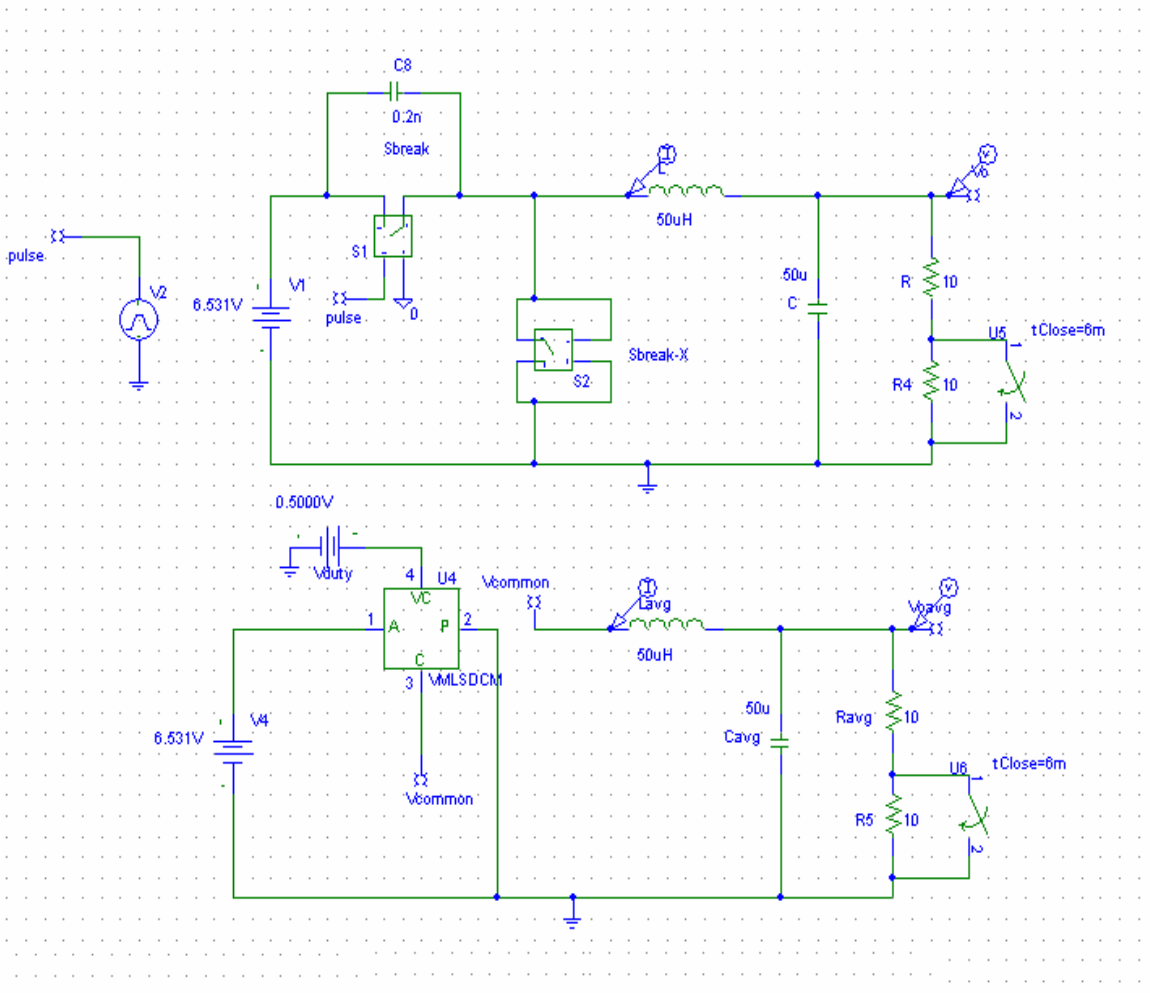

Figure 1-7: Simulation of actual buck circuit and average model in PSPICE

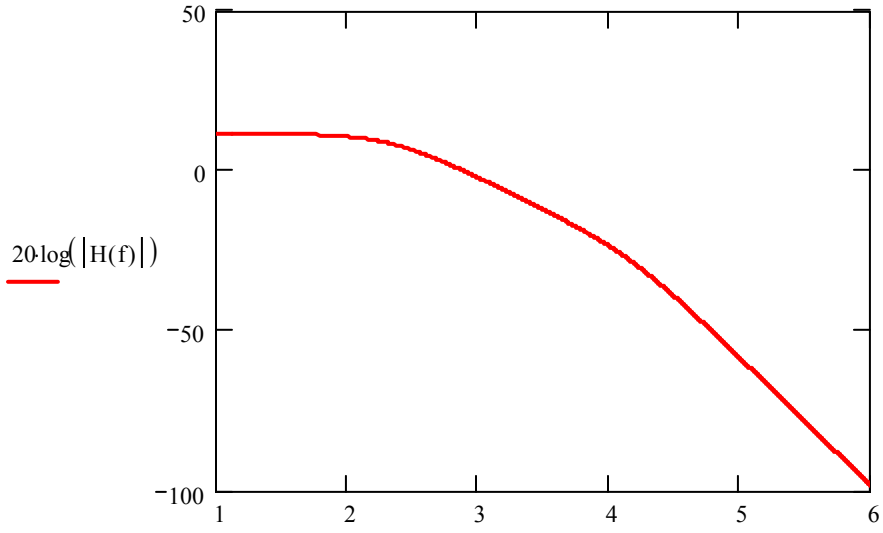

(a)

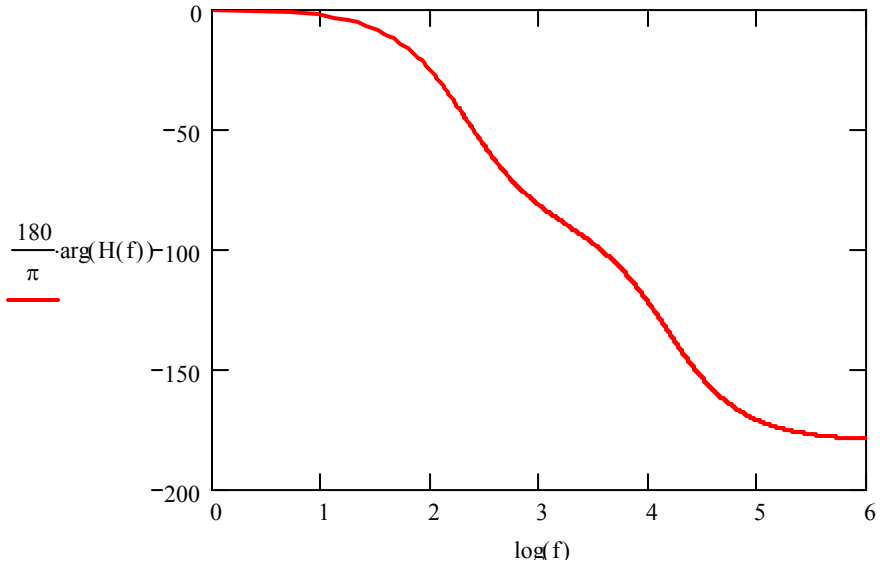

(b)

Figure 1-8 : Frequency response of Buck , (a) Magnitude , (b) Phase

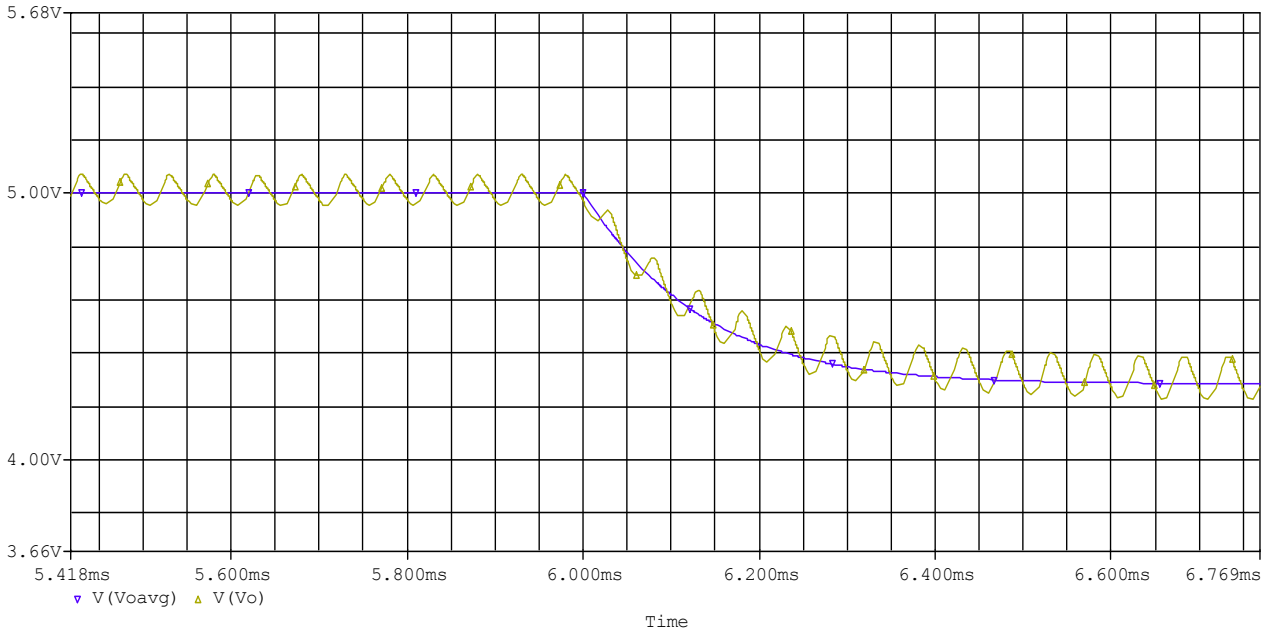

Figure 1-9 : Comparison between Average Model vs actual circuit simulation

1.3 Introduction to Digital Control and Discrete modeling of PWM converters

Conventional averaging methods for dynamic modeling yield models that are inaccurate at the upper frequency range because they ignore the sampled nature of the Duty Cycle signals that drive the power stage. Furthermore they predict frequency response content at higher than half the switching frequency, of course such information is meaningless.

The objective of this Thesis is to derive a general unified large and small discrete-space models for PWM converters in CCM so as they can be utilized for digital control of the power stage. It was shown in [5] that discrete models are more accurate in predicting the dynamics of

switching converters since switching is a naturally discrete phenomena and as thus the methodology used there will be implemented in this work. The main line of attack will be the recognition of the different modes of operation of the power stage and finding their state space matrices. This can be done since in each mode the converter is essentially a linear system. Ultimately the transient and forced time responses within each mode are derived and after relating them with each other a discrete state-space system can be deduced. Thus we arrive at the discrete model and having it in state-space form makes it versatile since it can be used to obtain pulsed filter transfer functions or simply plugged directly into a numerical package like MATLAB. Different control techniques and different topologies will result in different modes of operation thus alter the results of the model.

One of the useful utilizations of the discrete model is to obtain frequency response curves for the open loop power stage. Phase and gain margin techniques can then be used to design an appropriate compensator for stabilization of the closed loop response and furthermore the compensator can be discretized and implemented through a DSP controller. Such a methodology is an indirect digital design method since the compensator is first designed in the analog domain and then mapped into the digital domain. Having a discrete model of the Power stage in the first place makes it prudent to use a direct design method such as pole-placement where the coefficients of the digital compensator are directly obtained.

The discrepancy in the frequency response between the discrete models derived in this thesis and the average continuous models is examined in chapter 5 for the Half-Bridge topology, and is found to be substantial at high frequencies approaching one half the switching frequency.

1.4 Thesis Outline

After this introductory chapter of this Thesis chapter 2 will start with an overview of the general switched State -Space equation describing the operation of DC/DC converters. Then for the purpose of increasing the accuracy of the modeling the problem of evaluating the Steady-State waveforms is attacked using a Fourier analysis technique, and sample MATLAB code demonstrating how to implement the analysis results.

Chapter 3 and 4 commence with the task of Discrete modeling .Both chapters incorporate any general topology with at most two switches and two freewheeling modes where the phase shift between the duty cycle pulses is a variable within the models. Chapter 3 uses an impulse approximation of the duty cycle modulations to somewhat simplify the analysis that ends up with a small signal model, while chapter 4 examines the large signal discrete model and introduces small-signal analysis directly to it without any impulse approximations. Finally chapter 5 applies the developed models to the Half-Bridge DC/DC converter for all its prominent control methods (Symmetric , Asymmetric , DCS). Then Chapter 6 presents a GUI platform developed in MATLAB as an implementations of the models of this thesis, this platforms is essentially used to aid digital controller design. Chapter 7 is the conclusion and future work section of this Thesis.

CHAPTER 2

OVERVIEW AND STEADY-STATE HARMONIC ANALYSIS

2.1 General State-Space Switched Model.

Any switching power converter has switches that turn on and off in a predetermined manner to alter between different modes of operation and therefore achieve power transfer in a controlled way. A general State-Space switched equation is presented here to account for the very general case of converters that have two switches or less and two freewheeling modes or less. That is not to say other situations are not accounted for, as will be explained later. So the general switching equation , assuming the converter has two switches S1 and S2, is,

$$\frac{d\mathbf{x}}{dt} = \left[d_1(t)\mathbf{A}_1 + d_2(t)\mathbf{A_2} + d_3(t)\mathbf{A_3}\right]\mathbf{x} + \left[d_1(t)\mathbf{b}_1 + d_2(t)\mathbf{b_2} + d_3(t)\mathbf{b_3}\right]v_g \qquad (2.1)$$

where $d_1(t)$, $d_2(t)$ and $d_3(t)$ in steady state operation are as shown in Figure 2-1 , and their definition is,

$$d_1(t) = \begin{cases} 1 & \text{if S1 on} \\ 0 & \text{Otherwise} \end{cases} \qquad (2.2)$$

$$d_2(t) = \begin{cases} 1 & \text{if S2 on} \\ 0 & \text{Otherwise} \end{cases} \tag{2.3}$$

and,

$$d_3(t) = 1 - d_1(t) - d_2(t) \tag{2.4}$$

In figure 2-1 there is a phase shift α between the duty pulses for S1 and S2 , this phase shift is useful when a certain topology like the Half-Bridge has different control schemes controlled by the phase shift between the different duty cycle pulses. It will be shown in chapter 5 that this phase shift does affect the dynamics of the converter in a visible manner.

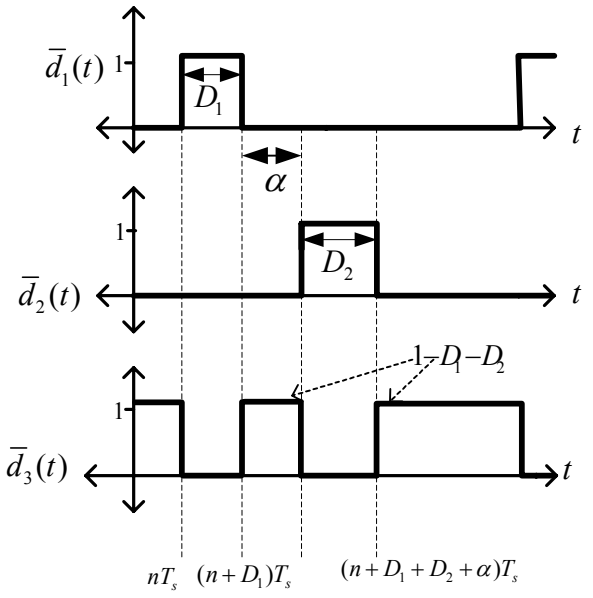

Figure 2-1 : Switching functions $\overline{d}_1(t)$ and $\overline{d}_2(t)$ for two switches in steady-state.

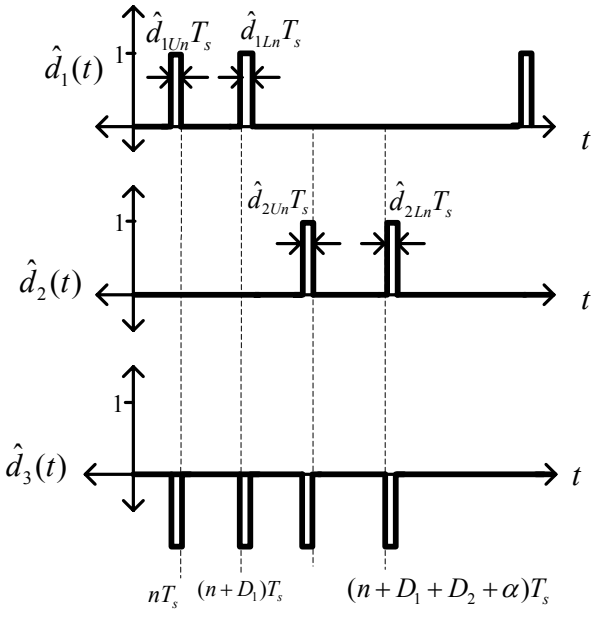

Figure 2-2 : Perturbation of Switching functions $\hat{d}_1(t)$ and $\hat{d}_2(t)$ for two switches

2.2 Small Signal perturbation.

Since it is desired to obtain a dynamic model from the switched state-space form the first step whether the main interest is discrete or continuous modeling is to apply small signal perturbation about steady state conditions. The particular notation used here marks all steady state signals with a bar over the variable ($\bar{a}$) while small signal perturbations are marked with the hat symbol ($\hat{a}$). The components of each state variable, switching functions and the input voltage are,

$$x = \bar{x} + \hat{x}\ , d_1(t) = \bar{d}_1(t) + \hat{d}_1(t)\ ,\ d_2(t) = \bar{d}_2(t) + \hat{d}_2(t)\ ,\ v_g = V_g + \hat{v}_g$$

and when substituted into (2.1) they cause its decomposition into two equations, a steady-state one and a small-signal one. The Steady-State equation is :

$$\begin{aligned}\frac{d\bar{\mathbf{x}}}{dt} = &\left[\bar{d}_1(t)\mathbf{A}_1 + \bar{d}_2(t)\mathbf{A}_2 + \left(1-\bar{d}_1(t)-\bar{d}_2(t)\right)\mathbf{A}_3\right]\bar{\mathbf{x}} \\ &+\left[\bar{d}_1(t)\mathbf{b}_1 + \bar{d}_2(t)\mathbf{b}_2 + \left(1-\bar{d}_1(t)-\bar{d}_2(t)\right)\mathbf{b}_3\right]V_g\end{aligned} \tag{2.5}$$

While the small signal equation is :

$$\begin{aligned}\frac{d\hat{\mathbf{x}}}{dt} = &\left[\bar{d}_1(t)\mathbf{A}_1 + \bar{d}_2(t)\mathbf{A}_2 + \left(1-\bar{d}_1(t)-\bar{d}_2(t)\right)\mathbf{A}_3\right]\hat{\mathbf{x}} \\ &+\left[\bar{d}_1(t)\mathbf{b}_1 + \bar{d}_2(t)\mathbf{b}_2 + \left(1-\bar{d}_1(t)-\bar{d}_2(t)\right)\mathbf{b}_3\right]\hat{v}_g \\ &+\left[\left(\mathbf{b}_1-\mathbf{b}_3\right)V_g - \left(\mathbf{A}_1-\mathbf{A}_3\right)\bar{\mathbf{X}}(t)\right]\hat{d}_1(t) \\ &+\left[\left(\mathbf{b}_2-\mathbf{b}_3\right)V_g - \left(\mathbf{A}_2-\mathbf{A}_3\right)\bar{\mathbf{X}}(t)\right]\hat{d}_2(t)\end{aligned} \tag{2.6}$$

The small signals $\hat{d}_1(t)$ and $\hat{d}_2(t)$ are the small signal perturbations of the switching signal and are as shown in figure 2-2. So now the stage is set for the derivation of a small-signal discrete model from equation (2.6).But first operation of the converter at steady state needs to be considered. This is due to the fact that $\overline{\mathbf{X}}(t)$ is a component of equation (2.6).

2.3 Motivation for Harmonic Analysis:

Throughout the literature [1]-[8] the small ripple approximation is incorporated into the analysis either for obtaining the steady-state operation point for its own sake or because the derived small-signal dynamic model requires it as an input parameter. But while the small ripple approximation is reasonable for any capacitor voltage in the converter it certainly is not for inductor currents. In the context of a continuous average model [1] errors from this assumption will not be significant since all state variables are averaged anyway , but it will make a difference for models (discrete or not) that depend on the values of the states at different instants of time in one switching cycle. The model derived in this thesis needs the values of the states at the instants where the converter switches from one mode to another , and that is the justification for the analysis presented in this section.

2.4 Fourier Series:

Going back to equation (2.5) since $\bar{\mathbf{x}}$ is the steady state vector and is periodic with respect to time Fourier analysis can be applied to it and it can be represented in the following fourirer series form,

$$\bar{\mathbf{x}} = \sum_{n=-\infty}^{\infty} \left(\overline{\mathbf{X}}_{\mathbf{n}} e^{j\frac{2\pi n}{T_s}t} \right) \tag{2.7}$$

where $\overline{\mathbf{X}}_{\mathbf{n}}$ is the n^{th} complex Fourier coefficient (harmonic) of $\bar{\mathbf{x}}(t)$. And in a similar fashion other periodic functions of time in (2.5) can be decomposed as,

$$V_g = \sum_{n=-\infty}^{\infty} \left(V_{g_n} e^{j\frac{2\pi n}{T_s}t} \right) \tag{2.8}$$

where ,

$$V_{g_n} = \frac{1}{T_s} \int_0^{T_s} V_g(t) e^{-j\frac{2\pi n}{T_s}t} dt \tag{2.9}$$

also,

$$\bar{d}_1(t) = \sum_{n=-\infty}^{\infty} \left(\overline{D_{1\mathbf{n}}} e^{j\frac{2\pi n}{T_s}t} \right) \tag{2.10}$$

$$\bar{d}_2(t) = \sum_{n=-\infty}^{\infty} \left(\overline{D_{2\mathbf{n}}} e^{j\frac{2\pi n}{T_s}t} \right) \tag{2.11}$$

where,

$$\overline{D_{1\mathbf{n}}} = \begin{cases} D_1 & ,n = 0 \\ j\dfrac{e^{-jD_1 2\pi n} - 1}{2\pi n} & ,Otherwise \end{cases} \tag{2.12}$$

$$\overline{D_{2\mathbf{n}}} = \begin{cases} D_2 & ,n = 0 \\ j\dfrac{e^{-j(D_1+\alpha)2\pi n}\left[e^{-jD_2 2\pi n} - 1\right]}{2\pi n} & ,Otherwise \end{cases} \tag{2.13}$$

Complex harmonics in (2.12) and (2.13) are plotted for n=-20 till n=20 , it can be noted that higher coefficients approach zero in magnitude , but not in a fast manner.

So , substituting (2.7)-(2.13) into (2.5) , and also entering the differentiation operator into the summation on the left hand side gives,

$$\begin{aligned} \sum_{n=-\infty}^{\infty}\left(j\frac{2\pi n}{T_s}\overline{\mathbf{X}}_{\mathbf{n}} e^{j\frac{2\pi n}{T_s}t}\right) = \\ \left[\sum_{n=-\infty}^{\infty}\left(\overline{D_{1\mathbf{n}}} e^{j\frac{2\pi n}{T_s}t}\left[\mathbf{A}_1 - \mathbf{A_3}\right]\right) + \sum_{n=-\infty}^{\infty}\left(\overline{D_{2\mathbf{n}}} e^{j\frac{2\pi n}{T_s}t}\left[\mathbf{A_2} - \mathbf{A_3}\right]\right) + \mathbf{A_3}\right]\left[\sum_{n=-\infty}^{\infty}\left(\overline{\mathbf{X}}_{\mathbf{n}} e^{j\frac{2\pi n}{T_s}t}\right)\right] \\ + \left[\sum_{n=-\infty}^{\infty}\left(\overline{D_{1\mathbf{n}}} e^{j\frac{2\pi n}{T_s}t}\left[\mathbf{b_1} - \mathbf{b_3}\right]\right) + \sum_{n=-\infty}^{\infty}\left(\overline{D_{2\mathbf{n}}} e^{j\frac{2\pi n}{T_s}t}\left[\mathbf{b}_2 - \mathbf{b_3}\right]\right) + \mathbf{b_3}\right]\left[\sum_{n=-\infty}^{\infty}\left(V_{g_n} e^{j\frac{2\pi n}{T_s}t}\right)\right] \end{aligned} \tag{2.14}$$

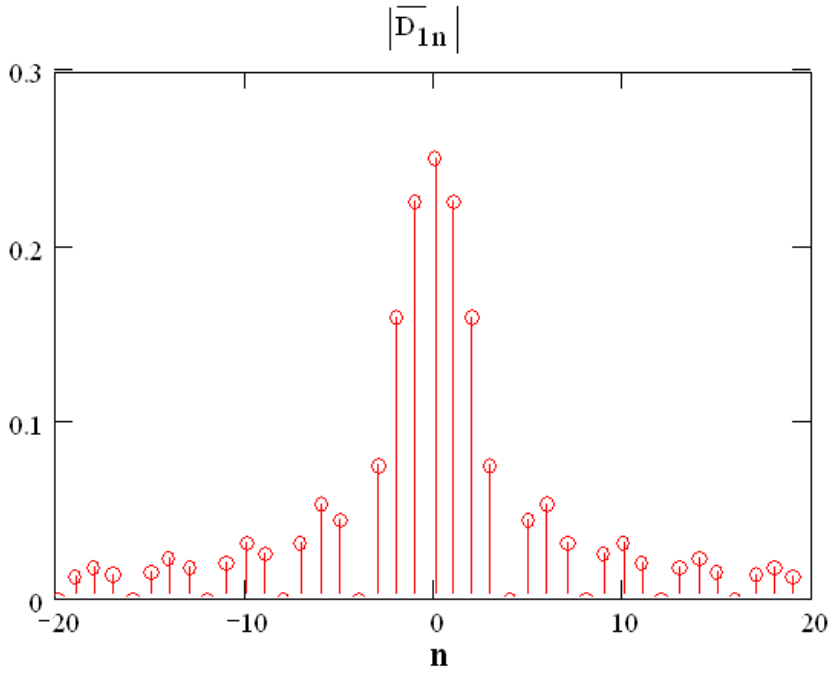

Figure 2-3: Magnitude of Fourier Coefficients of $\bar{d}_1(t)$

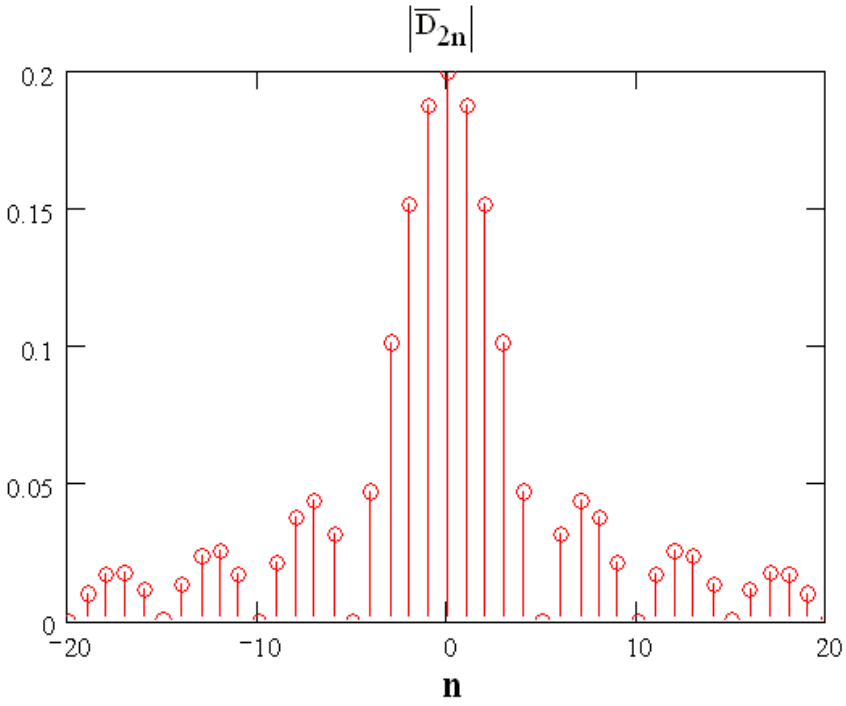

Figure 2-4: Magnitude of Fourier Coefficients of $\bar{d}_2(t)$

After some algebraic and summation sign and index manipulations, the process leads to,

$$\begin{aligned}\sum_{n=-\infty}^{\infty}\left(j\frac{2\pi n}{T_s}\overline{\mathbf{X}}_{\mathbf{n}}e^{j\frac{2\pi n}{T_s}t}\right)=&\sum_{n=-\infty}^{\infty}\sum_{m=-\infty}^{\infty}\left(\overline{D_{1\mathbf{n}}}\left[\mathbf{A}_1-\mathbf{A}_3\right]\overline{\mathbf{X}}_{\mathbf{m}}e^{j\frac{2\pi n}{T_s}t}e^{j\frac{2\pi m}{T_s}t}\right)\\&+\sum_{n=-\infty}^{\infty}\sum_{m=-\infty}^{\infty}\left(\overline{D_{2\mathbf{n}}}\left[\mathbf{A}_2-\mathbf{A}_3\right]\overline{\mathbf{X}}_{\mathbf{m}}e^{j\frac{2\pi n}{T_s}t}e^{j\frac{2\pi m}{T_s}t}\right)\\&+\sum_{m=-\infty}^{\infty}\left(\mathbf{A}_3\overline{\mathbf{X}}_{\mathbf{m}}e^{j\frac{2\pi m}{T_s}t}\right)\\&+\sum_{n=-\infty}^{\infty}\sum_{m=-\infty}^{\infty}\left(\overline{D_{1\mathbf{n}}}\left[\mathbf{b}_1-\mathbf{b}_3\right]V_{g_m}e^{j\frac{2\pi n}{T_s}t}e^{j\frac{2\pi m}{T_s}t}\right)\\&+\sum_{n=-\infty}^{\infty}\sum_{m=-\infty}^{\infty}\left(\overline{D_{2\mathbf{n}}}\left[\mathbf{b}_2-\mathbf{b}_3\right]V_{g_m}e^{j\frac{2\pi n}{T_s}t}e^{j\frac{2\pi m}{T_s}t}\right)\\&+\sum_{m=-\infty}^{\infty}\left(\mathbf{b}_3V_{g_m}e^{j\frac{2\pi m}{T_s}t}\right)\end{aligned}\tag{2.15}$$

2.5 Theoretical acquisition of Harmonics of steady-state waveforms:

What is derived up to now can be reduced to a simpler form by applying the following kernel (2.16) to both sides of (2.15). This particular kernel was used because it represents a dot product with a complex exponential function that is orthogonal to the exponential functions in the Fourier series only for some components on each side of (2.15) , otherwise its value is zero. This greatly reduces the complexity of (2.15).The kernel is shown below,

$$K\{f(t)\}=\frac{1}{T_s}\int_0^{T_s}f(t)e^{-j\frac{2\pi k}{T_s}t}dt\tag{2.16}$$

and the orthogonality property is demonstrated by,

$$\frac{1}{T_s}\int_0^{T_s} e^{j\frac{2\pi n}{T_s}t} e^{-j\frac{2\pi k}{T_s}t} dt = \begin{cases} 1 & ,n = k \\ 0 & ,n \neq k \end{cases} \tag{2.17}$$

and,

$$\frac{1}{T_s}\int_0^{T_s} e^{j\frac{2\pi n}{T_s}t} e^{j\frac{2\pi m}{T_s}t} e^{-j\frac{2\pi k}{T_s}t} dt = \begin{cases} 1 & ,n+m = k \\ 0 & ,n+m \neq k \end{cases} \tag{2.18}$$

So, after applying the aforementioned kernel equation (2.15) reduces to,

$$\begin{aligned} j\frac{2\pi k}{T_s}\overline{\mathbf{X}}_{\mathbf{k}} = &\sum_{m=-\infty}^{\infty} \overline{D}_{1\,k-m}\left[\mathbf{A}_1 - \mathbf{A}_3\right]\overline{\mathbf{X}}_{\mathbf{m}} + \sum_{m=-\infty}^{\infty} \overline{D}_{2\,k-m}\left[\mathbf{A}_2 - \mathbf{A}_3\right]\overline{\mathbf{X}}_{\mathbf{m}} + \mathbf{A}_3\overline{\mathbf{X}}_{\mathbf{k}} \\ &+ \sum_{m=-\infty}^{\infty} \overline{D}_{1\,k-m}\left[\mathbf{b}_1 - \mathbf{b}_3\right]V_{g_m} + \sum_{m=-\infty}^{\infty} \overline{D}_{2\,k-m}\left[\mathbf{b}_2 - \mathbf{b}_3\right]V_{g_m} + \mathbf{b}_3 V_{g_k} \end{aligned} \tag{2.19}$$

Since the input voltage V_g is almost constant in value and varies at a much slower rate than the switching frequency, the substitution $V_{gm} = 0$ for m≠0 can be applied. So again equation (2.19) reduces to,

$$\begin{aligned} \sum_{m=-\infty}^{\infty}\left[\overline{D}_{1\,k-m}\left[\mathbf{A}_1 - \mathbf{A}_3\right] + \overline{D}_{2\,k-m}\left[\mathbf{A}_2 - \mathbf{A}_3\right]\right]\overline{\mathbf{X}}_{\mathbf{m}} + \left[\mathbf{A}_3 - j\frac{2\pi k}{T_s}\mathbf{I}\right]\overline{\mathbf{X}}_{\mathbf{k}} \\ = -\left[\overline{D}_{1\,k}\left[\mathbf{b}_1 - \mathbf{b}_3\right] + \overline{D}_{2\,k}\left[\mathbf{b}_2 - \mathbf{b}_3\right]\right]V_{go} - \mathbf{b}_3 V_{gk} \end{aligned} \tag{2.20}$$

For the purpose of simplifying the notation the following defined substitutions are introduced,

$$\boldsymbol{\gamma}_{\mathbf{A},k-m} = \overline{D}_{1\,k-m}\left[\mathbf{A}_1 - \mathbf{A}_3\right] + \overline{D}_{2\,k-m}\left[\mathbf{A}_2 - \mathbf{A}_3\right] \tag{2.21}$$

$$\boldsymbol{\gamma}_{\mathbf{b},k} = \overline{D}_{1\,k}\left[\mathbf{b}_1 - \mathbf{b}_3\right] + \overline{D}_{2\,k}\left[\mathbf{b}_2 - \mathbf{b}_3\right] \tag{2.22}$$

$$\boldsymbol{\Omega}_{\mathbf{k}} = \mathbf{A}_3 - j\frac{2\pi k}{T_s}\mathbf{I} \tag{2.23}$$

So finally (2.20) reduces to,

$$\sum_{n=-\infty}^{\infty} \boldsymbol{\gamma}_{\mathbf{A},k-m}\overline{\mathbf{X}}_{\mathbf{m}} + \boldsymbol{\Omega}_{\mathbf{k}}\overline{\mathbf{X}}_{\mathbf{k}} = -\boldsymbol{\gamma}_{\mathbf{b},k}V_{go} - \mathbf{b}_3 V_{gk} \tag{2.24}$$

Since any converter system is a physical system this means that it essentially is low pass and higher frequency harmonics will approach zero. This allows the reduction of the infinite series in (2.24) into a finite one. Assuming that it is required to acquire N harmonics then k can be swept in integer increments form –N till +N. Thus giving the following set of vector equations,

$$\begin{aligned} k = -N \Rightarrow & \left(\boldsymbol{\gamma}_{\mathbf{A},o} + \boldsymbol{\Omega}_{-N}\right)\overline{\mathbf{X}}_{-N} + \boldsymbol{\gamma}_{\mathbf{A},-1}\overline{\mathbf{X}}_{-N+1} + \boldsymbol{\gamma}_{\mathbf{A},-2}\overline{\mathbf{X}}_{-N+2} + \ldots\ldots \\ & + \boldsymbol{\gamma}_{\mathbf{A},-N}\overline{\mathbf{X}}_{o} + \boldsymbol{\gamma}_{\mathbf{A},-N-1}\overline{\mathbf{X}}_{1} + \ldots\ldots\ldots + \boldsymbol{\gamma}_{\mathbf{A},-2N}\overline{\mathbf{X}}_{N} = -\boldsymbol{\gamma}_{\mathbf{b},-N}V_{go} \end{aligned}$$

$$\begin{aligned} k = -N+1 \Rightarrow & \boldsymbol{\gamma}_{\mathbf{A},1}\overline{\mathbf{X}}_{-N} + \left(\boldsymbol{\gamma}_{\mathbf{A},o} + \boldsymbol{\Omega}_{-N+1}\right)\overline{\mathbf{X}}_{-N+1} + \boldsymbol{\gamma}_{\mathbf{A},-1}\overline{\mathbf{X}}_{-N+2} + \ldots\ldots \\ & + \boldsymbol{\gamma}_{\mathbf{A},-N+1}\overline{\mathbf{X}}_{o} + \boldsymbol{\gamma}_{\mathbf{A},-N}\overline{\mathbf{X}}_{1} + \ldots\ldots\ldots + \boldsymbol{\gamma}_{\mathbf{A},-2N+1}\overline{\mathbf{X}}_{N} = -\boldsymbol{\gamma}_{\mathbf{b},-N+1}V_{go} \end{aligned}$$

$$\begin{aligned} k = -N+2 \Rightarrow & \boldsymbol{\gamma}_{\mathbf{A},2}\overline{\mathbf{X}}_{-N} + \boldsymbol{\gamma}_{\mathbf{A},1}\overline{\mathbf{X}}_{-N+1} + \left(\boldsymbol{\gamma}_{\mathbf{A},o} + \boldsymbol{\Omega}_{-N+2}\right)\overline{\mathbf{X}}_{-N+2} + \ldots\ldots \\ & + \boldsymbol{\gamma}_{\mathbf{A},-N+2}\overline{\mathbf{X}}_{o} + \boldsymbol{\gamma}_{\mathbf{A},-N+1}\overline{\mathbf{X}}_{1} + \ldots\ldots\ldots + \boldsymbol{\gamma}_{\mathbf{A},-2N+2}\overline{\mathbf{X}}_{N} = -\boldsymbol{\gamma}_{\mathbf{b},-N+2}V_{go} \end{aligned}$$

$$
\begin{aligned}
&\cdots\cdots\cdots \\
&\cdots\cdots\cdots \\
&k=0 \Rightarrow \boldsymbol{\gamma}_{\mathbf{A},N}\overline{\mathbf{X}}_{-N}+\boldsymbol{\gamma}_{\mathbf{A},N-1}\overline{\mathbf{X}}_{-N+1}+\boldsymbol{\gamma}_{\mathbf{A},N-2}\overline{\mathbf{X}}_{-N+2}+\cdots\cdots \\
&\qquad\qquad +\left(\boldsymbol{\gamma}_{\mathbf{A},o}+\boldsymbol{\Omega}_o\right)\overline{\mathbf{X}}_o+\boldsymbol{\gamma}_{\mathbf{A},-1}\overline{\mathbf{X}}_1+\cdots\cdots\cdots+\boldsymbol{\gamma}_{\mathbf{A},-N}\overline{\mathbf{X}}_N=\left(-\boldsymbol{\gamma}_{\mathbf{b},0}-\mathbf{b_3}\right)V_{go} \\
&\cdots\cdots\cdots \\
&k=N \Rightarrow \boldsymbol{\gamma}_{\mathbf{A},2N}\overline{\mathbf{X}}_{-N}+\boldsymbol{\gamma}_{\mathbf{A},2N-1}\overline{\mathbf{X}}_{-N+1}+\boldsymbol{\gamma}_{\mathbf{A},2N-2}\overline{\mathbf{X}}_{-N+2}+\cdots\cdots \\
&\qquad\qquad +\boldsymbol{\gamma}_{\mathbf{A},N}\overline{\mathbf{X}}_o+\boldsymbol{\gamma}_{\mathbf{A},N-1}\overline{\mathbf{X}}_1+\cdots\cdots\cdots+\left(\boldsymbol{\gamma}_{\mathbf{A},o}+\boldsymbol{\Omega}_N\right)\overline{\mathbf{X}}_N=-\boldsymbol{\gamma}_{\mathbf{b},N}V_{go}
\end{aligned}
\tag{2.25}
$$

Equations (2.25) can be accumulated into one system of linear equations as shown below,

$$
\begin{bmatrix}
\boldsymbol{\gamma}_{\mathbf{A},o}+\boldsymbol{\Omega}_{-N} & \boldsymbol{\gamma}_{\mathbf{A},-1} & \boldsymbol{\gamma}_{\mathbf{A},-2} & \cdots & \boldsymbol{\gamma}_{\mathbf{A},-N} & \boldsymbol{\gamma}_{\mathbf{A},-N-1} & \cdots & \boldsymbol{\gamma}_{\mathbf{A},-2N} \\
\boldsymbol{\gamma}_{\mathbf{A},1} & \boldsymbol{\gamma}_{\mathbf{A},o}+\boldsymbol{\Omega}_{-N+1} & \boldsymbol{\gamma}_{\mathbf{A},-1} & \cdots & \boldsymbol{\gamma}_{\mathbf{A},-N+1} & \boldsymbol{\gamma}_{\mathbf{A},-N} & \cdots & \boldsymbol{\gamma}_{\mathbf{A},-2N+1} \\
\boldsymbol{\gamma}_{\mathbf{A},2} & \boldsymbol{\gamma}_{\mathbf{A},1} & \boldsymbol{\gamma}_{\mathbf{A},o}+\boldsymbol{\Omega}_{-N+2} & \cdots & \boldsymbol{\gamma}_{\mathbf{A},-N+2} & \boldsymbol{\gamma}_{\mathbf{A},-N+1} & \cdots & \boldsymbol{\gamma}_{\mathbf{A},-2N+2} \\
\cdots & \cdots & \cdots & \cdots & \cdots & \cdots & \cdots & \cdots \\
\cdots & \cdots & \cdots & \cdots & \cdots & \cdots & \cdots & \cdots \\
\boldsymbol{\gamma}_{\mathbf{A},N} & \boldsymbol{\gamma}_{\mathbf{A},N-1} & \boldsymbol{\gamma}_{\mathbf{A},N-2} & \cdots & \boldsymbol{\gamma}_{\mathbf{A},o}+\boldsymbol{\Omega}_o & \boldsymbol{\gamma}_{\mathbf{A},-1} & \cdots & \boldsymbol{\gamma}_{\mathbf{A},-N} \\
\cdots & \cdots & \cdots & \cdots & \cdots & \cdots & \cdots & \cdots \\
\cdots & \cdots & \cdots & \cdots & \cdots & \cdots & \cdots & \cdots \\
\boldsymbol{\gamma}_{\mathbf{A},2N} & \boldsymbol{\gamma}_{\mathbf{A},2N-1} & \boldsymbol{\gamma}_{\mathbf{A},2N-2} & \cdots & \boldsymbol{\gamma}_{\mathbf{A},N} & \boldsymbol{\gamma}_{\mathbf{A},N-1} & \cdots & \boldsymbol{\gamma}_{\mathbf{A},o}+\boldsymbol{\Omega}_N
\end{bmatrix}
\begin{bmatrix}
\overline{\mathbf{X}}_{-N} \\ \cdots \\ \overline{\mathbf{X}}_o \\ \cdots \\ \overline{\mathbf{X}}_N
\end{bmatrix}
=
\begin{bmatrix}
-\boldsymbol{\gamma}_{\mathbf{b},-N} \\ \cdots \\ -\boldsymbol{\gamma}_{\mathbf{b},o}-\mathbf{b_3} \\ \cdots \\ -\boldsymbol{\gamma}_{\mathbf{b},N}
\end{bmatrix}
\tag{2.26}
$$

All that remains is to solve the system of linear equations shown in (2.26) to obtain the fourier complex coefficients for each state in the DC/DC converter circuit. Those coefficients can then be utilized to construct the steady-state waveforms by using (2.7). Any linear algebra computer package can be used for solving (2.7) , but MATLAB was utilized for obtaining the results presented in this Thesis. The matrix on the left-hand side of (2.7) can be large depending on the number needed harmonics. For example if the converter has 6 state-variables (6^{th} degree system) and 20 harmonics are needed then the matrix will be a 246 x 246, but still such a matrix

equation will just need a fraction of a second to solve in modern computers , so this is much faster than iterative simulation packages like Spice. A note about accuracy though, (2.7) should not be solved by matrix inversion because its large size will compound round off error , rather it should be solved by Gaussian Elimination which gives machine accuracy and is available in MATLAB.

2.6 Implementation in MATLAB

Sample MATLAB code is presented in this section as an example of how its scripting language can be relatively easily implemented towards solving (2.7). Results from such an implementation are plotted in chapter 5.

Code I : Harmonic Analysis implementation using MATLAB

```
function sswaveforms=SteadyStatesim(D1,D2,alpha,Ts,A1,A2,A3,b1,b2,b3,C,Vg,N,t)

%Generates CCM steady state waveforms given
%state-space matrices for different modes.

n=-2.*N:1:2.*N;
n=n+(n==0).*realmin;
D1fc=j.*(exp(-j.*2.*pi.*n.*D1)-1)./2./pi./n;
D2fc=j.*exp(-j.*2.*pi.*n.*(D1+alpha))./2./pi./n.*(exp(-j.*2.*pi.*n.*D2)-1);

temp1=[];
btemp=[];
for k=0:(2.*N),
   temp2=[];
   for m=k:-1:(-2.*N+k),
      gamma=D1fc(2.*N+1+m).*(A1-A3)+D2fc(2.*N+1+m).*(A2-A3);
      if m==0,
         omega=A3-j.*2.*pi.*(-N+k)./Ts.*eye(size(A3));
      else
         omega=0;
      end
      temp2=[temp2 gamma+omega];
   end
   temp1=[temp1 ; temp2];
   gamma=D1fc(N+1+k).*(b1-b3)+D2fc(N+1+k).*(b2-b3);
   if k==N,
      omega=b3;
   else
      omega=0;
   end
   btemp=[btemp;-(gamma+omega).*Vg];
end

AA=temp1;
clear temp1;

bb=btemp;
clear btemp;

fcoef=AA\bb;
fcoef=reshape(fcoef,length(b1),2.*N+1);
temp=0;

n=diag(-N:1:N);
t=ones(2.*N+1,1)*t;
t=n*t;
t=exp(t.*2.*pi./Ts.*j);

sswaveforms=fcoef*t;
```

CHAPTER 3

SMALL-SIGNAL DYNAMIC ANALYSIS USING IMPULSE APPROXIMATION

3.1 Motivation

The purpose of this chapter is to achieve a small-signal linear time invariant discrete state-space model from (2.6), which although being linear is time variant. Such a model will be useful for obtaining a pulse transfer function for the converter and therefore a frequency response that inherently includes the effects of sampling.

3.2 Discrete small signal State-Space Model

The methodology used here for attaining the model is to consider each mode separately and relate the small-signal state of the converter at the end of each mode to the state at its start. Then all the relations are telescoped until the state at a point is described by a function of a previous state exactly one switching cycle in the past and all the duty cycle impulse perturbations in between. This process will be elaborated more by the derivation presented in this section. A discrete model will be arrived at which relates $\hat{\mathbf{x}}\left[(n+1+D_1)T_s\right]$ to $\hat{\mathbf{x}}\left[(n+D_1)T_s\right]$, the choice of

considering the state sample at $t=(n+D_1)T_s$ is arbitrary , But for cases where an analog compensator is used for closing the loop it is preferable to consider the sampling time which corresponds with the natural sampling of the PWM modulator.

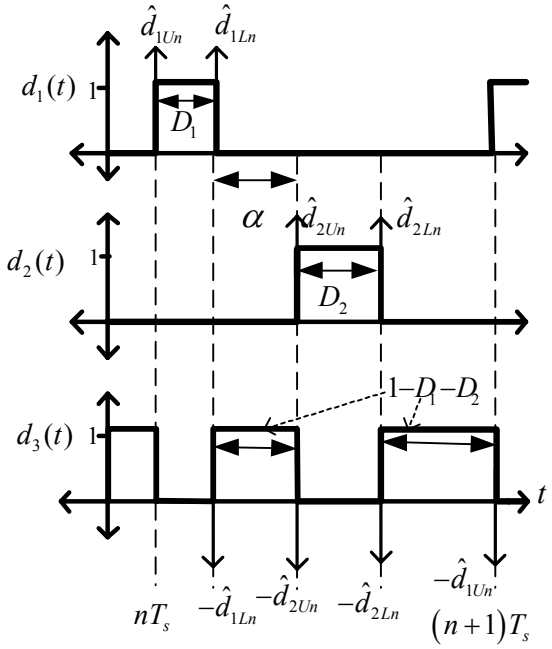

Figure 3-1 : Approximation of Duty cycle perturbations as impulse functions

The Duty cycle perturbations shown in figure 2-2 can be approximated as weighted impulse functions with weights equal to the amount of perturbation at any edge throughout the pulses. Equations (3.1)-(3.2) describe this approximation as a train of impulses

$$\hat{d}_1(t) \approx T_s \sum_{n=-\infty}^{\infty} \hat{d}_{1Ln}\delta\left[t-nT_s\right] + T_s \sum_{n=-\infty}^{\infty} \hat{d}_{1Un}\delta\left[t-(n+D_1)T_s\right] \tag{3.1}$$

$$\hat{d}_2(t) \approx T_s \sum_{n=-\infty}^{\infty} \hat{d}_{2Ln}\delta\left[t-\left(n+D_1+\alpha\right)T_s\right] + T_s \sum_{n=-\infty}^{\infty} \hat{d}_{2Un}\delta\left[t-\left(n+D_1+\alpha+D_2\right)T_s\right] \tag{3.2}$$

The variables $\hat{d}_{2Ln}$, $\hat{d}_{2Un}$, $\hat{d}_{1Ln}$, $\hat{d}_{1Un}$ represent the amount of change at each boundary edge as shown in figure (3-1).They don't necessarily have equal values , actually their values depend on the type of PWM modulator used. So describing the change in each boundary edge separately like this guarantees the accommodation into the model many diverse PWM generation circuits or even the direct output of a digital controller. Essentially the model will be a four input multiple output State-Space equation.

In (2.6) , assuming that $\hat{v}_g = \hat{v}_{gn}$,that is , assuming that the input voltage is almost constant in value through one switching cycle, which is an adequate assumption since any disturbance in the input voltage has a much less frequency than the switching frequency. So, considering (2.6) for $(n+D_1)T_s \le t \le (n+D_1+\alpha)T_s$, it becomes,

$$\frac{d\hat{\mathbf{x}}}{dt} = \mathbf{A_3}\hat{\mathbf{x}} + \mathbf{b_3}\hat{v}_{gn} + \left[\left(\mathbf{b_1}-\mathbf{b_3}\right)V_g - \left(\mathbf{A}_1-\mathbf{A_3}\right)\overline{\mathbf{X}}[t]\right]\hat{d}_{1Un}T_s\delta\left[t-\left(n+D_1\right)T_s\right] \tag{3.3}$$

In any region in time where a dynamic system is linear and its states governed by a general state-space equation such as,

$$\frac{d\mathbf{w}}{dt} = \mathbf{A}\mathbf{w}(t) + \mathbf{b}\mathbf{u}(t) \tag{3.4}$$

if the state of the system is known at an initial time t_o then the solution of (3.4) is given as:

$$\mathbf{w}(t) = e^{A(t-t_o)}\mathbf{w}(t_o) + \int_{t_o}^{t} e^{A(t-\lambda)}\mathbf{bu}(\lambda)\,d\lambda \tag{3.5}$$

So , returning to equation (3.3) it is apparent that $\mathbf{x}[(n+D_1+\alpha)T_s]$,which is at the upper edge of the first piecewise linear region of the converter system, is a function of $\mathbf{x}[(n+D_1)T_s]$ as stated before. So,

$$\begin{aligned}\hat{\mathbf{x}}\left[\left(n+D_1+\alpha\right)T_s\right] = e^{\alpha A_3 T_s}\hat{\mathbf{x}}\left[\left(n+D_1\right)T_s\right] + \left[\int_{(n+D_1)T_s}^{(n+D_1+\alpha)T_s} e^{\mathbf{A_3}\left[(n+D_1+\alpha)T_s-\lambda\right]}d\lambda\right]\mathbf{b_3}\hat{v}_{gn} \\ + \left(\int_{(n+D_1)T_s}^{(n+D_1+\alpha)T_s} e^{\mathbf{A_3}\left[(n+D_1+\alpha)T_s-\lambda\right]}\left[\left(\mathbf{b_1}-\mathbf{b_3}\right)V_g - \left(\mathbf{A}_1-\mathbf{A_3}\right)\overline{\mathbf{X}}\left[\lambda\right]\right]\delta\left[\lambda-\left(n+D_1\right)T_s\right]d\lambda\right)\hat{d}_{1Un}T_s\end{aligned} \tag{3.6}$$

And due to the sifting property of the impulse function,

$$\begin{aligned}\hat{\mathbf{x}}\left[\left(n+D_1+\alpha\right)T_s\right] = e^{\alpha\mathbf{A_3}T_s}\hat{\mathbf{x}}\left[\left(n+D_1\right)T_s\right] + \left[\int_{(n+D_1)T_s}^{(n+D_1+\alpha)T_s} e^{\mathbf{A_3}\left[(n+D_1+\alpha)T_s-\lambda\right]}d\lambda\right]\mathbf{b_3}\hat{v}_{gn} \\ + T_s e^{\alpha\mathbf{A_3}T_s}\left[\left(\mathbf{b_1}-\mathbf{b_3}\right)V_g - \left(\mathbf{A}_1-\mathbf{A_3}\right)\overline{\mathbf{X}}\left[\left(n+D_1\right)T_s\right]\right]\hat{d}_{1Un}\end{aligned} \tag{3.7}$$

Before moving to the next linear region it is worth noting that there is a certain symmetry to the state-space form of the model that suggests the following definitions which ease the size and tediousness of the notation to a large extent. These definitions are,

$$\mathbf{\Psi_1} = e^{\alpha \mathbf{A_3} T_s} \tag{3.8}$$

$$\mathbf{\Psi_2} = e^{D_2 \mathbf{A_2} T_s} \tag{3.9}$$

$$\mathbf{\Psi_3} = e^{(1-D_1-D_2-\alpha)\mathbf{A_3} T_s} \tag{3.10}$$

$$\mathbf{\Psi_4} = e^{D_1 \mathbf{A_1} T_s} \tag{3.11}$$

and,

$$\mathbf{\Delta_n}(\lambda) = (\mathbf{b_n} - \mathbf{b_3}) V_g + (\mathbf{A_n} - \mathbf{A_3}) \overline{\mathbf{X}}(\lambda) \tag{3.12}$$

also,

$$\mathbf{S_1} = \int_{(n+D_1)T_s}^{(n+D_1+\alpha)T_s} e^{\mathbf{A_3}\left[(n+D_1+\alpha)T_s - \lambda\right]} d\lambda \tag{3.13}$$

$$\mathbf{S_2} = \int_{(n+D_1+\alpha)T_s}^{(n+D_1+\alpha+D_2)T_s} e^{\mathbf{A_2}\left[(n+D_1+\alpha+D_2)T_s - \lambda\right]} d\lambda \tag{3.14}$$

$$\mathbf{S_3} = \int_{(n+D_1+\alpha+D_2)T_s}^{(n+1)T_s} e^{\mathbf{A_3}\left[(n+1)T_s - \lambda\right]} d\lambda \tag{3.15}$$

$$\mathbf{S_4} = \int_{(n+1)T_s}^{(n+1+D_1)T_s} e^{\mathbf{A_1}\left[(n+1+D_1)T_s - \lambda\right]} d\lambda \tag{3.16}$$

For the special case where the A matrices in each particular mode of operation are invertible, Equations (3.13)-(3.16) can be written as,

$$\mathbf{S_1} = \left[\mathbf{\Psi_1} - \mathbf{I}\right]\mathbf{A_3^{-1}} \tag{3.17}$$

$$\mathbf{S_2} = \left[\mathbf{\Psi_2} - \mathbf{I}\right]\mathbf{A_2^{-1}} \tag{3.18}$$

$$\mathbf{S_3} = \left[\mathbf{\Psi_3} - \mathbf{I}\right]\mathbf{A_3^{-1}} \tag{3.19}$$

$$\mathbf{S_4} = \left[\mathbf{\Psi_4} - \mathbf{I}\right]\mathbf{A_1^{-1}} \tag{3.20}$$

and finally the following is defined,

$$\mathbf{\Psi_{n:m}} = \prod_{\mathbf{k=0}}^{\mathbf{n-m}} \mathbf{\Psi_{n-k}} \tag{3.21}$$

$$\mathbf{S_{n:m}} = \prod_{\mathbf{k=0}}^{\mathbf{n-m}} \mathbf{S_{n-k}} \tag{3.22}$$

Now , continuing the derivation using the definitions (3.8)-(3.22) and substituting them into (3.7) gives,

$$\hat{\mathbf{x}}\left[\left(n + D_1 + \alpha\right)T_s\right] = \mathbf{\Psi_1}\hat{\mathbf{x}}\left[\left(n + D_1\right)T_s\right] + \mathbf{S_1 b_3}\hat{v}_{gn} + T_s\mathbf{\Psi_1 \Delta_1}\left[\left(n + D_1\right)T_s\right]\hat{d}_{1Un} \tag{3.23}$$

For the next linear region , $(n+D_1+\alpha)T_s \le t \le (n+D_1+\alpha+D_2)T_s$,

$$\frac{d\hat{\mathbf{x}}}{dt} = \mathbf{A_2}\hat{\mathbf{x}} + \mathbf{b_2}\hat{v}_g + \mathbf{\Delta_2}\left(t\right)\hat{d}_{2Ln}T_s\delta\left[t-\left(n+D_1+\alpha\right)T_s\right] \tag{3.24}$$

so,

$$\hat{\mathbf{x}}\left[\left(n+D_1+\alpha+D_2\right)T_s\right] = \mathbf{\Psi_2}\hat{\mathbf{x}}\left[\left(n+D_1+\alpha\right)T_s\right] + \mathbf{S_2}\mathbf{b_2}v_{gn} + T_s\mathbf{\Psi_2}\mathbf{\Delta_2}\left[\left(n+D_1+\alpha\right)T_s\right]\hat{d}_{2Ln} \tag{3.25}$$

Substituting (3.23) into (3.25) gives:

$$\begin{aligned}\hat{\mathbf{x}}\left[\left(n+D_1+\alpha+D_2\right)T_s\right] = {} & \mathbf{\Psi_{2:1}}\hat{\mathbf{x}}\left[\left(n+D_1\right)T_s\right] + \left(\mathbf{\Psi_2}\mathbf{S_1}\mathbf{b_3} + \mathbf{S_2}\mathbf{b_2}\right)\hat{v}_{gn} \\ & + T_s\mathbf{\Psi_{2:1}}\mathbf{\Delta_1}\left[\left(n+D_1\right)T_s\right]\hat{d}_{1Un} \\ & + T_s\mathbf{\Psi_2}\mathbf{\Delta_2}\left[\left(n+D_1+\alpha\right)T_s\right]\hat{d}_{2Ln}\end{aligned} \tag{3.26}$$

Then in the interval $(n+D_1+\alpha+D_2)T_s \le t \le (n+1)T_s$,

$$\frac{d\hat{\mathbf{x}}}{dt} = \mathbf{A_3}\hat{\mathbf{x}} + \mathbf{b_3}\hat{v}_g + \mathbf{\Delta_2}\left(t\right)\hat{d}_{2Un}T_s\delta\left[t-\left(n+D_1+\alpha+D_2\right)T_s\right] \tag{3.27}$$

So,

$$\hat{\mathbf{x}}\left[\left(n+1\right)T_s\right] = \mathbf{\Psi_3}\hat{\mathbf{x}}\left[\left(n+D_1+\alpha+D_2\right)T_s\right] + \mathbf{S_3}b_3\hat{v}_{gn} + T_s\mathbf{\Psi_3}\mathbf{\Delta_2}\left[\left(n+D_1+\alpha+D_2\right)T_s\right]\hat{d}_{2Un} \tag{3.28}$$

Again , Substituting (3.26) into (3.28) gives,

$$\begin{aligned}\hat{\mathbf{x}}\left[\left(n+1\right)T_s\right] = \boldsymbol{\Psi}_{\mathbf{3:1}}\hat{\mathbf{x}}\left[\left(n+D_1\right)T_s\right] + \left(\boldsymbol{\Psi}_{\mathbf{3:2}}\mathbf{S_1}\mathbf{b_3} + \boldsymbol{\Psi}_{\mathbf{3}}\mathbf{S_2}\mathbf{b_2} + \mathbf{S_3}\mathbf{b_3}\right)\hat{v}_{gn} \\ + T_s\boldsymbol{\Psi}_{\mathbf{3:1}}\boldsymbol{\Delta}_{\mathbf{1}}\left[\left(n+D_1\right)T_s\right]\hat{d}_{1Un} \\ + T_s\boldsymbol{\Psi}_{\mathbf{3:2}}\boldsymbol{\Delta}_{\mathbf{2}}\left[\left(n+D_1+\alpha\right)T_s\right]\hat{d}_{2Ln} \\ + T_s\boldsymbol{\Psi}_{\mathbf{3}}\boldsymbol{\Delta}_{\mathbf{2}}\left[\left(n+D_1+\alpha+D_2\right)T_s\right]\hat{d}_{2Un}\end{aligned} \tag{3.29}$$

Finally the final linear region is encountered , when $(n+1)T_s \le t \le (n+1+D_1)T_s$,

$$\frac{d\hat{\mathbf{x}}}{dt} = \mathbf{A}_1\hat{\mathbf{x}} + \mathbf{b_1}\hat{v}_{gn} + \boldsymbol{\Delta}_{\mathbf{1}}\left(t\right)T_s\hat{d}_{1Ln}\delta\left[t - nT_s\right] \tag{3.30}$$

so,

$$\hat{\mathbf{x}}\left[\left(n+1+D_1\right)T_s\right] = \boldsymbol{\Psi}_{\mathbf{4}}\hat{\mathbf{x}}\left[\left(n+1\right)T_s\right] + \mathbf{S_4}\mathbf{b_1}\hat{v}_{gn} + T_s\boldsymbol{\Psi}_{\mathbf{4}}\boldsymbol{\Delta}_{\mathbf{1}}\left[\left(n+1\right)T_s\right]\hat{d}_{1Ln} \tag{3.31}$$

Then substituting (3.29) into (3.31) yields:

$$\begin{aligned}\hat{\mathbf{x}}\left[\left(n+1+D_1\right)T_s\right] = \boldsymbol{\Psi}_{\mathbf{4:1}}\hat{\mathbf{x}}\left[\left(n+D_1\right)T_s\right] + \left(\boldsymbol{\Psi}_{\mathbf{4:2}}\mathbf{S_1}\mathbf{b_3} + \boldsymbol{\Psi}_{\mathbf{4:3}}\mathbf{S_2}\mathbf{b_2} + \boldsymbol{\Psi}_{\mathbf{4}}\mathbf{S_3}\mathbf{b_3} + \mathbf{S_4}\mathbf{b_1}\right)\hat{v}_{gn} \\ + T_s\boldsymbol{\Psi}_{\mathbf{4:1}}\boldsymbol{\Delta}_{\mathbf{1}}\left[\left(n+D_1\right)T_s\right]\hat{d}_{1Un} \\ + T_s\boldsymbol{\Psi}_{\mathbf{4:2}}\boldsymbol{\Delta}_{\mathbf{2}}\left[\left(n+D_1+\alpha\right)T_s\right]\hat{d}_{2Ln} \\ + T_s\boldsymbol{\Psi}_{\mathbf{4:3}}\boldsymbol{\Delta}_{\mathbf{2}}\left[\left(n+D_1+\alpha+D_2\right)T_s\right]\hat{d}_{2Un} \\ + T_s\boldsymbol{\Psi}_{\mathbf{4}}\boldsymbol{\Delta}_{\mathbf{1}}\left[\left(n+1\right)T_s\right]\hat{d}_{1Ln}\end{aligned} \tag{3.32}$$

Equation (3.32) is the general form of the small signal discrete model in state-space form, and it can be tailored for the different control schemes for various topologies by adjusting the values of α , D_1 and D_2 as necessary. For example it can even be used to model the three main topologies (Buck , Boost and Buckboost) or any topology that is controlled by two or less switches and has a freewheeling mode. Of course different topologies can share the same α, D1 and D2 parameters depending on how their switches are operated , yet the A and b for each mode should be different.

Table 3-1 : Model parameters substitution for various topologies with different control schemes

Buck	$\alpha = 0$	$D_2 = 1 - D_1$
Boost	$\alpha = 0$	$D_2 = 1 - D_1$
BuckBoost	$\alpha = 0$	$D_2 = 1 - D_1$
Symmetric	$\alpha = \frac{1 - D_1 - D_2}{2}$	$D_2 = D_1$
Asymmetric	$\alpha = 0$	$D_2 = 1 - D_1$
DCS	$\alpha = 0$	$D_2 = D_1$

Equation (3.32) is in the form of a discrete state equation that can be implemented within a linear system software package. Various useful information for stability analysis and compensation can be obtained through the model, such as the frequency response curves, root locus plots or Nyquist diagrams. Moreover, having the discrete model in state space form allows the use of modern control methods such as pole-placement.

It is worth noticing that (3.32) has four small duty cycle modulations as input signals. Normally in a completely digital closed loop system the digital compensator directly controls the modulations in the duty cycle ratios, or its output may be connected to an analog PWM generator. This PWM generator, whether analog or digital is modeled with small signal approximation as a linear operator as shown in (3.33),

$$\begin{bmatrix} \hat{d}_{1un} \\ \hat{d}_{2ln} \\ \hat{d}_{2un} \\ \hat{d}_{1ln} \end{bmatrix} = Mc[n] \tag{3.33}$$

where $M=[m_1 \;\; m_2 \; m_3 \; m_4]^T$ and c[n] is the output of the discrete compensator or the input of the pulse width modulator. Substituting (3.33) into (3.32) gives a more useful and complete model for pulse transfer function acquisition. Considering what was stated above, and selecting the output voltage of the converter to be the output of the model , for the case where the modulator input to output voltage pulse transfer function is required, the complete representation of the discrete model is,

$$\hat{\mathbf{x}}[n+1] = \mathbf{A_d}\hat{x}[n] + \mathbf{b_d}c[n] \tag{3.34}$$

$$\hat{y}[n] = \mathbf{C_d}\hat{x}[n] \tag{3.35}$$

Since the interest is stability analysis it is assumed that $\hat{v}_{gn} = 0$, so,

$$\mathbf{A_d} = \mathbf{\Psi_{4:1}} \tag{3.36}$$

and,

$$\mathbf{b_d} = T_s \left[\begin{array}{c} \mathbf{\Psi_{4:1}\Delta_1}\left[\left(n + D_1\right)T_s\right] \\ \hline \mathbf{\Psi_{4:2}\Delta_2}\left[\left(n + D_1 + \alpha\right)T_s\right] \\ \hline \mathbf{\Psi_{4:3}\Delta_2}\left[\left(n + D_1 + \alpha + D_2\right)T_s\right] \\ \hline \mathbf{\Psi_4\Delta_1}\left[\left(n+1\right)T_s\right] \end{array} \right]^T M \tag{3.37}$$

$\mathbf{C_d}$ normally depends on the particular topology , and is the C matrix at or just right before the moment of sampling.

Note that $\hat{y}[n]$ represents the perturbation in the converter output voltage. Equations (3.34)-(3.35) are the general state-space representation of a discrete-time system from which finally the desired pulse transfer function is derived in (3.38),

$$\frac{v_o(z)}{c(z)} = C_d \left[zI - A_d\right]^{-1} b_d \tag{3.38}$$

With the derivation of the pulse transfer function in general comes the conclusion of this chapter.

CHAPTER 4

LARGE AND SMALL SIGNAL STATE-SPACE DISCRETE MODEL WITHOUT IMPULSE APPROXIMATION

4.1 Motivation

In the previous chapter a small signal State-Space dynamic model was developed, and it utilized approximating the perturbations of the duty cycle functions controlling the converter switches as impulse functions. The main assumption of course is that those perturbations are small in magnitude and the converter states remain close to the steady state operating point. Due to this approximation the large signal dynamics are lost , that is large signal response could not be obtained. In this chapter a large signal Discrete model will be derived without any approximations other than that the input voltage is almost constant throughout one switching cycle. The small signal model can then be obtained through Taylor series expansion with cancellation of higher order terms.

4.2 Discrete Large signal State-Space Mode

As was done in chapter 3 the basis of the Discrete model is the state space switching model described in equation (2.1) .But now the relation between edges of each piecewise linear region is derived before the application of small signal perturbation. Figure 4-1 show those linear regions between switching instants , and emphasizes that the time of switching between one mode to the next can vary by any amount within some constraints. These constraints are,

$$d_{1un} < \left(\alpha - d_{2ln}\right) < \left(\alpha + D_2 + d_{2un}\right) < \left(1 - D_1 - d_{1ln}\right)$$

Since the desired model will be used for large signal discrete simulation it is desirous to choose a sampling instant within the switching cycle that is as close as possible to the average magnitudes of the state variables within that period. Choosing an instant of switching as a beginning point will result in a model that tracks the peaks of the state waveforms so for this thesis the midpoint of the first duty cycle switching is chosen to be the sampling instant.

So ,to begin the derivation process the interval $(n+D_1/2)T_s \le t \le (n+D_1+d_{1u})T_s$ is considered were from (2.1) ,

$$\frac{d\mathbf{x}}{dt} = \mathbf{A_1}\mathbf{x} + \mathbf{b_1}\mathbf{u} \tag{4.1}$$

$$\begin{aligned}\mathbf{x}\left[\left(n + D_1 + d_{1un}\right)T_s\right] = e^{\mathbf{A_1}\left(\frac{D_1}{2}+d_{1un}\right)T_s}\mathbf{x}\left[\left(n+\frac{D_1}{2}\right)T_s\right] \\ + \left(\int_{\left(n+\frac{D_1}{2}\right)T_s}^{(n+D_1+d_{1un})T_s} e^{\mathbf{A_1}\left[(n+D_1+d_{1un})T_s-\lambda\right]}d\lambda\right)\mathbf{b_1}\mathbf{u}\left[nT_s\right]\end{aligned} \tag{4.2}$$

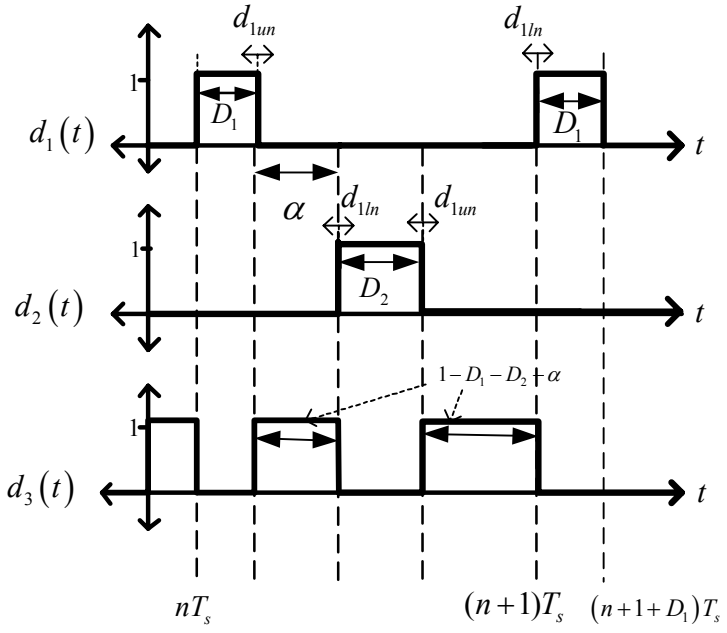

Figure 4-1 : Switching Model Piecewise linear regions with varying switching instants

Now , the next interval to consider is $(n+D_1+d_{1u})T_s \le t \le (n+D_1+\alpha-d_{2l})T_s$ where,

$$\frac{d\mathbf{x}}{dt} = \mathbf{A_3}\mathbf{x} + \mathbf{b_3}\mathbf{u} \tag{4.3}$$

$$\begin{aligned}\mathbf{x}\left[\left(n+D_1+\alpha-d_{2ln}\right)T_s\right] &= e^{\mathbf{A_3}(\alpha-d_{2ln}-d_{1un})T_s}\mathbf{x}\left[\left(n+D_1+d_{1un}\right)T_s\right] \\ &+\left(\int_{(n+D_1+d_{1un})T_s}^{(n+D_1+\alpha-d_{2ln})T_s} e^{\mathbf{A_3}\left[(n+D_1+\alpha-d_{2ln})T_s-\lambda\right]}d\lambda\right)\mathbf{b_3}\mathbf{u}\left[nT_s\right]\end{aligned} \tag{4.4}$$

Substituting (4.2) into (4.4) yields ,

$$\mathbf{x}\left[\left(n+D_1+\alpha-d_{2ln}\right)T_s\right]=e^{\mathbf{A_3}(\alpha-d_{2ln}-d_{1un})T_s}e^{\mathbf{A_1}\left(\frac{D_1}{2}+d_{1un}\right)T_s}\mathbf{x}\left[\left(n+\frac{D_1}{2}\right)T_s\right]$$
$$+\left[e^{\mathbf{A_3}(\alpha-d_{2ln}-d_{1un})T_s}\left(\int_{\left(n+\frac{D_1}{2}\right)T_s}^{(n+D_1+d_{1un})T_s}e^{\mathbf{A_1}\left[(n+D_1+d_{1un})T_s-\lambda\right]}d\lambda\right)\mathbf{b_1}\right. \tag{4.5}$$
$$\left.+\left(\int_{(n+D_1+d_{1un})T_s}^{(n+D_1+\alpha-d_{2ln})T_s}e^{\mathbf{A_3}\left[(n+D_1+\alpha-d_{2ln})T_s-\lambda\right]}d\lambda\right)\mathbf{b_3}\right]\mathbf{u}\left[nT_s\right]$$

It seems that the form of the discrete difference equation will be of a cumbersome nature from a notational perspective. Yet the same symmetry first encountered in chapter 3 still holds , and the notation can be immensely simplified through making some appropriate definitions as follows,

$$\mathbf{\Psi_1}=e^{\mathbf{A_1}\left(\frac{D_1}{2}+d_{1un}\right)T_s} \tag{4.6}$$

$$\mathbf{\Psi_2}=e^{\mathbf{A_3}(\alpha-d_{2ln}-d_{1un})T_s} \tag{4.7}$$

$$\mathbf{\Psi_3}=e^{\mathbf{A_2}(D_2+d_{2ln}+d_{2un})T_s} \tag{4.8}$$

$$\mathbf{\Psi_4}=e^{\mathbf{A_3}(1-D_1-\alpha-D_2-d_{2un}-d_{1ln})T_s} \tag{4.9}$$

$$\mathbf{\Psi_5}=e^{\mathbf{A_1}\left(\frac{D_1}{2}+d_{1ln}\right)T_s} \tag{4.10}$$

also,

$$\mathbf{S_1}=\int_{\left(n+\frac{D_1}{2}\right)T_s}^{(n+D_1+d_{1un})T_s}e^{\mathbf{A_1}\left[(n+D_1+d_{1un})T_s-\lambda\right]}d\lambda \tag{4.11}$$

$$\mathbf{S_2}=\int_{(n+D_1+d_{1un})T_s}^{(n+D_1+\alpha-d_{2ln})T_s}e^{\mathbf{A_3}\left[(n+D_1+\alpha-d_{2ln})T_s-\lambda\right]}d\lambda \tag{4.12}$$

$$\mathbf{S_3} = \int_{(n+D_1+\alpha-d_{2ln})T_s}^{(n+D_1+\alpha+D_2+d_{2un})T_s} e^{\mathbf{A_2}\left[(n+D_1+\alpha+D_2+d_{2un})T_s-\lambda\right]}d\lambda \tag{4.13}$$

$$\mathbf{S_4} = \int_{(n+D_1+\alpha+D_2+d_{2un})T_s}^{(n+1-d_{1ln})T_s} e^{\mathbf{A_3}\left[(n+1-d_{1ln})T_s-\lambda\right]}d\lambda \tag{4.14}$$

$$\mathbf{S_5} = \int_{(n+1-d_{1ln})T_s}^{\left(n+1+\frac{D_1}{2}\right)T_s} e^{\mathbf{A_1}\left[\left(n+1+\frac{D_1}{2}\right)T_s-\lambda\right]}d\lambda \tag{4.15}$$

The integrals in $\mathbf{S_1}$ till $\mathbf{S_5}$ can be evaluated using a numerical integration method such as Simpsons Rule , or the matrix exponential within each integral could be expanded into its Taylor Series and integrated term by term. So in that case ,

$$\mathbf{S_1} = \sum_{k=0}^{\infty} \frac{\mathbf{A_1}^k}{(k+1)!}\left[\left(\frac{D_1}{2}+d_{1un}\right)T_s\right]^{k+1} \tag{4.16}$$

$$\mathbf{S_2} = \sum_{k=0}^{\infty} \frac{\mathbf{A_3}^k}{(k+1)!}\left[\left(\alpha-d_{2ln}-d_{1un}\right)T_s\right]^{k+1} \tag{4.17}$$

$$\mathbf{S_3} = \sum_{k=0}^{\infty} \frac{\mathbf{A_2}^k}{(k+1)!}\left[\left(D_2+d_{2ln}+d_{2un}\right)T_s\right]^{k+1} \tag{4.18}$$

$$\mathbf{S_4} = \sum_{k=0}^{\infty} \frac{\mathbf{A_3}^k}{(k+1)!}\left[\left(1-D_1-\alpha-D_2-d_{2un}-d_{1ln}\right)T_s\right]^{k+1} \tag{4.19}$$

$$\mathbf{S_5} = \sum_{k=0}^{\infty} \frac{\mathbf{A_1}^k}{(k+1)!}\left[\left(\frac{D_1}{2}+d_{1ln}\right)T_s\right]^{k+1} \tag{4.20}$$

For the case where the switching period is very small (which is almost always true for switching DC/DC power converters) the terms for k>0 in (4.16) to (4.20) can be eliminated. The most accurate path though is to use an integral numerical method since the speed of convergence of the presented power series depends also on the norms of the A matrices which is a parameter that varies with the circuit components values. Also the results (4.16) to (4.20) verify that $\mathbf{S_1}$ till $\mathbf{S_5}$ are not dependant on n when all the duty cycle perturbations are zero and the converter is in steady state, so n can be set to zero in that case.

So, continuing the same procedure outlined before for the region $(n+D_1+\alpha-d_{2l})T_s \le t \le (n+D_1+\alpha+D_2+d_{2u})T_s$ and every following region until the interval where $(n+1-d_{1l})T_s \le t \le (n+D_1/2)T_s$ is reached, and without repeating the same algebraic manipulation in chapter 2 the followed result is induced,

$$\begin{aligned}\mathbf{x}\left[\left(n+1+D_1\right)T_s\right] &= \mathbf{\Psi_{5:1}}\mathbf{x}\left[\left(n+D_1\right)T_s\right] \\ &+\left(\mathbf{\Psi_{5:2}}\mathbf{S_1}\mathbf{b_1}+\mathbf{\Psi_{5:3}}\mathbf{S_2}\mathbf{b_3}+\mathbf{\Psi_{5:4}}\mathbf{S_3}\mathbf{b_2}+\mathbf{\Psi_5}\mathbf{S_4}\mathbf{b_3}+\mathbf{S_5}\mathbf{b_1}\right)\mathbf{u}\left[nT_s\right] \qquad (4.21)\end{aligned}$$

Equation (4.21) represents the Large Signal model , it should be noted that for any fixed switching duty cycles the converter behaves as a discrete linear system when the states are a function of the system input (input voltage for example , or perhaps load current). The nonlinearity appears only when the effect of modulating the switching cycles is considered. It is apparent that all the $\mathbf{\Psi_n}, \mathbf{\Psi_{n:m}}$ and $\mathbf{S_n}$ matrices are functions of the duty cycle modulations in a nonlinear manner. The achieved model can be easily implemented using computer linear algebra software such as MATLAB.

4.3 Discrete Small signal State-Space Model without impulse approximation.

As was mentioned in section 2, all the $\mathbf{\Psi_n}, \mathbf{\Psi_{n:m}}$ and $\mathbf{S_n}$ matrices are functions of the duty cycle modulations in a nonlinear fashion So the first step for linearizing the Discrete model would be to reduce those matrices to a form that is linear with respect to the cycle modulations. This form comes through the small signal assumption which leads to the desired small signal dynamic model for any steady-state operating point. But before continuing the steady state operating point needs to be found , so going back to (4.21) and assuming that,

$$d_{1u} = d_{2l} = d_{2u} = d_{1l} = 0 \tag{4.22}$$

and noting that the converter reaches steady-state after a certain N when for all n>N ,

$$\mathbf{x}\left[n+1\right] = \mathbf{x}[n] = \overline{\mathbf{X}} \tag{4.23}$$

of course the input also should be constant otherwise a constant steady state won't be reached , the constant input is denoted for all n as,

$$\mathbf{u}[n] = \overline{\mathbf{U}} \tag{4.24}$$

Now , substituting (4.23) and (4.24) into (4.21) and solving gives,

$$\overline{\mathbf{X}} = \left(\mathbf{I} - \overline{\mathbf{\Psi}}_{5:1}\right)^{-1}\left(\overline{\mathbf{\Psi}}_{5:2}\overline{\mathbf{S}}_1\mathbf{b}_1 + \overline{\mathbf{\Psi}}_{5:3}\overline{\mathbf{S}}_2\mathbf{b}_3 + \overline{\mathbf{\Psi}}_{5:4}\overline{\mathbf{S}}_3\mathbf{b}_2 + \overline{\mathbf{\Psi}}_5\overline{\mathbf{S}}_4\mathbf{b}_3 + \overline{\mathbf{S}}_5\mathbf{b}_1\right)\overline{\mathbf{U}} \tag{4.25}$$

where any matrix that has a bar on it indicates that (4.22) is satisfied. So from this point forward any steady state component of a matrix is represented with the same matrix name but with a bar on it. On the other hand and matrix with a hat on it signifies a matrix with a small signal simplification.

For the small signal analysis a certain simplification of the binomial expansion where one of the variables has small values will be used. The general form of the binomial expansion is,

$$\left(a+\hat{b}\right)^n = a^n + \binom{n}{1} a^{n-1}\hat{b} + \binom{n}{2} a^{n-2}\hat{b}^2 + \bullet\bullet\bullet\bullet\bullet\bullet + \binom{n}{n-1} a\hat{b}^{n-1} + \hat{b}^n \tag{4.26}$$

where,

$$\binom{n}{k} = \frac{n!}{k!(n-k)!} \tag{4.27}$$

and since $\hat{b}$ is small when compared to a all high order powers can be eliminated to give,

$$\left(a+\hat{b}\right)^n \approx a^n + na^{n-1}\hat{b} \tag{4.28}$$

The line of attack will be to use the approximation in (4.28) and the Taylor series truncation to express the matrices in the discrete model as linear functions of the duty cycle modulations , so each matrix presented in (4.21) is investigated and manipulated to reach the desired result. Then , starting with $\mathbf{S_1}$ and manipulating it algebraically to get,

$$\mathbf{S_1} = \sum_{k=0}^{\infty} \frac{\mathbf{A_1}^k}{(k+1)!}\left[\frac{D_1}{2}T_s + \hat{d}_{1un}T_s\right]^{k+1} \tag{4.29}$$

then by applying the binomial approximation and taking the summation sign inside , then doing the appropriate cancellations ,

$$\hat{\mathbf{S}}_1 = \sum_{k=0}^{\infty} \frac{\mathbf{A_1}^k}{(k+1)!}\left(\frac{D_1}{2}T_s\right)^{k+1} + \sum_{k=0}^{\infty} \frac{\mathbf{A_1}^k}{k!}\left(\frac{D_1}{2}T_s\right)^{k} \hat{d}_{1un}T_s \tag{4.30}$$

so,

$$\hat{\mathbf{S}}_1 = \overline{\mathbf{S}}_1 + \overline{\mathbf{\Psi}}_1 T_s \hat{d}_{1un} \tag{4.31}$$

Repeating the same process with the other $\mathbf{S}$ matrices gives,

$$\hat{\mathbf{S}}_{\mathbf{2}} = \bar{\mathbf{S}}_{\mathbf{2}} - \overline{\mathbf{\Psi}}_{\mathbf{2}} T_s \hat{d}_{2ln} - \overline{\mathbf{\Psi}}_{\mathbf{2}} T_s \hat{d}_{1un} \tag{4.32}$$

$$\hat{\mathbf{S}}_{\mathbf{3}} = \bar{\mathbf{S}}_{\mathbf{3}} + \overline{\mathbf{\Psi}}_{\mathbf{3}} T_s \hat{d}_{2ln} + \overline{\mathbf{\Psi}}_{\mathbf{3}} T_s \hat{d}_{2un} \tag{4.33}$$

$$\hat{\mathbf{S}}_{\mathbf{4}} = \bar{\mathbf{S}}_{\mathbf{4}} - \overline{\mathbf{\Psi}}_{\mathbf{4}} T_s \hat{d}_{2un} - \overline{\mathbf{\Psi}}_{\mathbf{4}} T_s \hat{d}_{1ln} \tag{4.34}$$

$$\hat{\mathbf{S}}_{\mathbf{5}} = \bar{\mathbf{S}}_{\mathbf{5}} + \overline{\mathbf{\Psi}}_{\mathbf{5}} T_s \hat{d}_{1ln} \tag{4.35}$$

Moving on to the $\mathbf{\Psi}$ matrices their Taylor Series expansions can be used to arrive at their small signal forms , for example for $\mathbf{\Psi}_{\mathbf{1}}$,

$$\mathbf{\Psi}_{\mathbf{1}} = e^{\mathbf{A}_{\mathbf{1}}\left(\frac{D_1}{2} + d_{1un}\right)T_s} = e^{\mathbf{A}_{\mathbf{1}}\frac{D_1}{2}T_s} e^{\mathbf{A}_{\mathbf{1}} d_{1un} T_s} \tag{4.36}$$

So,

$$\mathbf{\Psi}_{\mathbf{1}} = \overline{\mathbf{\Psi}}_{\mathbf{1}} \sum_{k=0}^{\infty} \frac{\mathbf{A}_{\mathbf{1}}^{\,k}}{k!} \left(d_{1un} T_s\right)^k \tag{4.37}$$

and if d_{1un} is small all terms where k>1 can be ignored so what remains would be,

$$\hat{\mathbf{\Psi}}_{\mathbf{1}} = \overline{\mathbf{\Psi}}_{\mathbf{1}} \left[\mathbf{I} + \mathbf{A}_{\mathbf{1}} T_s \hat{d}_{1un} \right] \tag{4.38}$$

and in the same manner,

$$\hat{\mathbf{\Psi}}_{2} = \overline{\mathbf{\Psi}}_{2} \left[\mathbf{I} - \mathbf{A}_{3} T_s \hat{d}_{2ln} - \mathbf{A}_{3} T_s \hat{d}_{1un} \right] \tag{4.39}$$

$$\hat{\mathbf{\Psi}}_{\mathbf{3}} = \overline{\mathbf{\Psi}}_{\mathbf{3}} \left[\mathbf{I} + \mathbf{A}_{\mathbf{2}} T_s \hat{d}_{2ln} + \mathbf{A}_{\mathbf{2}} T_s \hat{d}_{2un} \right] \tag{4.40}$$

$$\hat{\mathbf{\Psi}}_{\mathbf{4}} = \overline{\mathbf{\Psi}}_{\mathbf{4}} \left[\mathbf{I} - \mathbf{A}_{\mathbf{3}} T_s \hat{d}_{2un} - \mathbf{A}_{\mathbf{3}} T_s \hat{d}_{1ln} \right] \tag{4.41}$$

$$\hat{\mathbf{\Psi}}_{\mathbf{5}} = \overline{\mathbf{\Psi}}_{\mathbf{5}} \left[\mathbf{I} + \mathbf{A}_{\mathbf{1}} T_s \hat{d}_{1ln} \right] \tag{4.44}$$

If the $\boldsymbol{\Psi}_{5:1}$ matrix is examined in (4.21) after substituting the small signal forms in (4.38) to (4.44) into it the following algebraic manipulations can be done ,

$$\hat{\boldsymbol{\Psi}}_{5:1} = \hat{\boldsymbol{\Psi}}_5 \hat{\boldsymbol{\Psi}}_4 \hat{\boldsymbol{\Psi}}_3 \hat{\boldsymbol{\Psi}}_2 \hat{\boldsymbol{\Psi}}_1 \tag{4.45}$$

but,

$$\hat{\boldsymbol{\Psi}}_5 \hat{\boldsymbol{\Psi}}_4 = \left[\overline{\boldsymbol{\Psi}}_5 + \overline{\boldsymbol{\Psi}}_5 \mathbf{A}_1 T_s \hat{d}_{1ln} \right] \left[\overline{\boldsymbol{\Psi}}_4 - \overline{\boldsymbol{\Psi}}_4 \mathbf{A}_3 T_s \hat{d}_{2un} - \overline{\boldsymbol{\Psi}}_4 \mathbf{A}_3 T_s \hat{d}_{1ln} \right]$$

So,

$$\hat{\boldsymbol{\Psi}}_5 \hat{\boldsymbol{\Psi}}_4 = \overline{\boldsymbol{\Psi}}_{5:4} - \overline{\boldsymbol{\Psi}}_{5:4} \mathbf{A}_3 T_s \hat{d}_{2un} + \left(\overline{\boldsymbol{\Psi}}_5 \mathbf{A}_1 \overline{\boldsymbol{\Psi}}_4 - \overline{\boldsymbol{\Psi}}_{5:4} \mathbf{A}_3 \right) T_s \hat{d}_{1ln} \tag{4.46}$$

and in a similar manner,

$$\begin{aligned} \hat{\boldsymbol{\Psi}}_5 \hat{\boldsymbol{\Psi}}_4 \hat{\boldsymbol{\Psi}}_3 = \overline{\boldsymbol{\Psi}}_{5:3} &+ \overline{\boldsymbol{\Psi}}_{5:3} \mathbf{A}_2 T_s \hat{d}_{2ln} + \left(\overline{\boldsymbol{\Psi}}_{5:3} \mathbf{A}_2 - \overline{\boldsymbol{\Psi}}_{5:4} \mathbf{A}_3 \overline{\boldsymbol{\Psi}}_3 \right) T_s \hat{d}_{2un} \\ &+ \left(\overline{\boldsymbol{\Psi}}_5 \mathbf{A}_1 \overline{\boldsymbol{\Psi}}_{4:3} - \overline{\boldsymbol{\Psi}}_{5:4} \mathbf{A}_3 \overline{\boldsymbol{\Psi}}_3 \right) T_s \hat{d}_{1ln} \end{aligned} \tag{4.47}$$

$$\begin{aligned} \hat{\boldsymbol{\Psi}}_5 \hat{\boldsymbol{\Psi}}_4 \hat{\boldsymbol{\Psi}}_3 \hat{\boldsymbol{\Psi}}_2 = \overline{\boldsymbol{\Psi}}_{5:2} &\\ &- \overline{\boldsymbol{\Psi}}_{5:2} \mathbf{A}_3 T_s \hat{d}_{1un} \\ &+ \left(\overline{\boldsymbol{\Psi}}_{5:3} \mathbf{A}_2 \overline{\boldsymbol{\Psi}}_2 - \overline{\boldsymbol{\Psi}}_{5:2} \mathbf{A}_3 \right) T_s \hat{d}_{2ln} \\ &+ \left(\overline{\boldsymbol{\Psi}}_{5:3} \mathbf{A}_2 \overline{\boldsymbol{\Psi}}_2 - \overline{\boldsymbol{\Psi}}_{5:4} \mathbf{A}_3 \overline{\boldsymbol{\Psi}}_{3:2} \right) T_s \hat{d}_{2un} \\ &+ \left(\overline{\boldsymbol{\Psi}}_5 \mathbf{A}_1 \overline{\boldsymbol{\Psi}}_{4:2} - \overline{\boldsymbol{\Psi}}_{5:4} \mathbf{A}_3 \overline{\boldsymbol{\Psi}}_{3:2} \right) T_s \hat{d}_{1ln} \end{aligned} \tag{4.48}$$

Finally,

$$\begin{aligned} \hat{\boldsymbol{\Psi}}_5 \hat{\boldsymbol{\Psi}}_4 \hat{\boldsymbol{\Psi}}_3 \hat{\boldsymbol{\Psi}}_2 \hat{\boldsymbol{\Psi}}_1 = \overline{\boldsymbol{\Psi}}_{5:1} &\\ &+ \left(\overline{\boldsymbol{\Psi}}_{5:1} \mathbf{A}_1 - \overline{\boldsymbol{\Psi}}_{5:2} \mathbf{A}_3 \overline{\boldsymbol{\Psi}}_1 \right) T_s \hat{d}_{1un} \\ &+ \left(\overline{\boldsymbol{\Psi}}_{5:3} \mathbf{A}_2 \overline{\boldsymbol{\Psi}}_{2:1} - \overline{\boldsymbol{\Psi}}_{5:2} \mathbf{A}_3 \overline{\boldsymbol{\Psi}}_1 \right) T_s \hat{d}_{2ln} \\ &+ \left(\overline{\boldsymbol{\Psi}}_{5:3} \mathbf{A}_2 \overline{\boldsymbol{\Psi}}_{2:1} - \overline{\boldsymbol{\Psi}}_{5:4} \mathbf{A}_3 \overline{\boldsymbol{\Psi}}_{3:1} \right) T_s \hat{d}_{2un} \\ &+ \left(\overline{\boldsymbol{\Psi}}_5 \mathbf{A}_1 \overline{\boldsymbol{\Psi}}_{4:1} - \overline{\boldsymbol{\Psi}}_{5:4} \mathbf{A}_3 \overline{\boldsymbol{\Psi}}_{3:1} \right) T_s \hat{d}_{1ln} \end{aligned} \tag{4.49}$$

Now attention is turned to the $\left(\mathbf{\Psi}_{5:2}\mathbf{S}_1\mathbf{b}_1+\mathbf{\Psi}_{5:3}\mathbf{S}_2\mathbf{b}_3+\mathbf{\Psi}_{5:4}\mathbf{S}_3\mathbf{b}_2+\mathbf{\Psi}_5\mathbf{S}_4\mathbf{b}_3+\mathbf{S}_5\mathbf{b}_1\right)$ matrix in (4.21) , which can be attacked component by component , but first to simplify the analysis the matrix is rearranged as,

$$\left(\mathbf{\Psi}_5\left(\mathbf{\Psi}_4\left(\mathbf{\Psi}_3\left(\mathbf{\Psi}_2\mathbf{S}_1\mathbf{b}_1+\mathbf{S}_2\mathbf{b}_3\right)+\mathbf{S}_3\mathbf{b}_2\right)+\mathbf{S}_4\mathbf{b}_3\right)+\mathbf{S}_5\mathbf{b}_1\right)$$

So starting with ,

$$\hat{\mathbf{\Psi}}_2\hat{\mathbf{S}}_1\mathbf{b}_1+\hat{\mathbf{S}}_2\mathbf{b}_3\approx\left[\overline{\mathbf{\Psi}}_2-\overline{\mathbf{\Psi}}_2\mathbf{A}_3T_s\hat{d}_{2ln}-\overline{\mathbf{\Psi}}_2\mathbf{A}_3T_s\hat{d}_{1un}\right]\left(\overline{\mathbf{S}}_1+\overline{\mathbf{\Psi}}_1T_s\hat{d}_{1un}\right)\mathbf{b}_1+\left(\overline{\mathbf{S}}_2-\overline{\mathbf{\Psi}}_2T_s\hat{d}_{2ln}-\overline{\mathbf{\Psi}}_2T_s\hat{d}_{1un}\right)\mathbf{b}_3$$

gives,

$$\begin{aligned}\hat{\mathbf{\Psi}}_2\hat{\mathbf{S}}_1\mathbf{b}_1+\hat{\mathbf{S}}_2\mathbf{b}_3\approx{}&\overline{\mathbf{\Psi}}_2\overline{\mathbf{S}}_1\mathbf{b}_1+\overline{\mathbf{S}}_2\mathbf{b}_3\\&+\left(\overline{\mathbf{\Psi}}_{2:1}\mathbf{b}_1-\overline{\mathbf{\Psi}}_2\mathbf{A}_3\overline{\mathbf{S}}_1\mathbf{b}_1-\overline{\mathbf{\Psi}}_2\mathbf{b}_3\right)T_s\hat{d}_{1un}\\&+\left(-\overline{\mathbf{\Psi}}_2\mathbf{A}_3\overline{\mathbf{S}}_1\mathbf{b}_1-\overline{\mathbf{\Psi}}_2\mathbf{b}_3\right)T_s\hat{d}_{2ln}\end{aligned}\tag{4.50}$$

and by continuing along this path ,

$$\begin{aligned}\hat{\mathbf{\Psi}}_3\left(\hat{\mathbf{\Psi}}_2\hat{\mathbf{S}}_1\mathbf{b}_1+\hat{\mathbf{S}}_2\mathbf{b}_3\right)+\hat{\mathbf{S}}_3\mathbf{b}_2={}&\overline{\mathbf{\Psi}}_{3:2}\overline{\mathbf{S}}_1\mathbf{b}_1+\overline{\mathbf{\Psi}}_3\overline{\mathbf{S}}_2\mathbf{b}_3+\overline{\mathbf{S}}_3\mathbf{b}_2\\&+\left(\overline{\mathbf{\Psi}}_{3:1}\mathbf{b}_1-\overline{\mathbf{\Psi}}_{3:2}\mathbf{A}_3\overline{\mathbf{S}}_1\mathbf{b}_1-\overline{\mathbf{\Psi}}_{3:2}\mathbf{b}_3\right)T_s\hat{d}_{1un}\\&+\left(-\overline{\mathbf{\Psi}}_{3:2}\mathbf{A}_3\overline{\mathbf{S}}_1\mathbf{b}_1-\overline{\mathbf{\Psi}}_{3:2}\mathbf{b}_3+\overline{\mathbf{\Psi}}_3\mathbf{A}_2\overline{\mathbf{\Psi}}_2\overline{\mathbf{S}}_1\mathbf{b}_1+\overline{\mathbf{\Psi}}_3\mathbf{A}_2\overline{\mathbf{S}}_2\mathbf{b}_3+\overline{\mathbf{\Psi}}_3\mathbf{b}_2\right)T_s\hat{d}_{2ln}\\&+\left(\overline{\mathbf{\Psi}}_3\mathbf{A}_2\overline{\mathbf{\Psi}}_2\overline{\mathbf{S}}_1\mathbf{b}_1+\overline{\mathbf{\Psi}}_3\mathbf{A}_2\overline{\mathbf{S}}_2\mathbf{b}_3+\overline{\mathbf{\Psi}}_3\mathbf{b}_2\right)T_s\hat{d}_{2un}\end{aligned}\tag{4.51}$$

and ,

$$\begin{aligned}
&\hat{\boldsymbol{\Psi}}_4\left(\hat{\boldsymbol{\Psi}}_3\left(\hat{\boldsymbol{\Psi}}_2\hat{\mathbf{S}}_1\mathbf{b}_1+\hat{\mathbf{S}}_2\mathbf{b}_3\right)+\hat{\mathbf{S}}_3\mathbf{b}_2\right)= \\
&\quad \overline{\boldsymbol{\Psi}}_{4:2}\overline{\mathbf{S}}_1\mathbf{b}_1+\overline{\boldsymbol{\Psi}}_{4:3}\overline{\mathbf{S}}_2\mathbf{b}_3+\overline{\boldsymbol{\Psi}}_4\overline{\mathbf{S}}_3\mathbf{b}_2 \\
&\quad +\left(\overline{\boldsymbol{\Psi}}_{4:1}\mathbf{b}_1-\overline{\boldsymbol{\Psi}}_{4:2}\mathbf{A}_3\overline{\mathbf{S}}_1\mathbf{b}_1-\overline{\boldsymbol{\Psi}}_{4:2}\mathbf{b}_3\right)T_s\hat{d}_{1un} \\
&\quad +\begin{pmatrix}-\overline{\boldsymbol{\Psi}}_{4:2}\mathbf{A}_3\overline{\mathbf{S}}_1\mathbf{b}_1-\overline{\boldsymbol{\Psi}}_{4:2}\mathbf{b}_3+\overline{\boldsymbol{\Psi}}_{4:3}\mathbf{A}_2\overline{\boldsymbol{\Psi}}_2\overline{\mathbf{S}}_1\mathbf{b}_1 \\ +\overline{\boldsymbol{\Psi}}_{4:3}\mathbf{A}_2\overline{\mathbf{S}}_2\mathbf{b}_3+\overline{\boldsymbol{\Psi}}_{4:3}\mathbf{b}_2\end{pmatrix}T_s\hat{d}_{2ln} \\
&\quad +\begin{pmatrix}\overline{\boldsymbol{\Psi}}_{4:3}\mathbf{A}_2\overline{\boldsymbol{\Psi}}_2\overline{\mathbf{S}}_1\mathbf{b}_1+\overline{\boldsymbol{\Psi}}_{4:3}\mathbf{A}_2\overline{\mathbf{S}}_2\mathbf{b}_3+\overline{\boldsymbol{\Psi}}_{4:3}\mathbf{b}_2 \\ -\overline{\boldsymbol{\Psi}}_4\mathbf{A}_3\overline{\boldsymbol{\Psi}}_{3:2}\overline{\mathbf{S}}_1\mathbf{b}_1-\overline{\boldsymbol{\Psi}}_4\mathbf{A}_3\overline{\boldsymbol{\Psi}}_3\overline{\mathbf{S}}_2\mathbf{b}_3 \\ -\overline{\boldsymbol{\Psi}}_4\mathbf{A}_3\overline{\mathbf{S}}_3\mathbf{b}_2\end{pmatrix}T_s\hat{d}_{2un}
\end{aligned} \tag{4.52}$$

So finally,

$$\begin{aligned}
&\hat{\boldsymbol{\Psi}}_5\left(\hat{\boldsymbol{\Psi}}_4\left(\hat{\boldsymbol{\Psi}}_3\left(\hat{\boldsymbol{\Psi}}_2\hat{\mathbf{S}}_1\mathbf{b}_1+\hat{\mathbf{S}}_2\mathbf{b}_3\right)+\hat{\mathbf{S}}_3\mathbf{b}_2\right)+\hat{\mathbf{S}}_4\mathbf{b}_3\right)+\hat{\mathbf{S}}_5\mathbf{b}_1= \\
&\quad \overline{\boldsymbol{\Psi}}_{5:2}\overline{\mathbf{S}}_1\mathbf{b}_1+\overline{\boldsymbol{\Psi}}_{5:3}\overline{\mathbf{S}}_2\mathbf{b}_3+\overline{\boldsymbol{\Psi}}_{5:4}\overline{\mathbf{S}}_3\mathbf{b}_2+\overline{\boldsymbol{\Psi}}_5\overline{\mathbf{S}}_4\mathbf{b}_3+\overline{\mathbf{S}}_5\mathbf{b}_1 \\
&\quad +\left(\overline{\boldsymbol{\Psi}}_{5:1}\mathbf{b}_1-\overline{\boldsymbol{\Psi}}_{5:2}\mathbf{A}_3\overline{\mathbf{S}}_1\mathbf{b}_1-\overline{\boldsymbol{\Psi}}_{5:2}\mathbf{b}_3\right)T_s\hat{d}_{1un} \\
&\quad +\begin{pmatrix}-\overline{\boldsymbol{\Psi}}_{5:2}\mathbf{A}_3\overline{\mathbf{S}}_1\mathbf{b}_1-\overline{\boldsymbol{\Psi}}_{5:2}\mathbf{b}_3+\overline{\boldsymbol{\Psi}}_{5:3}\mathbf{A}_2\overline{\boldsymbol{\Psi}}_2\overline{\mathbf{S}}_1\mathbf{b}_1 \\ +\overline{\boldsymbol{\Psi}}_{5:3}\mathbf{A}_2\overline{\mathbf{S}}_2\mathbf{b}_3+\overline{\boldsymbol{\Psi}}_{5:3}\mathbf{b}_2\end{pmatrix}T_s\hat{d}_{2ln} \\
&\quad +\begin{pmatrix}\overline{\boldsymbol{\Psi}}_{5:3}\mathbf{A}_2\overline{\boldsymbol{\Psi}}_2\overline{\mathbf{S}}_1\mathbf{b}_1+\overline{\boldsymbol{\Psi}}_{5:3}\mathbf{A}_2\overline{\mathbf{S}}_2\mathbf{b}_3 \\ +\overline{\boldsymbol{\Psi}}_{5:3}\mathbf{b}_2-\overline{\boldsymbol{\Psi}}_{5:4}\mathbf{A}_3\overline{\boldsymbol{\Psi}}_{3:2}\overline{\mathbf{S}}_1\mathbf{b}_1-\overline{\boldsymbol{\Psi}}_{5:4}\mathbf{A}_3\overline{\boldsymbol{\Psi}}_3\overline{\mathbf{S}}_2\mathbf{b}_3 \\ -\overline{\boldsymbol{\Psi}}_{5:4}\mathbf{A}_3\overline{\mathbf{S}}_3\mathbf{b}_2-\overline{\boldsymbol{\Psi}}_{5:4}\mathbf{b}_3\end{pmatrix}T_s\hat{d}_{2un} \\
&\quad +\begin{pmatrix}\overline{\boldsymbol{\Psi}}_5\mathbf{A}_1\overline{\boldsymbol{\Psi}}_{4:2}\overline{\mathbf{S}}_1\mathbf{b}_1+\overline{\boldsymbol{\Psi}}_5\mathbf{A}_1\overline{\boldsymbol{\Psi}}_{4:3}\overline{\mathbf{S}}_2\mathbf{b}_3 \\ +\overline{\boldsymbol{\Psi}}_5\mathbf{A}_1\overline{\boldsymbol{\Psi}}_4\overline{\mathbf{S}}_3\mathbf{b}_2+\overline{\boldsymbol{\Psi}}_5\mathbf{A}_1\overline{\mathbf{S}}_4\mathbf{b}_3{}^4+\overline{\boldsymbol{\Psi}}_5\mathbf{b}_1 \\ -\overline{\boldsymbol{\Psi}}_{5:4}\mathbf{A}_3\overline{\boldsymbol{\Psi}}_{3:2}\overline{\mathbf{S}}_1\mathbf{b}_1-\overline{\boldsymbol{\Psi}}_{5:4}\mathbf{A}_3\overline{\boldsymbol{\Psi}}_3\overline{\mathbf{S}}_2\mathbf{b}_3 \\ -\overline{\boldsymbol{\Psi}}_{5:4}\mathbf{A}_3\overline{\mathbf{S}}_3\mathbf{b}_2-\overline{\boldsymbol{\Psi}}_{5:4}\mathbf{b}_3\end{pmatrix}T_s\hat{d}_{1ln}
\end{aligned} \tag{4.53}$$

After finding the small signal forms for the two matrices in (4.21) its time now to apply small signal perturbation to that equation and cancel out small signal products,so,

$$\begin{aligned}\overline{\mathbf{X}}+\hat{\mathbf{x}}[n]&=\hat{\boldsymbol{\Psi}}_{5:1}\left(\overline{\mathbf{X}}+\hat{\mathbf{x}}[n]\right)\\&+\left(\hat{\boldsymbol{\Psi}}_{5:2}\hat{\mathbf{S}}_1\mathbf{b}_1+\hat{\boldsymbol{\Psi}}_{5:3}\hat{\mathbf{S}}_2\mathbf{b}_3+\hat{\boldsymbol{\Psi}}_{5:4}\hat{\mathbf{S}}_3\mathbf{b}_2+\hat{\boldsymbol{\Psi}}_5\hat{\mathbf{S}}_4\mathbf{b}_3+\hat{\mathbf{S}}_5\mathbf{b}_1\right)\left(\overline{\mathbf{U}}+\hat{\mathbf{u}}[n]\right)\end{aligned}\tag{4.54}$$

notice that $\overline{\mathbf{X}}[n+1]=\overline{\mathbf{X}}[n]=\overline{\mathbf{X}}$ is constant at steady state and the same can be said about the large signal component of the input to the model , substituting (4.49) and (4.53) into (4.54) and doing all the cancellations and removing all constant components gives the final form of the small signal discrete model,

$$\hat{\mathbf{x}}[n+1] = \overline{\boldsymbol{\Psi}}_{5:1}\hat{\mathbf{x}}[n]$$
$$+\left(\overline{\boldsymbol{\Psi}}_{5:2}\overline{\mathbf{S}}_1\mathbf{b}_1 + \overline{\boldsymbol{\Psi}}_{5:3}\overline{\mathbf{S}}_2\mathbf{b}_3 + \overline{\boldsymbol{\Psi}}_{5:4}\overline{\mathbf{S}}_3\mathbf{b}_2 + \overline{\boldsymbol{\Psi}}_5\overline{\mathbf{S}}_4\mathbf{b}_3 + \overline{\mathbf{S}}_5\mathbf{b}_1\right)\hat{\mathbf{u}}[n]$$

$$+\left[\left(\overline{\boldsymbol{\Psi}}_{5:1}\mathbf{A}_1 - \overline{\boldsymbol{\Psi}}_{5:2}\mathbf{A}_3\overline{\boldsymbol{\Psi}}_1\right)\overline{\mathbf{X}} + \begin{pmatrix}\overline{\boldsymbol{\Psi}}_{5:1}\mathbf{b}_1 - \overline{\boldsymbol{\Psi}}_{5:2}\mathbf{A}_3\overline{\mathbf{S}}_1\mathbf{b}_1 \\ -\overline{\boldsymbol{\Psi}}_{5:2}\mathbf{b}_3\end{pmatrix}\overline{\mathbf{U}}\right]T_s\hat{d}_{1un}$$

$$+\left[\left(\overline{\boldsymbol{\Psi}}_{5:3}\mathbf{A}_2\overline{\boldsymbol{\Psi}}_{2:1} - \overline{\boldsymbol{\Psi}}_{5:2}\mathbf{A}_3\overline{\boldsymbol{\Psi}}_1\right)\overline{\mathbf{X}} + \begin{pmatrix}-\overline{\boldsymbol{\Psi}}_{5:2}\mathbf{A}_3\overline{\mathbf{S}}_1\mathbf{b}_1 - \overline{\boldsymbol{\Psi}}_{5:2}\mathbf{b}_3 \\ +\overline{\boldsymbol{\Psi}}_{5:3}\mathbf{A}_2\overline{\boldsymbol{\Psi}}_2\overline{\mathbf{S}}_1\mathbf{b}_1 \\ +\overline{\boldsymbol{\Psi}}_{5:3}\mathbf{A}_2\overline{\mathbf{S}}_2\mathbf{b}_3 + \overline{\boldsymbol{\Psi}}_{5:3}\mathbf{b}_2\end{pmatrix}\overline{\mathbf{U}}\right]T_s\hat{d}_{2ln}$$

$$+\left[\left(\overline{\boldsymbol{\Psi}}_{5:3}\mathbf{A}_2\overline{\boldsymbol{\Psi}}_{2:1} - \overline{\boldsymbol{\Psi}}_{5:4}\mathbf{A}_3\overline{\boldsymbol{\Psi}}_{3:1}\right)\overline{\mathbf{X}} + \begin{pmatrix}\overline{\boldsymbol{\Psi}}_{5:3}\mathbf{A}_2\overline{\boldsymbol{\Psi}}_2\overline{\mathbf{S}}_1\mathbf{b}_1 + \overline{\boldsymbol{\Psi}}_{5:3}\mathbf{A}_2\overline{\mathbf{S}}_2\mathbf{b}_3 \\ +\overline{\boldsymbol{\Psi}}_{5:3}\mathbf{b}_2 - \overline{\boldsymbol{\Psi}}_{5:4}\mathbf{A}_3\overline{\boldsymbol{\Psi}}_{3:2}\overline{\mathbf{S}}_1\mathbf{b}_1 \\ -\overline{\boldsymbol{\Psi}}_{5:4}\mathbf{A}_3\overline{\boldsymbol{\Psi}}_3\overline{\mathbf{S}}_2\mathbf{b}_3 \\ -\overline{\boldsymbol{\Psi}}_{5:4}\mathbf{A}_3\overline{\mathbf{S}}_3\mathbf{b}_2 - \overline{\boldsymbol{\Psi}}_{5:4}\mathbf{b}_3\end{pmatrix}\overline{\mathbf{U}}\right]T_s\hat{d}_{2un}$$

$$+\left[\left(\overline{\boldsymbol{\Psi}}_5\mathbf{A}_1\overline{\boldsymbol{\Psi}}_{4:1} - \overline{\boldsymbol{\Psi}}_{5:4}\mathbf{A}_3\overline{\boldsymbol{\Psi}}_{3:1}\right)\overline{\mathbf{X}} + \begin{pmatrix}\overline{\boldsymbol{\Psi}}_5\mathbf{A}_1\overline{\boldsymbol{\Psi}}_{4:2}\overline{\mathbf{S}}_1\mathbf{b}_1 + \overline{\boldsymbol{\Psi}}_5\mathbf{A}_1\overline{\boldsymbol{\Psi}}_{4:3}\overline{\mathbf{S}}_2\mathbf{b}_3 \\ +\overline{\boldsymbol{\Psi}}_5\mathbf{A}_1\overline{\boldsymbol{\Psi}}_4\overline{\mathbf{S}}_3\mathbf{b}_2 + \overline{\boldsymbol{\Psi}}_5\mathbf{A}_1\overline{\mathbf{S}}_4\mathbf{b}_3 \\ +\overline{\boldsymbol{\Psi}}_5\mathbf{b}_1 - \overline{\boldsymbol{\Psi}}_{5:4}\mathbf{A}_3\overline{\boldsymbol{\Psi}}_{3:2}\overline{\mathbf{S}}_1\mathbf{b}_1 \\ -\overline{\boldsymbol{\Psi}}_{5:4}\mathbf{A}_3\overline{\boldsymbol{\Psi}}_3\overline{\mathbf{S}}_2\mathbf{b}_3 \\ -\overline{\boldsymbol{\Psi}}_{5:4}\mathbf{A}_3\overline{\mathbf{S}}_3\mathbf{b}_2 - \overline{\boldsymbol{\Psi}}_{5:4}\mathbf{b}_3\end{pmatrix}\overline{\mathbf{U}}\right]T_s\hat{d}_{1ln}$$

(4.55)

Although the small signal model here looks more complex than the one developed in chapter 3 , there is a certain symmetry to it that can be exploited when implementing it in a simulation or linear algebra package. With the arrival at the small signal discrete model with no impulse function approximation this chapter is concluded.

CHAPTER 5

APPLICATION OF DISCRETE MODELING METHOD TO THE HALF-BRIDGE DC/DC TOPOLOGY WITH CURRENT DOUBLER

5.1 Overview of Half-Bridge topology with three main control method

Established control techniques for the Half-Bridge DC/DC power converter are the symmetric and asymmetric (complimentary). While asymmetric control achieves ZVS conditions for converter switches its disadvantages are unbalanced component stresses and the existence of a nonzero DC magnetizing current in the isolation transformer, which increases the risk of transformer saturation and generally has a detrimental effect on the dynamics of the converter. A new control method called DCS PWM (Duty-Cycle Shifted) was proposed in [7] to achieve ZVS for at least one of the Half-Bridge switches , this control method is derived from symmetric control and entails switching S2 almost instantly after S1 turns off (see figure 5-1a). Of course meeting ZVS conditions is desirable because it allows the converter to operate at higher switching frequencies with greater efficiencies. Thus arises the need to accurately close the loop on this topology to meet design specifications, but as was stated in the introduction to this Thesis conventional averaging methods for dynamic modeling yield models that are inaccurate at the upper frequency range because they ignore the sampled nature of the Duty Cycle signals that

drive the power stage. Further more they predict frequency response content at higher than half the switching frequency,

5.2 State-Space representation of Modes of the Half-Bridge DC/DC topology with current doubler

Figure 5-1 shows the typical Half-Bridge topology and its three main modes of operation , Mode III being the freewheeling mode. All parasitics for the output filter and half-bridge capacitors are included. The system can be represented in piecewise state-space form as shown in the chapter 2 of this thesis and the parameters of the discrete model for the different control schemes are shown in Table 5-1, which shows the appropriate substitution of the parameters in equation (3.32)

Table 5-1 : Model parameter sunstitution for each control scheme

Symmetric	$\alpha = \frac{1 - D_1 - D_2}{2}$	$D_2 = D_1$
Asymmetric	$\alpha = 0$	$D_2 = 1 - D_1$
DCS	$\alpha = 0$	$D_2 = D_1$

So the first step now for applying the small signal model in chapter 3 is to find the A and b matrices for all the modes of operations , not forgetting of course to define the states. This is done in (5.1) till (5.7) shown below,

$$\hat{\mathbf{x}}^T = \begin{bmatrix} \hat{v}_{c1} & \hat{v}_{c2} & \hat{i}_{Lm} & \hat{i}_{L1} & \hat{i}_{L2} & \hat{v}_{co} \end{bmatrix} \tag{5.1}$$

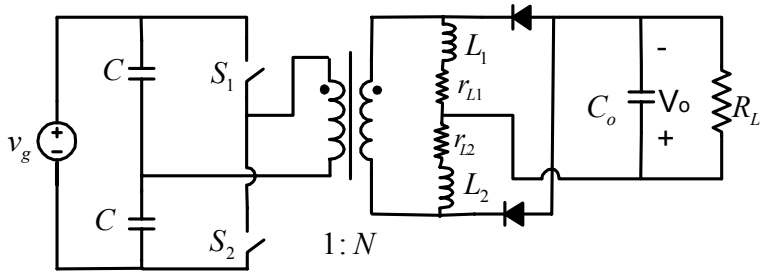

(a)

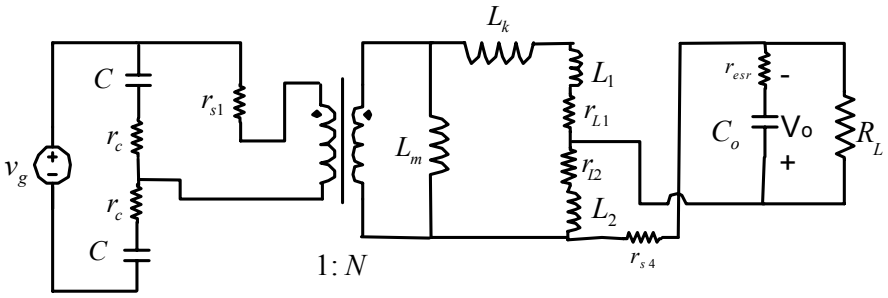

(b)

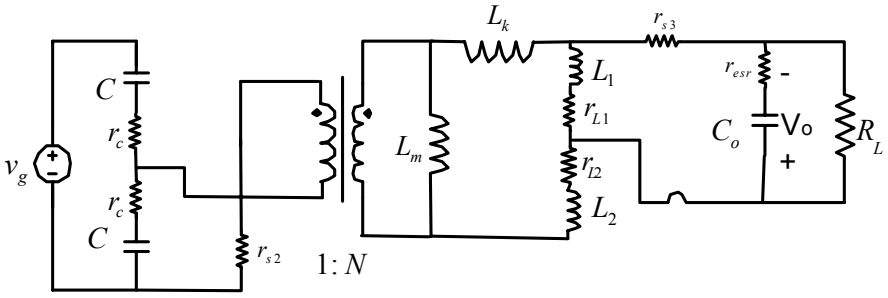

(c)

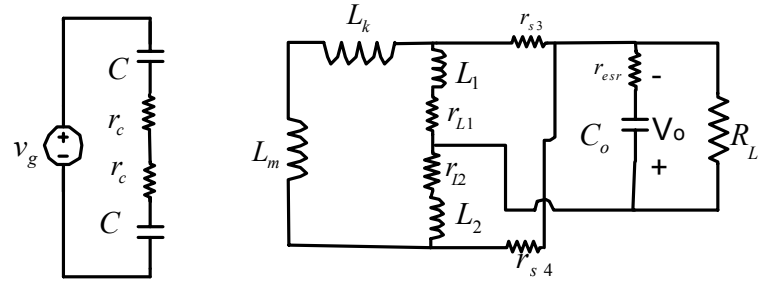

(d)

Figure 5-1: (a) Isolated Half-Bridge Converter, (b) Mode I (S1 on, S2 off), (b) Mode II (S1 off, S2 on), (c) Mode III (S1 off, S2 off)

$$\mathbf{b_1}^T = \begin{bmatrix} \frac{1}{2Cr_c} & \frac{1}{2Cr_c} & \frac{N}{2L_m} & \frac{N}{2\left(L_k + L_1\right)} & 0 & 0 \end{bmatrix} \tag{5.2}$$

$$\mathbf{b_2}^T = \begin{bmatrix} \frac{1}{2Cr_c} & \frac{1}{2Cr_c} & \frac{-N}{2L_m} & 0 & \frac{-N}{2\left(L_k + L_2\right)} & 0 \end{bmatrix} \tag{5.3}$$

$$\mathbf{b_3}^T = \begin{bmatrix} \frac{1}{2Cr_c} & \frac{1}{2Cr_c} & 0 & 0 & 0 & 0 \end{bmatrix} \tag{5.4}$$

and,

$$\mathbf{A_1} = \begin{bmatrix} \frac{-1}{2Cr_c} & \frac{-1}{2Cr_c} & \frac{-N}{2C} & \frac{-N}{2C} & 0 & 0 \\ \frac{-1}{2Cr_c} & \frac{-1}{2Cr_c} & \frac{N}{2C} & \frac{N}{2C} & 0 & 0 \\ \frac{N}{L_m} & \frac{-N}{L_m} & \frac{-\alpha_1}{2L_m} & \frac{-\alpha_1}{2L_m} & 0 & 0 \\ \frac{N}{2\left(L_k + L_1\right)} & \frac{-N}{2\left(L_k + L_1\right)} & \frac{-\alpha_1}{2\left(L_k + L_1\right)} & \frac{-\left(r_{L1} + \beta_4 + \frac{\alpha_1}{2}\right)}{L_k + L_1} & \frac{\beta_4}{L_k + L_1} & \frac{r_{esr} \| R_L}{r_{esr}\left(L_k + L_1\right)} \\ 0 & 0 & 0 & \frac{\beta_4}{L_2} & \frac{-\left(r_{L2} + \beta_4\right)}{L_2} & \frac{-\left(r_{esr} \| R_L\right)}{r_{esr} L_2} \\ 0 & 0 & 0 & \frac{-\left(r_{esr} \| R_L\right)}{r_{esr} C_o} & \frac{r_{esr} \| R_L}{r_{esr} C_o} & \frac{-1}{C_o\left(r_{esr} + R_L\right)} \end{bmatrix} \tag{5.5}$$

$$\mathbf{A_2} = \begin{bmatrix} \frac{-1}{2Cr_c} & \frac{-1}{2Cr_c} & \frac{-N}{2C} & 0 & \frac{-N}{2C} & 0 \\ \frac{-1}{2Cr_c} & \frac{-1}{2Cr_c} & \frac{N}{2C} & 0 & \frac{N}{2C} & 0 \\ \frac{N}{L_m} & \frac{-N}{L_m} & \frac{-\alpha_2}{2L_m} & 0 & \frac{-\alpha_1}{2L_m} & 0 \\ 0 & 0 & 0 & \frac{-(r_{L1}+\beta_3)}{L_1} & \frac{\beta_3}{L_1} & \frac{r_{esr}\|R_L}{r_{esr}L_1} \\ \frac{N}{2(L_k+L_2)} & \frac{-N}{2(L_k+L_2)} & \frac{-\alpha_2}{2(L_k+L_2)} & \frac{\beta_3}{L_k+L_2} & \frac{-\left(r_{L2}+\beta_3+\frac{\alpha_2}{2}\right)}{L_k+L_2} & \frac{-(r_{esr}\|R_L)}{r_{esr}(L_k+L_2)} \\ 0 & 0 & 0 & \frac{-(r_{esr}\|R_L)}{r_{esr}C_o} & \frac{r_{esr}\|R_L}{r_{esr}C_o} & \frac{-1}{C_o(r_{esr}+R_L)} \end{bmatrix} \tag{5.6}$$

$$\mathbf{A_3} = \begin{bmatrix} \frac{-1}{2Cr_c} & \frac{-1}{2Cr_c} & 0 & 0 & 0 & 0 \\ \frac{-1}{2Cr_c} & \frac{-1}{2Cr_c} & 0 & 0 & 0 & 0 \\ 0 & 0 & \frac{-(r_{s3}+r_{s4})}{L_m+L_k} & \frac{-r_{s3}}{L_m+L_k} & \frac{-r_{s4}}{L_m+L_k} & 0 \\ 0 & 0 & \frac{-r_{s3}}{L_1} & \frac{-(r_{L1}+\beta_3)}{L_1} & \frac{r_{esr}\|R_L}{L_1} & \frac{r_{esr}\|R_L}{r_{esr}L_1} \\ 0 & 0 & \frac{-r_{s4}}{L_2} & \frac{r_{esr}\|R_L}{L_2} & \frac{-(r_{L2}+\beta_4)}{L_2} & \frac{-(r_{esr}\|R_L)}{r_{esr}L_2} \\ 0 & 0 & 0 & \frac{-(r_{esr}\|R_L)}{r_{esr}C_o} & \frac{r_{esr}\|R_L}{r_{esr}C_o} & \frac{-1}{C_o(r_{esr}+R_L)} \end{bmatrix} \tag{5.7}$$

where,

$$\alpha_n = N^2(2r_{sn}+r_c) \tag{5.8}$$

$$\beta_n = r_{sn} + \left(r_{esr}\|R_L\right) \tag{5.9}$$

All constants in the previous definitions are referenced in figure 5-1.

5.3 Application of Chapter 3 small-signal model to the Half-Bridge DC/DC topology with current doubler

To demonstrate the model developed in this thesis in chapter 3, parameters will be taken from a prototype Half-Bridge converter with current doubler that was built in the lab. It had the following components and parameters,

$$Vin=48\ v\ ,\ Vo=1\ v\ ,\ Io=20\ A\ ,\ Fs=400\ KHz$$

$$L_1=L_2=180nH\ ,\ C_o=500\mu F\ ,\ r_{esr}=0.66m\Omega\ ,\ Lm=36\ \mu H$$

$$r_{L1}=r_{L2}=5e\text{-}3\ ,\ L_k=3.125nH\ ,\ N=1/6\ ,\ r_c=10m\Omega$$

$$r_{s1}=25\ m\Omega\ ,\ r_{s2}=25\ m\Omega\ ,\ r_{s3}=3\ m\Omega\ ,\ r_{s4}=3\ m\Omega;$$

The first step in applying the model is getting the steady-state waveforms, which can be done using MATLAB as shown in the sample code in section (2.7) . Figures (5-2) till (5-4) shows the results from running this code. The results of the harmonic analysis are verified for the asymmetric case by the simplorer simulation shown in Figure 5-5. After finding the waveforms they are utilized in evaluating the $\mathbf{\Delta_1}\left[\left(n+D_1\right)T_s\right]$, $\mathbf{\Delta_2}\left[\left(n+D_1+\alpha\right)T_s\right]$, $\mathbf{\Delta_2}\left[\left(n+D_1+\alpha+D_2\right)T_s\right]$ and $\mathbf{\Delta_1}\left[\left(n+1\right)T_s\right]$ matrices (or vectors depending on the number of inputs) in (2.32). Code II gives an example of how MATLAB can programmed with the discrete model. The resulting frequency response of the model is shown in figure 5-6. Figure 5-7 compare the frequency response obtained from the discrete model with the one obtained from the classical average model.

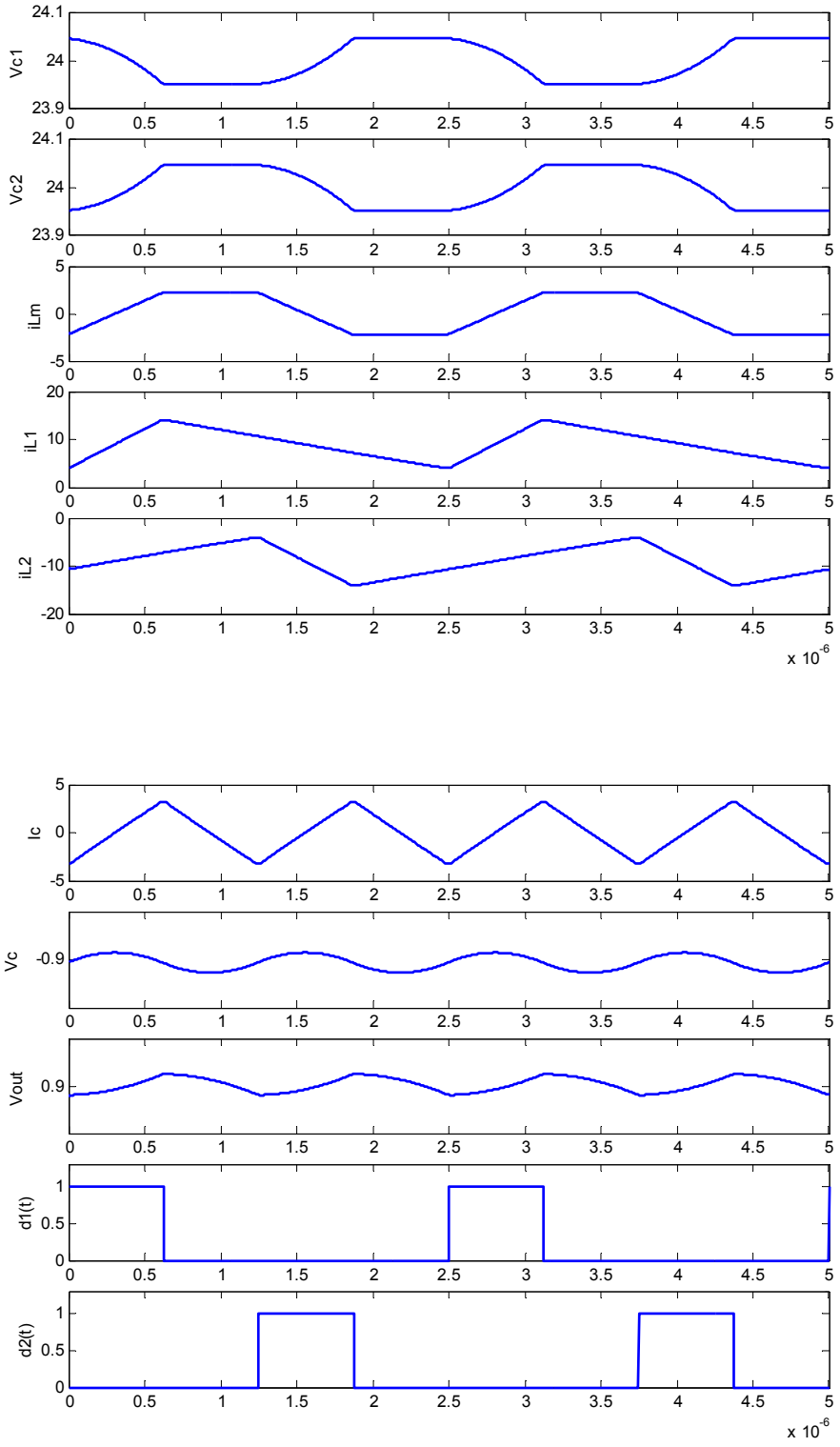

Figure 5-2 :HB DC/DC steady-state waveforms for symmetric control

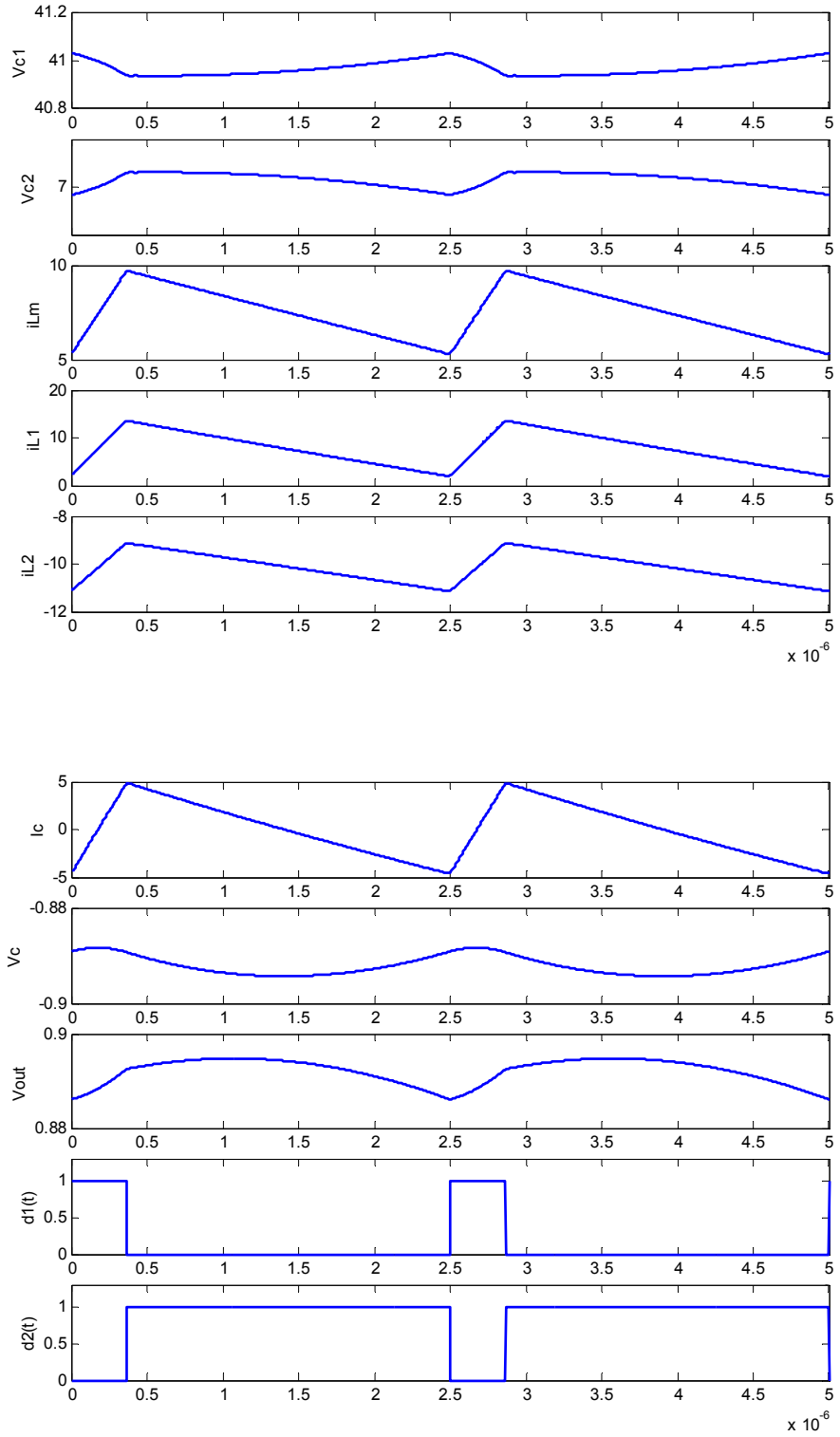

Figure 5-3 :HB DC/DC steady-state waveforms for asymmetric control

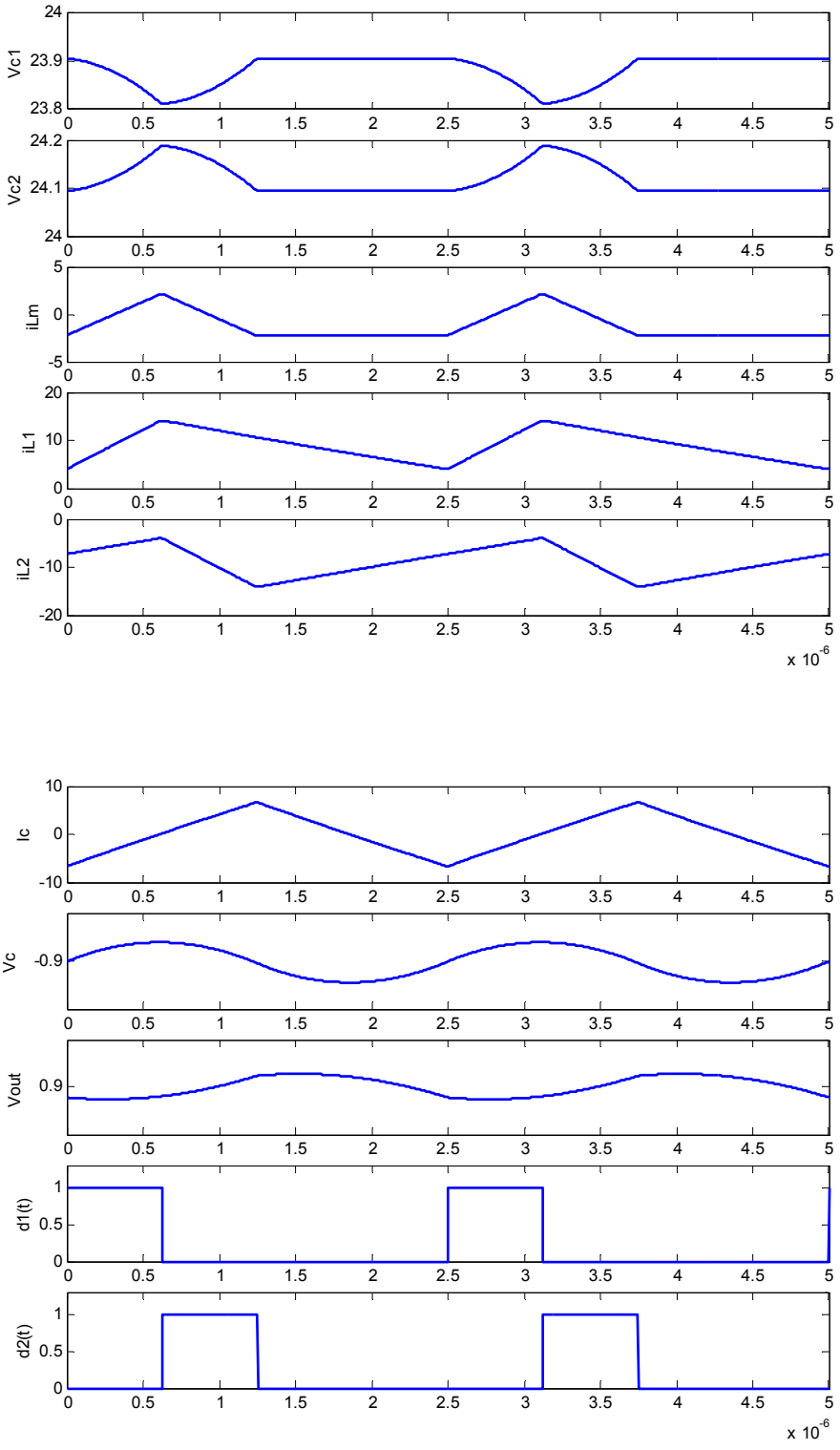

Figure 5-4 :HB DC/DC steady-state waveforms for DCS control

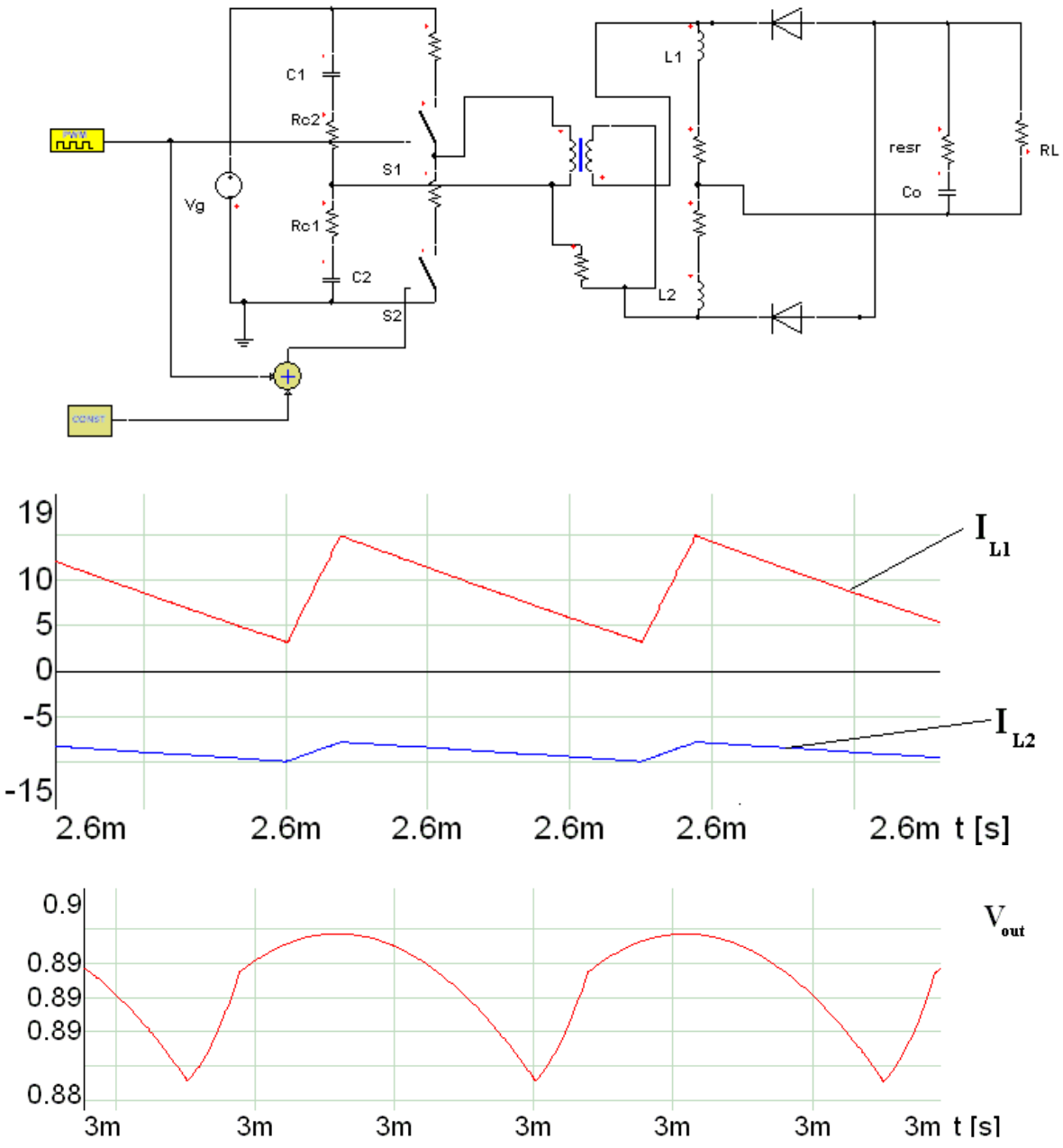

Figure 5-5 : Simplorer Simulation of the Asymmetric Control case

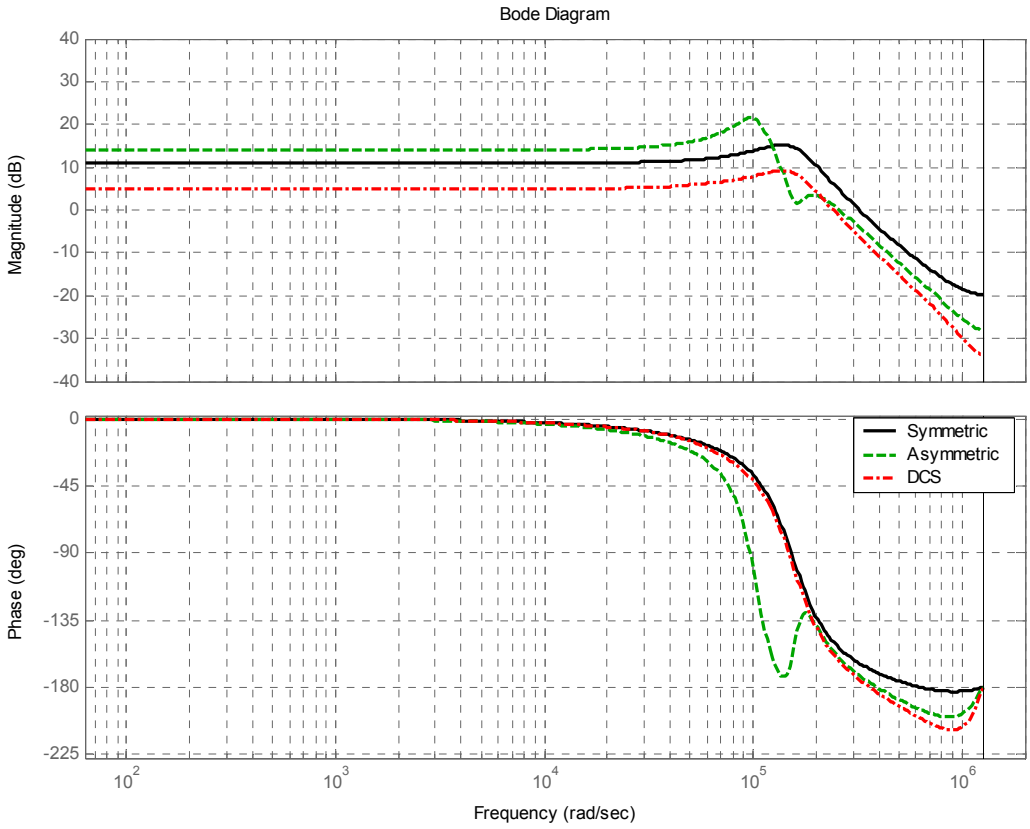

Figure 5-6 : Frequency Responce for HB DC/DC example for Symmetric , Asymmetric and DCS control respectively

Code II : Matlab Script to implement Discrete Model

```
clear all; close all; clc;

%Converter parameters and component values

a=1./64;        Vg=48;          Vo=1;
Io=20;          Fs=400e3;       Ts=1./Fs;
L1=180e-9;      L2=180e-9;      rL1=5e-3;
rL2=5e-3;       Co=500e-6;      resr=0.66e-3;
Lm=36e-6*a;     Lk=200e-9*a;    N=1/6;
RL=Vo/Io;       resrpRL=RL.*resr./(RL+resr);
rc=10e-3;       C=5e-6;         rs1=25e-3;
rs2=25e-3;      rs3=3e-3;       rs4=3e-3;

A1=[-1./(2.*C.*rc)  -1./(2.*C.*rc) ...
   -N./(2.*C)  -N./(2.*C)   0   0 ];
A1=[A1 ; -1./(2.*C.*rc)  -1./(2.*C.*rc) ...
   N./(2.*C)  N./(2.*C)   0   0 ];
A1=[A1 ; N./(2.*Lm) -N./(2.*Lm) ...
       -(N.^2).*(2.*rs1+rc)./2./Lm ...
       -(N.^2).*(2.*rs1+rc)./2./Lm   0   0];
A1=[A1 ; N./2./(Lk+L1)  -N./2./(Lk+L1) ...
       -(N.^2).*(2.*rs1+rc)./2./(Lk+L1)  ...
   -(rL1+rs4+resrpRL+(N.^2).*(2.*rs1+rc)./2)./(Lk+L1)...
   (rs4+resrpRL)./(Lk+L1)  resrpRL./resr./(Lk+L1)];
A1=[A1 ; 0 0 0  (rs4+resrpRL)./L2  ...
       -(rL2+rs4+resrpRL)./L2  -resrpRL./resr./L2 ];
A1=[A1 ; 0 0 0 -resrpRL./resr./Co  ...
       resrpRL./resr./Co   -1./Co./(resr+RL)];
b1=[1./(2.*C.*rc) ; 1./(2.*C.*rc) ; ...
       N./(2.*Lm)  ; N./2./(Lk+L1) ; 0 ; 0];

A2=[-1./(2.*C.*rc)  -1./(2.*C.*rc)...
       -N./(2.*C) 0  -N./(2.*C)  0 ];
A2=[A2; -1./(2.*C.*rc)  -1./(2.*C.*rc) ...
       N./(2.*C)   0  N./(2.*C)    0 ];
A2=[A2 ; N./(2.*Lm) -N./(2.*Lm) ...
       -(N.^2).*(2.*rs2+rc)./2./Lm   0 ...
       -(N.^2).*(2.*rs2+rc)./2./Lm   0 ];
A2=[A2; 0 0 0  -(rL1+rs3+resrpRL)./L1 ...
       (rs3+resrpRL)./L1     resrpRL./resr./L1 ];
A2=[A2;  N./2./(Lk+L2)  -N./2./(Lk+L2)  ...
       -(N.^2).*(2.*rs2+rc)./2./(Lk+L2) ...
   (rs3+resrpRL)./(Lk+L2) ...
   -(rL2+rs3+resrpRL+(N.^2).*(2.*rs2+rc)./2)./(Lk+L2) ...
   -resrpRL./resr./(Lk+L2)];
A2=[A2;  0 0 0 -resrpRL./resr./Co  ...
       resrpRL./resr./Co   -1./Co./(resr+RL)];

b2=[1./(2.*C.*rc) ; 1./(2.*C.*rc) ; ...
       -N./(2.*Lm)  ; 0 ;  -N./2./(Lk+L2)  ; 0];
```

```
A3=[-1./(2.*C.*rc)  -1./(2.*C.*rc) 0 0 0 0];
A3=[A3 ; -1./(2.*C.*rc)  -1./(2.*C.*rc) 0 0 0 0 ];
A3=[A3 ; 0 0 -(rs3+rs4)./(Lm+Lk) ...
      -rs3./(Lm+Lk) -rs4./(Lm+Lk) 0];
A3=[A3; 0 0 -rs3./L1 -(rL1+rs3+resrpRL)./L1 ...
      resrpRL./L1 resrpRL./resr./L1];
A3=[A3; 0 0 -rs4./L2  resrpRL./L2 ...
      -(rL2+rs4+resrpRL)./L2   -resrpRL./resr./L2];
A3=[A3;  0 0 0 -resrpRL./resr./Co  ...
      resrpRL./resr./Co   -1./Co./(resr+RL)];

b3=[1./(2.*C.*rc) ; 1./(2.*C.*rc)  ;  0  ; 0 ; 0  ; 0];

%Sym
D1=2.*Vo./N./Vg;
al=0; D2=D1;

% Asym
% D1=0.5-((1-4.*Vo./N./Vg).^0.5)./2;
% D2=1-D1;  al=0;

% DCS
% D2=D1;  al=0;

t=D1.*Ts;
[x1,sscoef]=SteadyStatesim(D1,D2,al,Ts,A1,A2,A3,b1,b2,b3,1,Vg,20,t);
t=(D1+al).*Ts;
[x2,sscoef]=SteadyStatesim(D1,D2,al,Ts,A1,A2,A3,b1,b2,b3,1,Vg,20,t);
t=(D1+al+D2).*Ts;
[x3,sscoef]=SteadyStatesim(D1,D2,al,Ts,A1,A2,A3,b1,b2,b3,1,Vg,20,t);
t=Ts;
[x4,sscoef]=SteadyStatesim(D1,D2,al,Ts,A1,A2,A3,b1,b2,b3,1,Vg,20,t);

x1=real(x1); x2=real(x2);
x3=real(x3); x4=real(x4);

delta1=(b1-b3)*Vg-(A1-A3)*x1; delta2=(b2-b3)*Vg-(A2-A3)*x2;
delta3=(b2-b3)*Vg-(A2-A3)*x3; delta4=(b1-b3)*Vg-(A1-A3)*x4;

lambda1=expm(al.*A3.*Ts); lambda2=expm(D2.*A2.*Ts);
lambda3=expm((1-D1-D2-al).*A3.*Ts); lambda4=expm(D1.*A1.*Ts);
lambda41=lambda4*lambda3*lambda2*lambda1;
lambda42=lambda4*lambda3*lambda2;
lambda43=lambda4*lambda3;

Ad=lambda41;
bd=Ts.*[lambda41*delta1 lambda42*delta2 lambda43*delta3 ...
      lambda4*delta4]*[0.5 ; 0 ; 0 ; 0.5];
dd=0;

HBf=ss(Ad,bd,cd,dd,Ts);
```

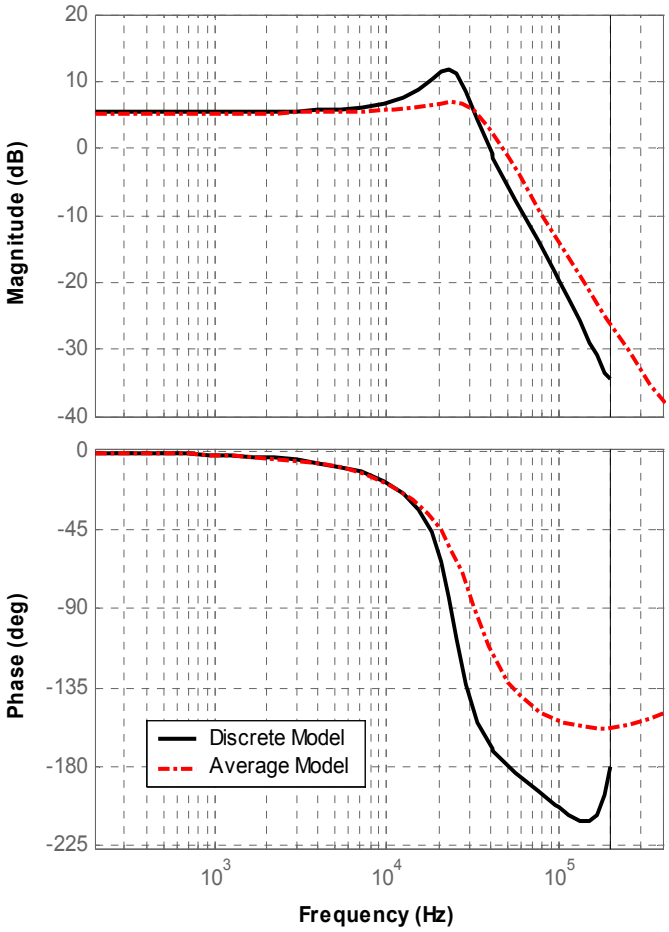

Figure 5-7 : Comparison between the Average Model and the Discrete Model for DCS control

5.4 Application of Chapter 4 Large-signal model to the Half-Bridge DC/DC topology with current doubler

The Large signal model represented by equation (4.21) is applied to the Half Bridge topology with parameters introduced in section 3. If a pulsating input is applied to it (for demonstration purposes) then the output of the model for DCS and Symmetric control is as shown in figure (5-8), while figure (5-9) is for Asymmetric control.

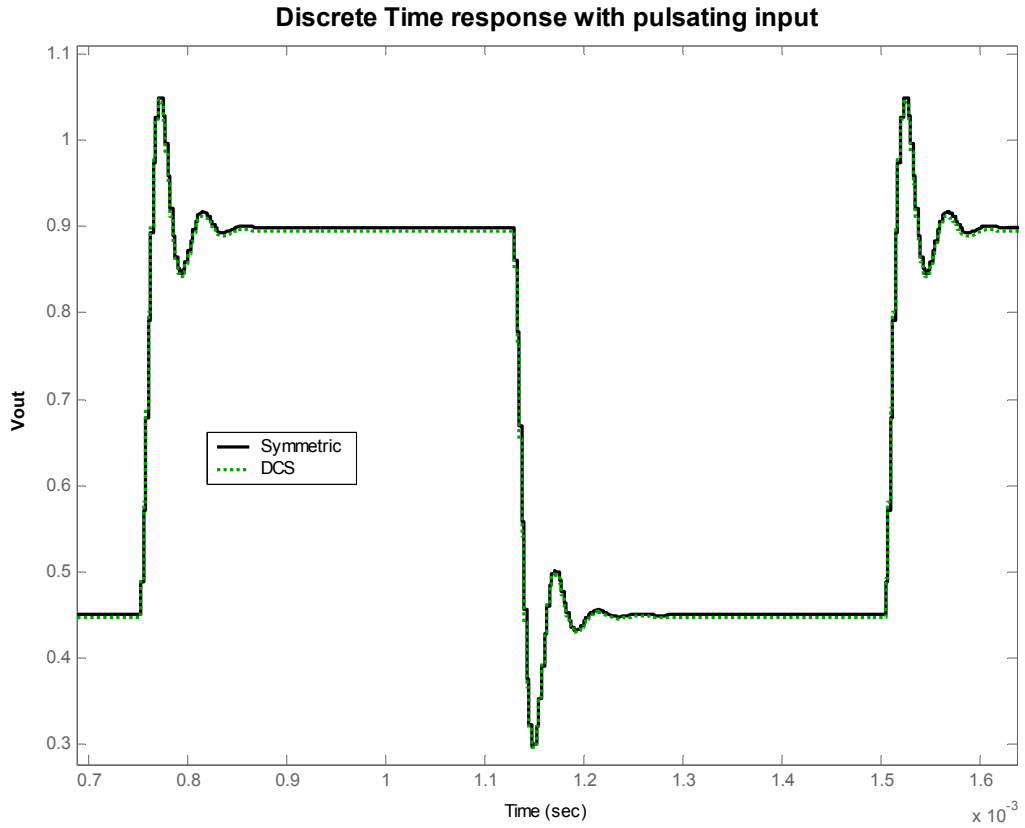

Figure 5-8 : Application of Large Signal model to HB DC/DC topology for Symmetric and DCS control respectively

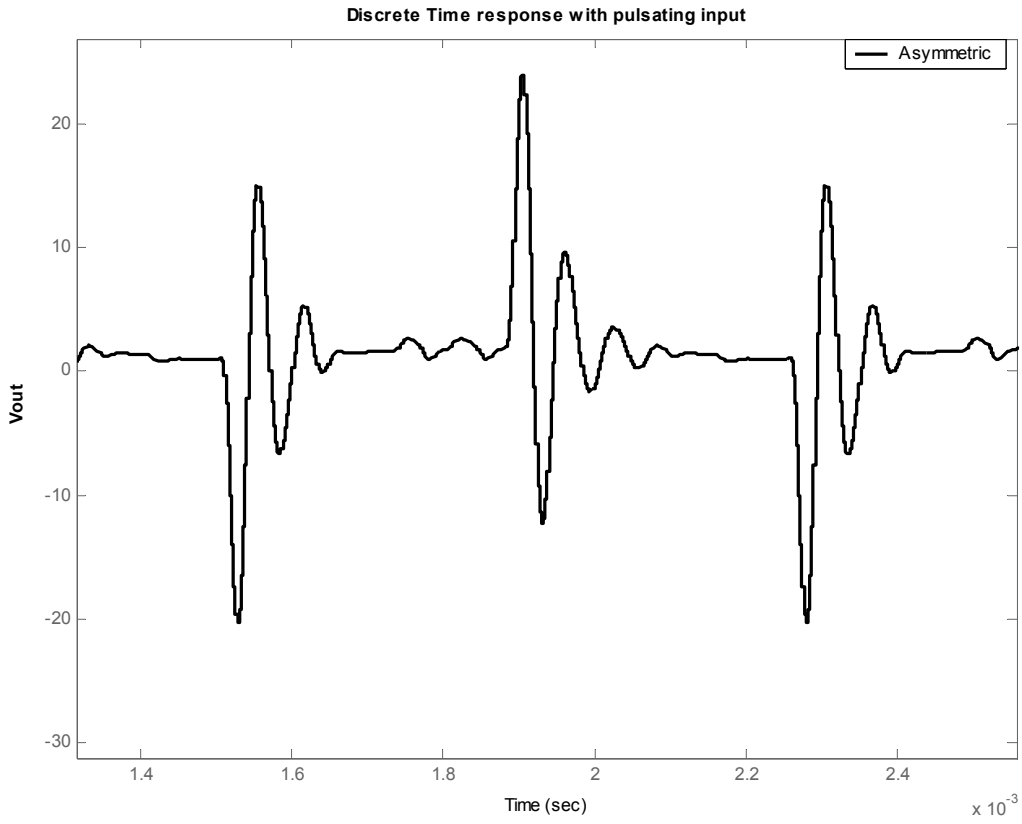

Figure 5-9 : Application of Large Signal model to HB DC/DC topology for Asymmetric control

It is apparent that Asymmetric control is the least stable control method for the Half-Bridge Topology as seen in figure (5-9) and as can be deduced from the smaller gain and phase margins in figure (5-6)

5.5 Comparison with an experimental prototype

An experimental lab prototype of a DCS controlled half-bridge Topology was used to compare with the derived models in chapter 3 and chapter 4. That pulse transfer function of the Discrete model of the converter in this case turns out to be,

$$\frac{\hat{v}_o(z)}{c(z)} = \frac{0.1542z^2 - 0.05593z - 0.08207}{z^3 - 2.633z^2 + 2.416z - 0.7744} \tag{5.10}$$

The frequency response is simply obtained by substituting $z=e^{jwTs}$. And from that frequency response (the one shown in figure 5-6 for DCS) one can design an appropriate compensator to improve the dynamics of the converter and maintain stability in closed loop. This compensator is found to be,

$$\frac{c(z)}{\hat{v}_o(z)} = \frac{2.065z^3 - 0.9179z^2 - 1.97z + 1.013}{z^3 - 0.1969z^2 - 0.6427z - 0.1604} \tag{5.11}$$

The built laboratory prototype with the compensator in (5.11) had its closed loop frequency response (power stage with compensator) examined with a frequency analyzer for verification purposes. The results of the comparison between the experimental and theoretical frequency responses are plotted in Figure 5-10 and show a very high correspondence from 1 KHz till Fs/2.

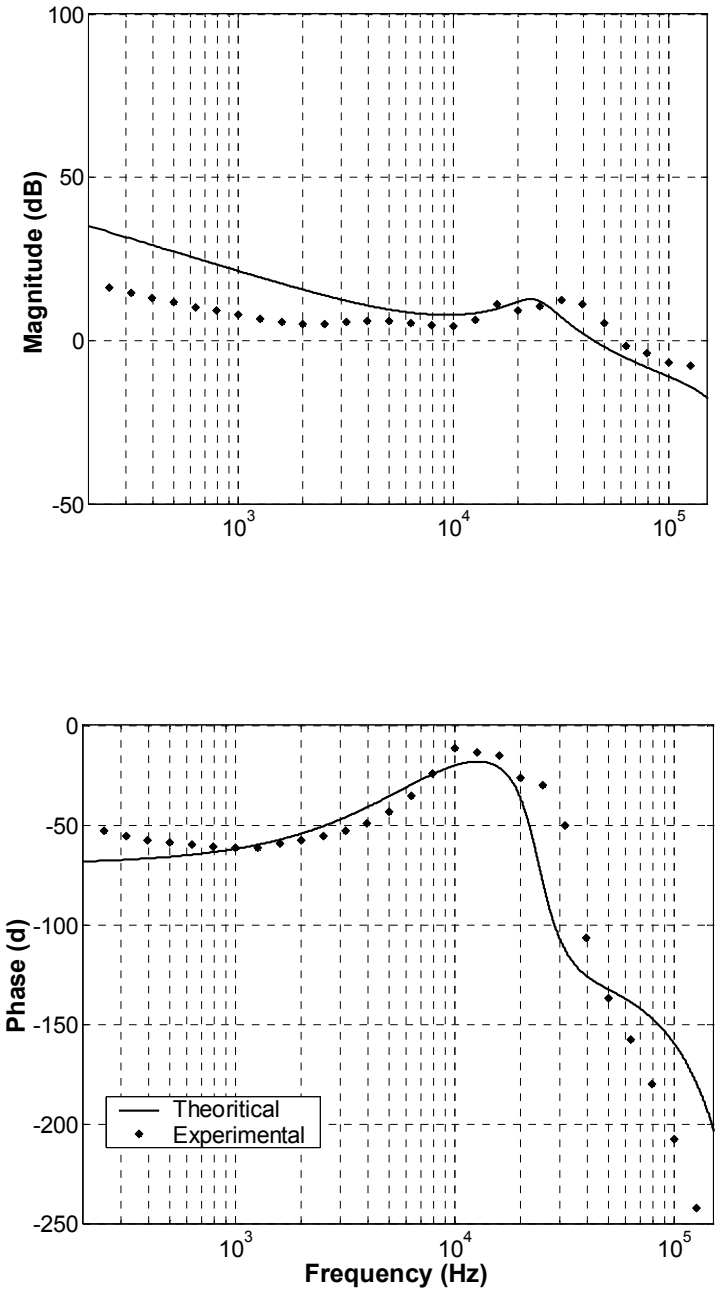

Figure 5-10 : Comparison of Closed loop frequency response between experiment and theory

It is worth noting that the Discrete model which was presented in state-space form is more adequate for direct design in the case where a digital controller is implemented, and it surpasses the continuous average models in accuracy at the higher frequency range. This last property is crucial for converters operating at high switching frequencies where modeling errors affect the robustness of the closed loop. Additionally the main reason discrete models are a more natural choice for switching converters is due to the fact that they are driven by discrete duty ratio modulations, so the sample and hold effect are implicitly included. As seen on the plots in (5-6) the measured phase at the higher frequencies has a large deviation from analog model predictions, which means if such a system was to be compensated depending on the continuous model, there would have been a high risk of instability, or at best lower transient performance than expected.

CHAPTER 6

IMPLEMENTATION OF DISCRETE MODEL IN A GUI FOR CONTROLLER DESIGN USING MATLAB

6.1 Overview of GUI platform

The purpose of this chapter is to review a GUI platform developed in MATLAB to aid controller design. Essentially this platform is a GUI wrapper for the discrete models developed in this thesis. Figures 6-1 till 6-6 show the main windows of the platform.

Starting with the main window shown in Figure 6-1 , the various numbered components are,

1. The topology popup list : many topologies with different control schemes are available here.
2. View Parameters Button : opens the window shown in Figure 6-2 were the converter circuit parameter can be entered.
3. Compensator Frame : this frame contains sliders and edit boxes that are used to specify the dynamics of the compensator used in terms of its poles or zero. A compensator with up to twelve poles and zeros with an integrator can be entered. Also ,the switching frequency and the compensator DC gain can be entered here.
4. Magnitude of Frequency Response.

5. Phase of Frequency Response.
6. Bode Plot Frame : contains checkboxes than when chosen causes the platform to plot the open loop , plant , compensator or closed loop frequency responses. More than one frequency response can be plotted at the same time.
7. Difference Equation Coefficients Button : this button gives the coefficients of the digital compensator equivalent to the compensator specified in the compensator frame (number 3)
8. Transfer Functions Button : this button gives the various continuous and discrete transfer functions of the compensator at hand.

Other functions can be accessed through the main window menu. For example there are menu items for saving and loading parameters and compensator data. Also the tools menu provides access to the time response window shown in Figure 6-3 , this window gives the closed loop response under step load conditions were the slew rate of the load step can be specified. Another tools menu item is the parameter sweep that opens the window of Figure 6-4 , in this window any parameter of the circuit can be swept across a defined range to observe the parameters effect on the frequency response. The root locus item produces the root locus of the closed loop of the system, and finally , the Steady-State ripple item calculates the steady-state waveforms utilizing the analysis described in chapter 2.

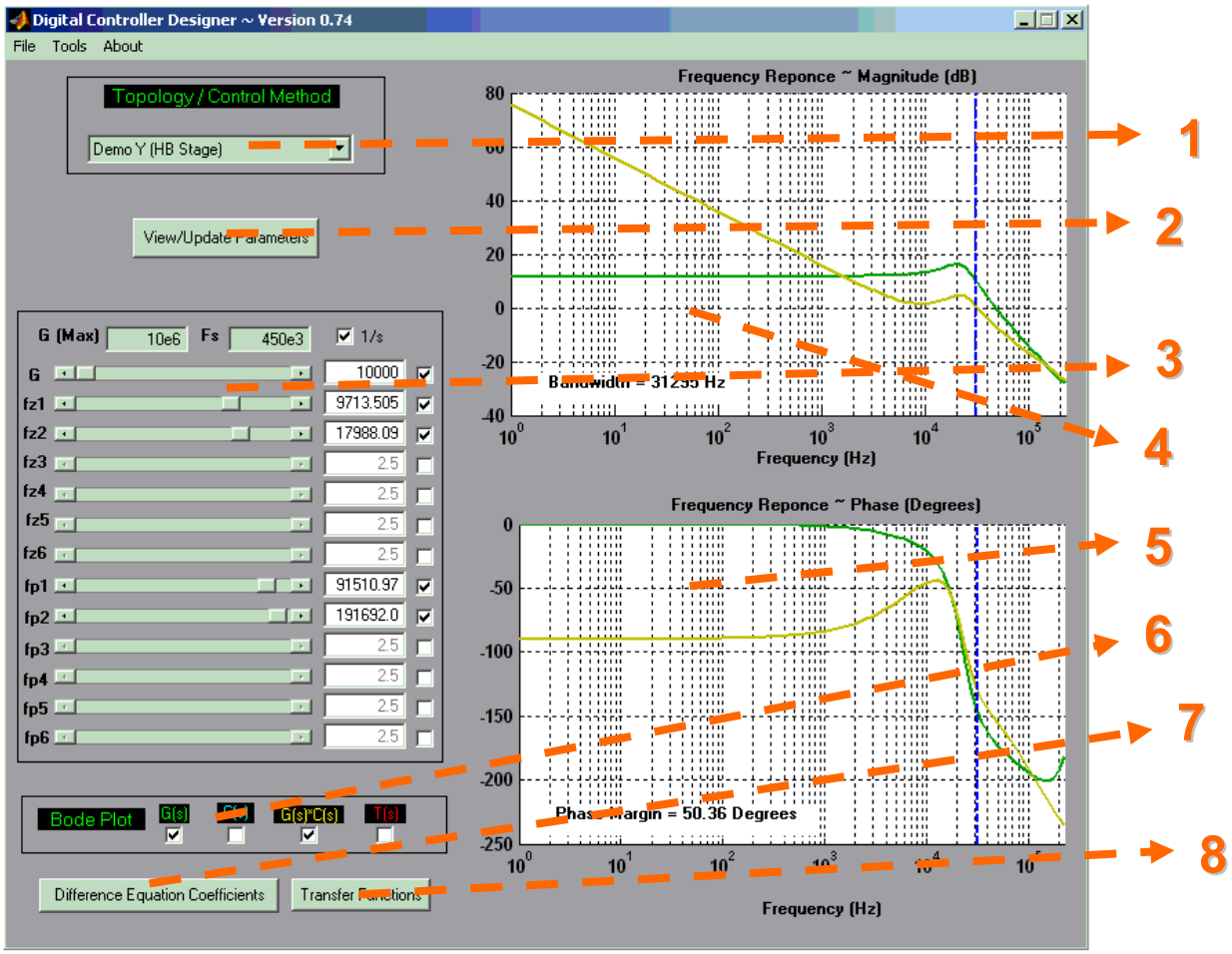

Figure 6-1 : Digital Controller Designer main window

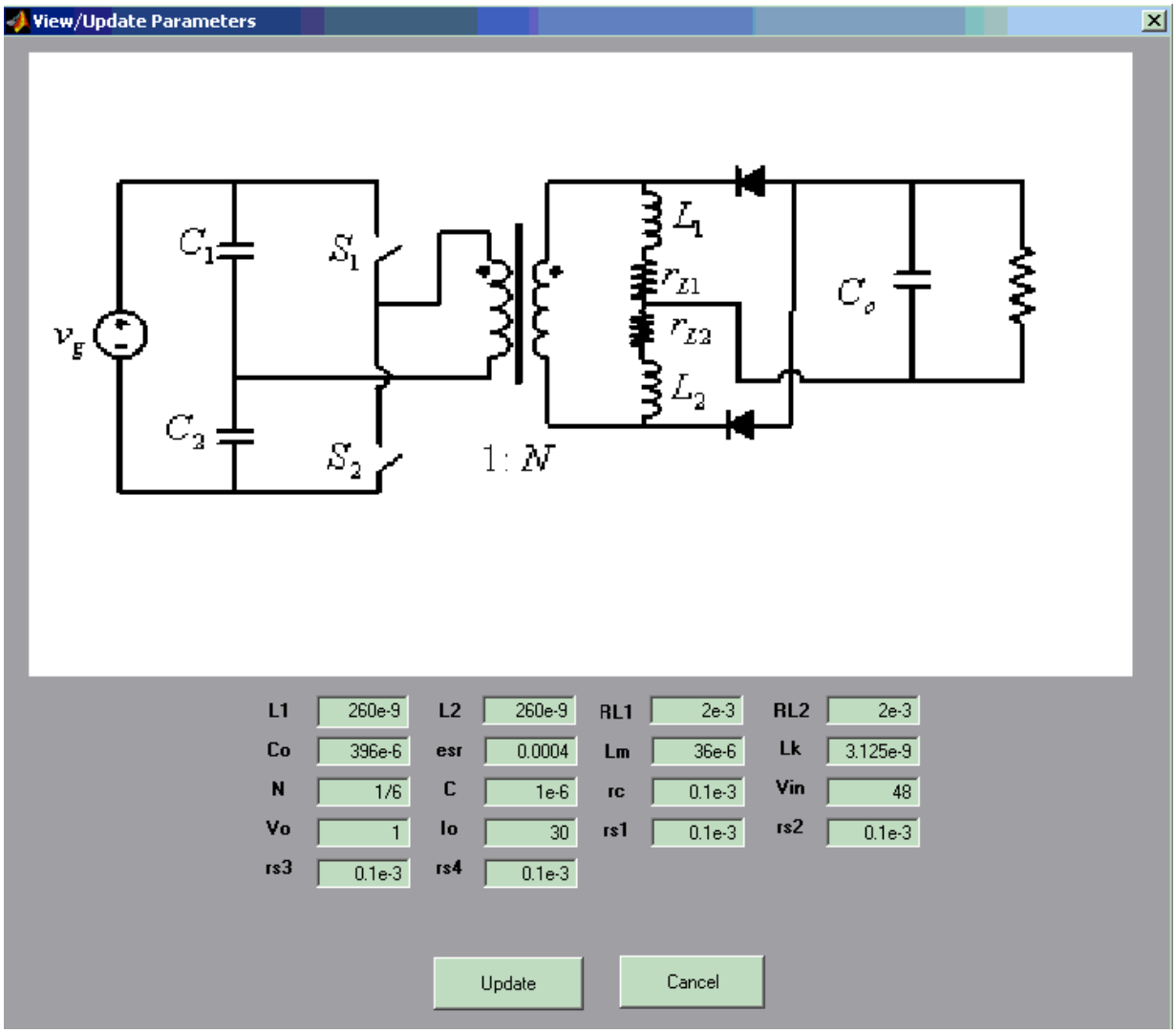

Figure 6-2 : Digital Controller Designer parameters window

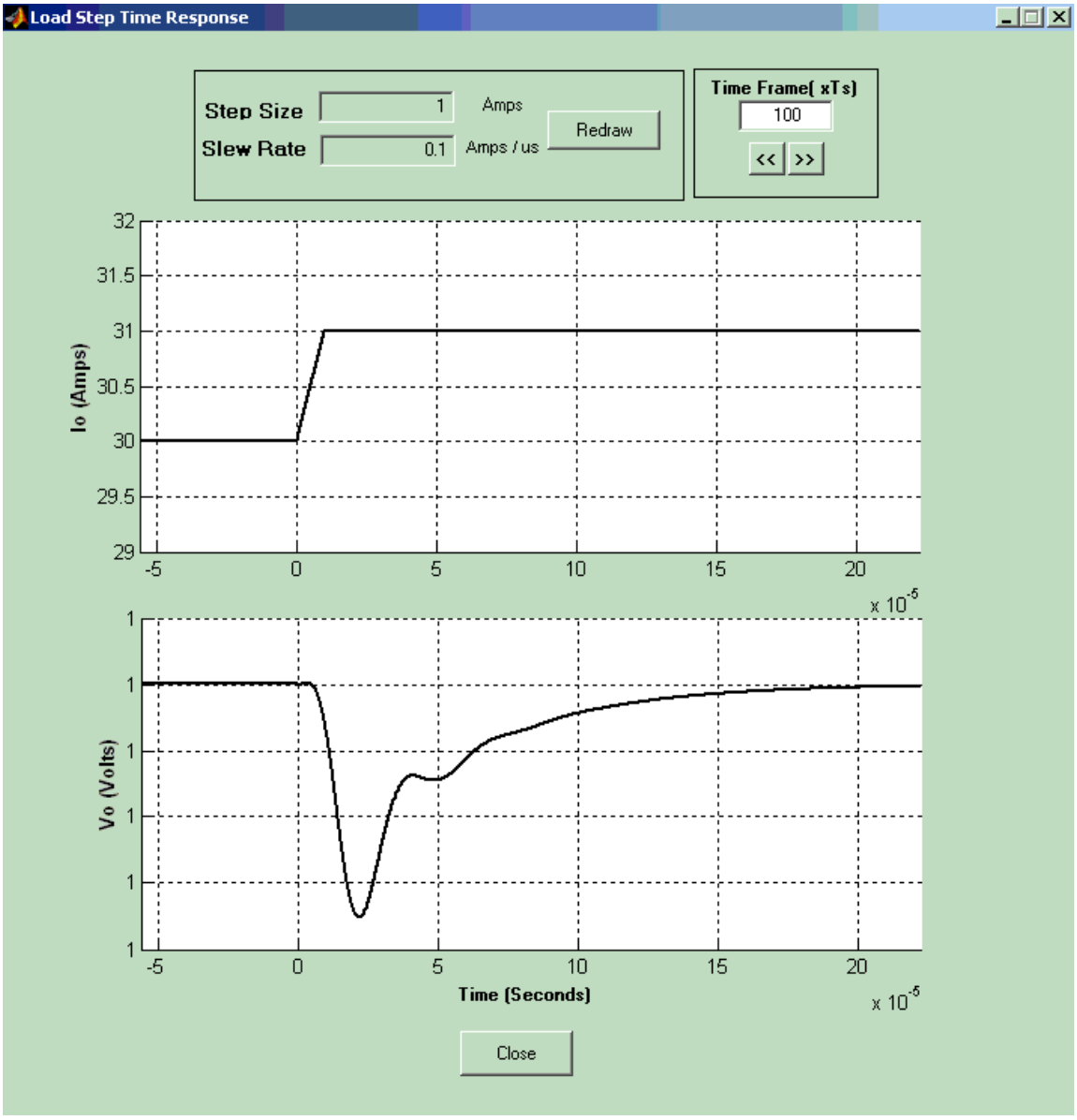

Figure 6-3 : Digital Controller Designer Time response window

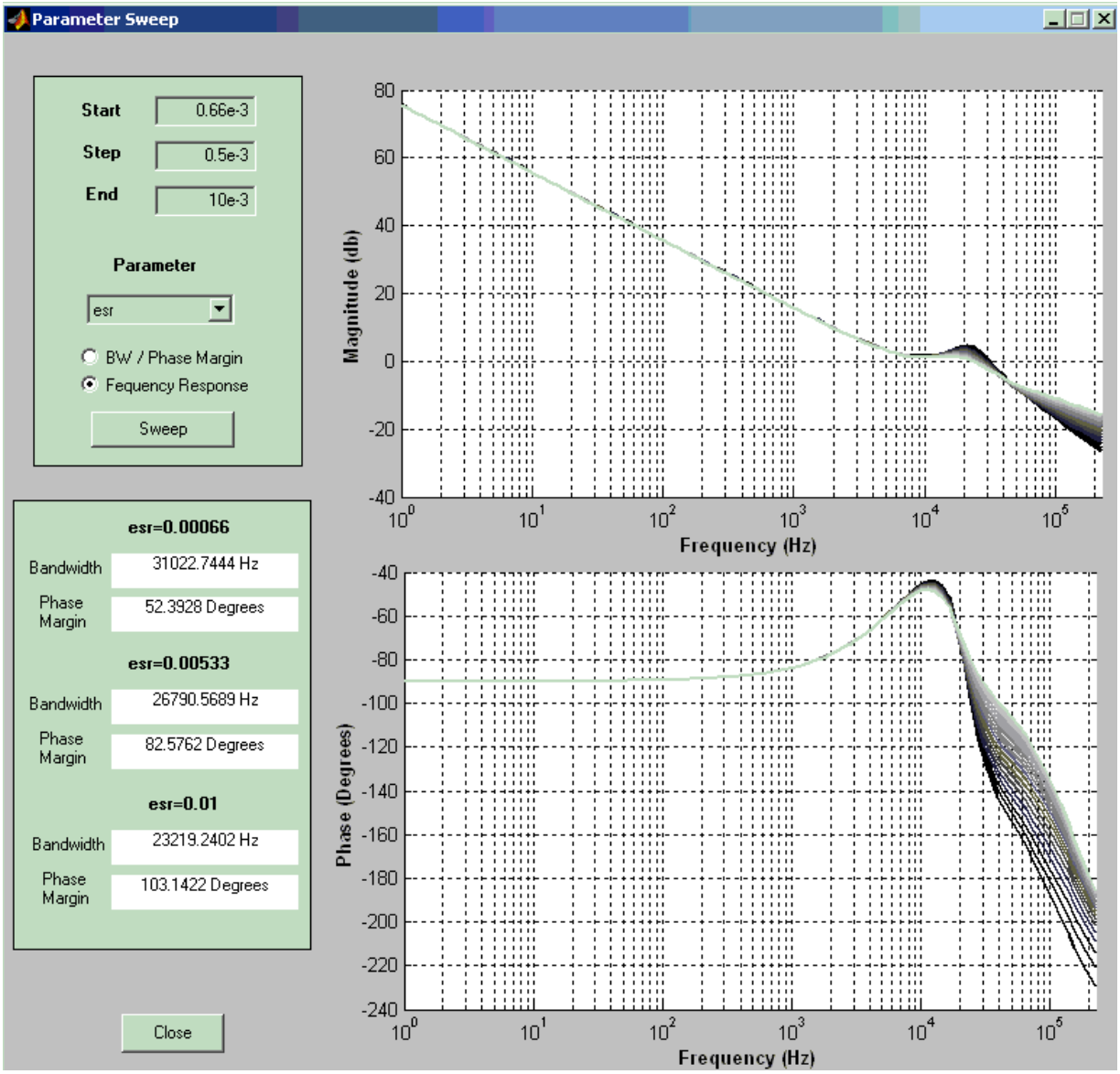

Figure 6-4 : Digital Controller Designer parameter sweep window

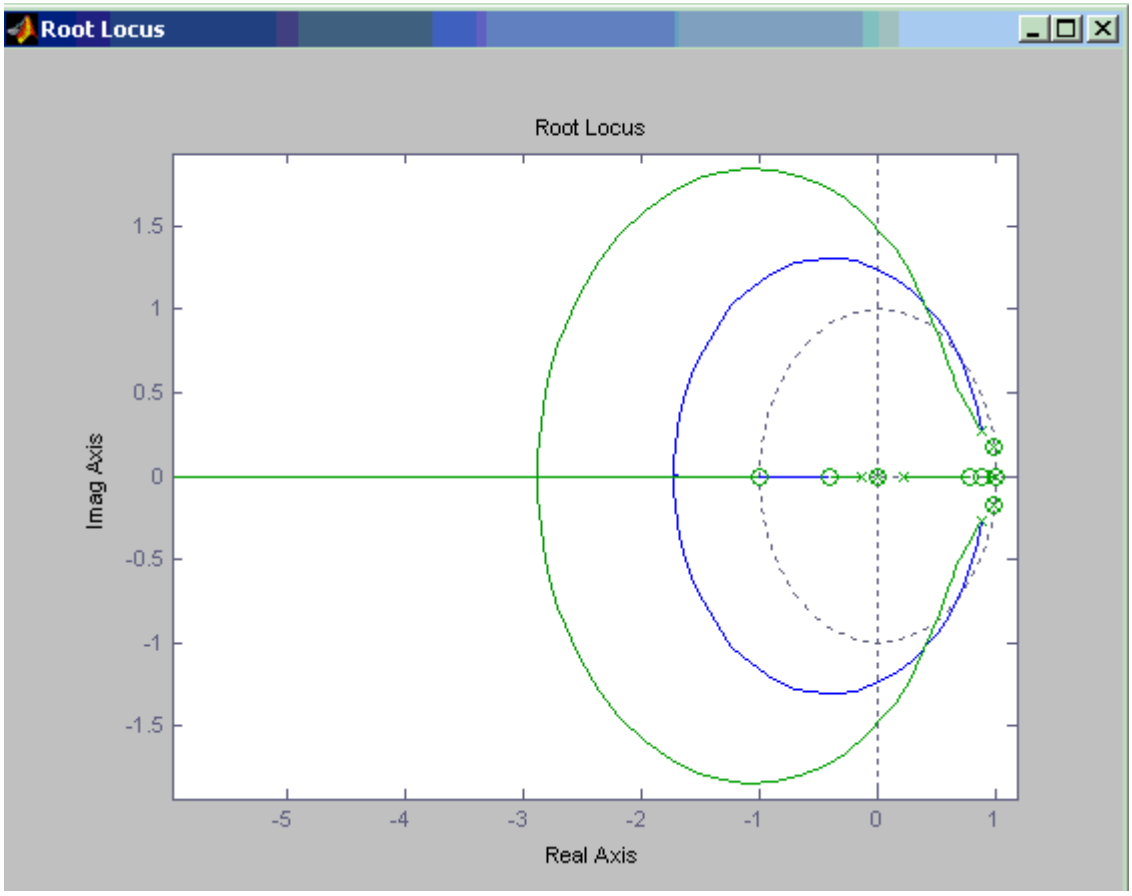

Figure 6-5 : Digital Controller Designer Root Locus window

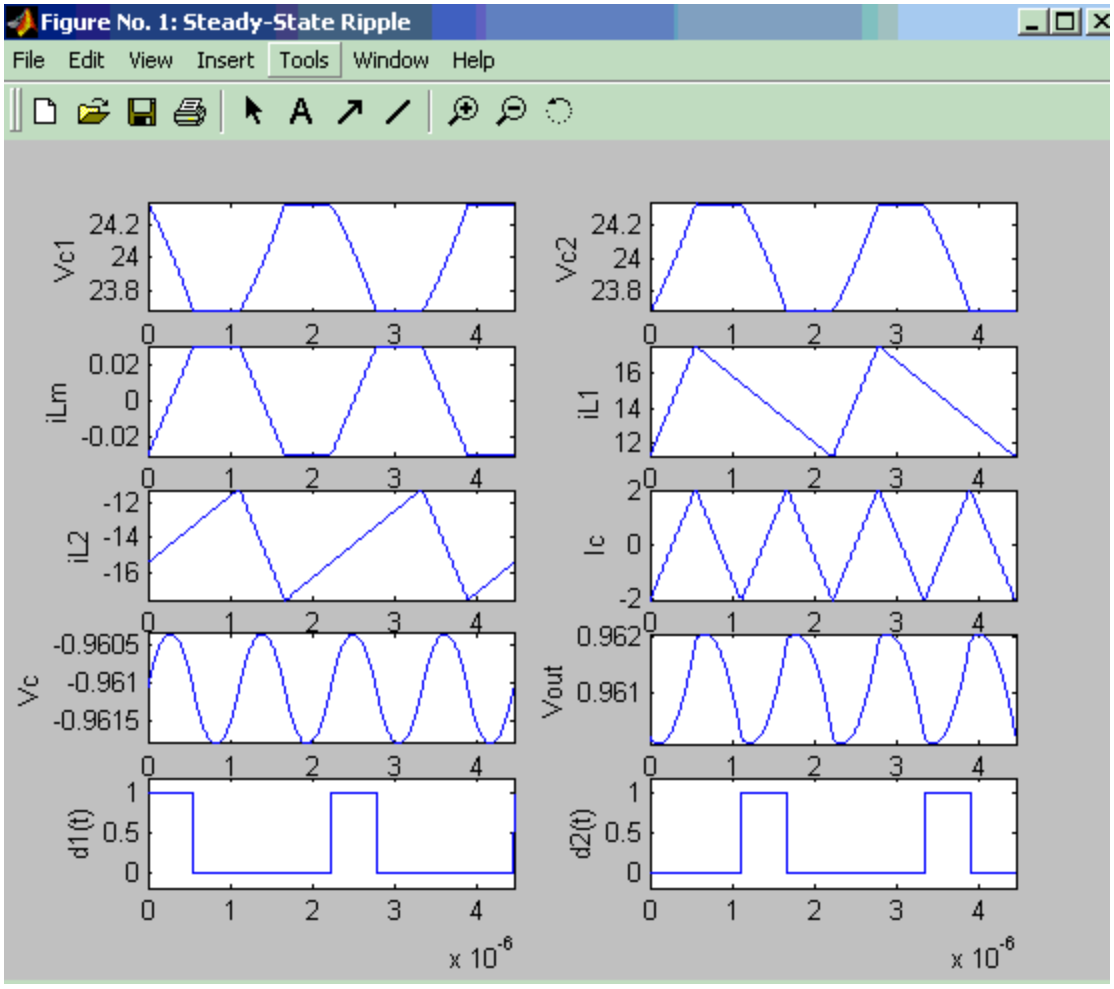

Figure 6-6 : Digital Controller Designer Steady-State waveforms window

6.2 Design Example

As an example of utilizing this GUI platform parameters from a lab prototype were entered into the parameters window those parameters are as shown below,

Figure 6-7 : Parameters for Lab Prototype Half-Bridge with current doubler and Symmetric control

The next step in the controller design process is to check two poles and two zeros with DC gain and an integrator in the compensator frame of the main window. This specific compensator is the general PID that is most generally used in many cases for compensator realization. The sliders of the poles and zeros are then adjusted until the desired bandwidth and phase margins are achieved, as shown in Figure 6-8. The achieved compensator parameters can then be used to design an analog realization as shown in Figure 6-9 , or they can be used to obtain the parameters of a linear discrete compensator (a difference equation) through the use of the Difference Coefficients Button in the main window as shown in Figure 6-10.

With this design example this chapter is concluded.

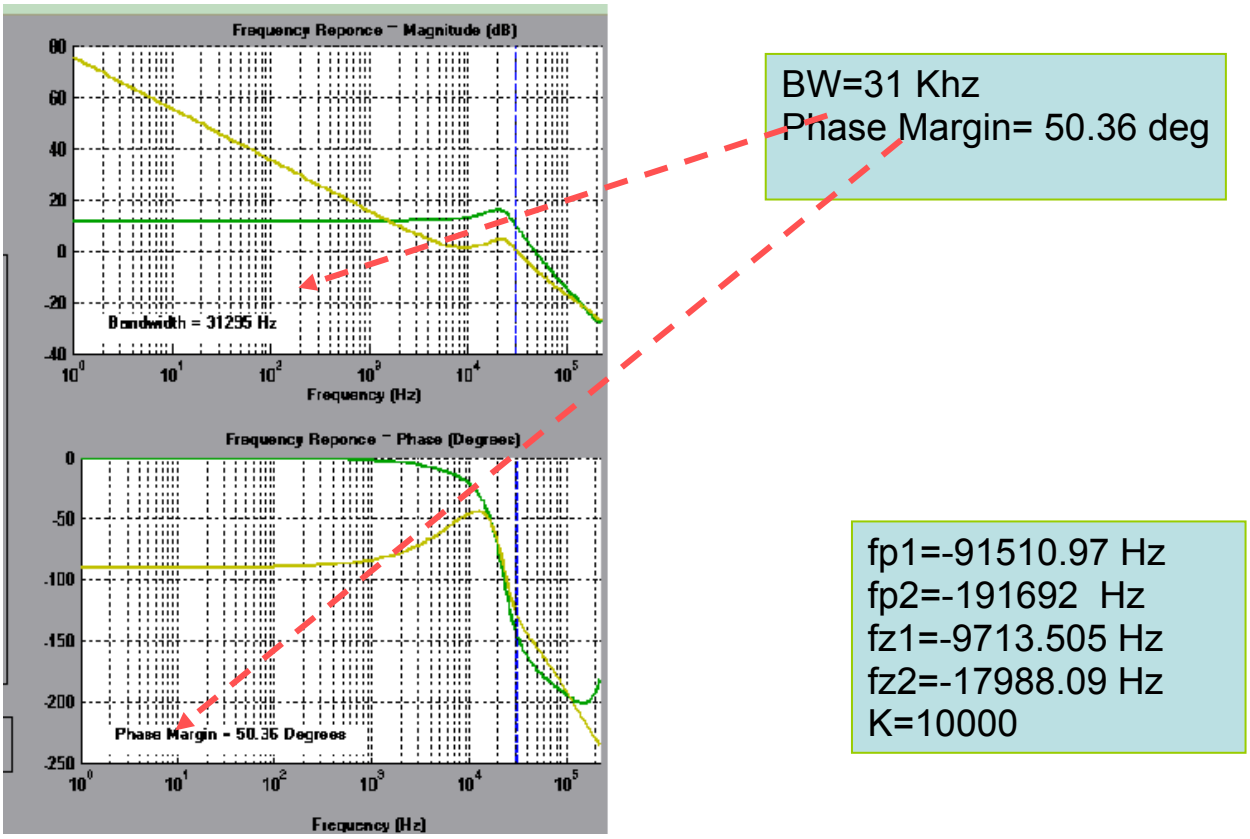

Figure 6-8 : Desired Bandwidth and phase margin with required compensator poles and zeros

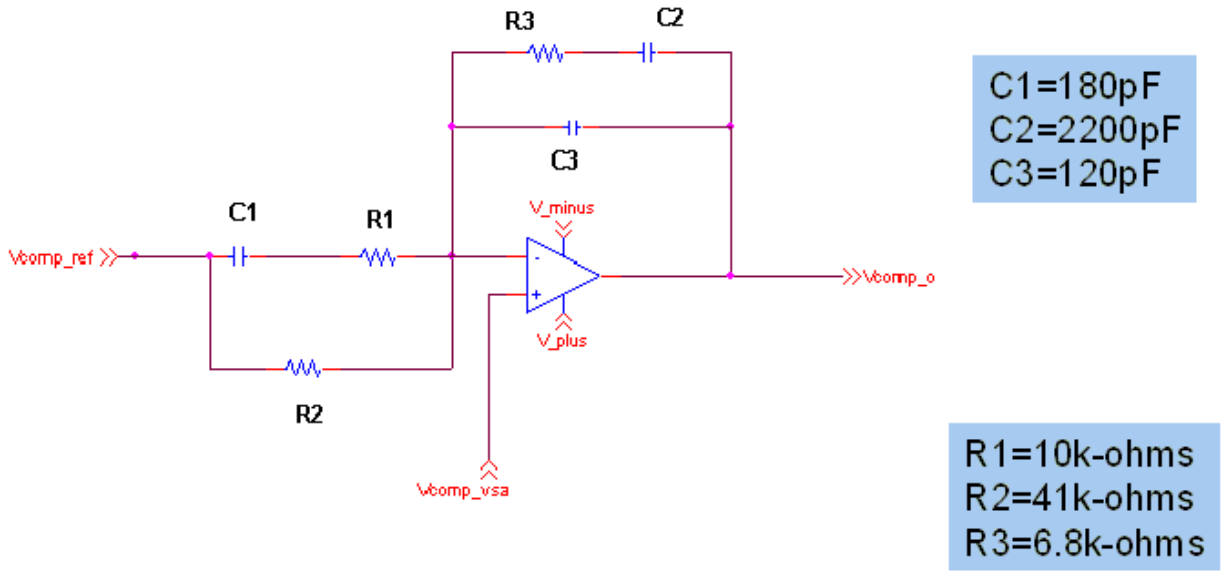

Figure 6-9 : Compensator realization in the analog domain

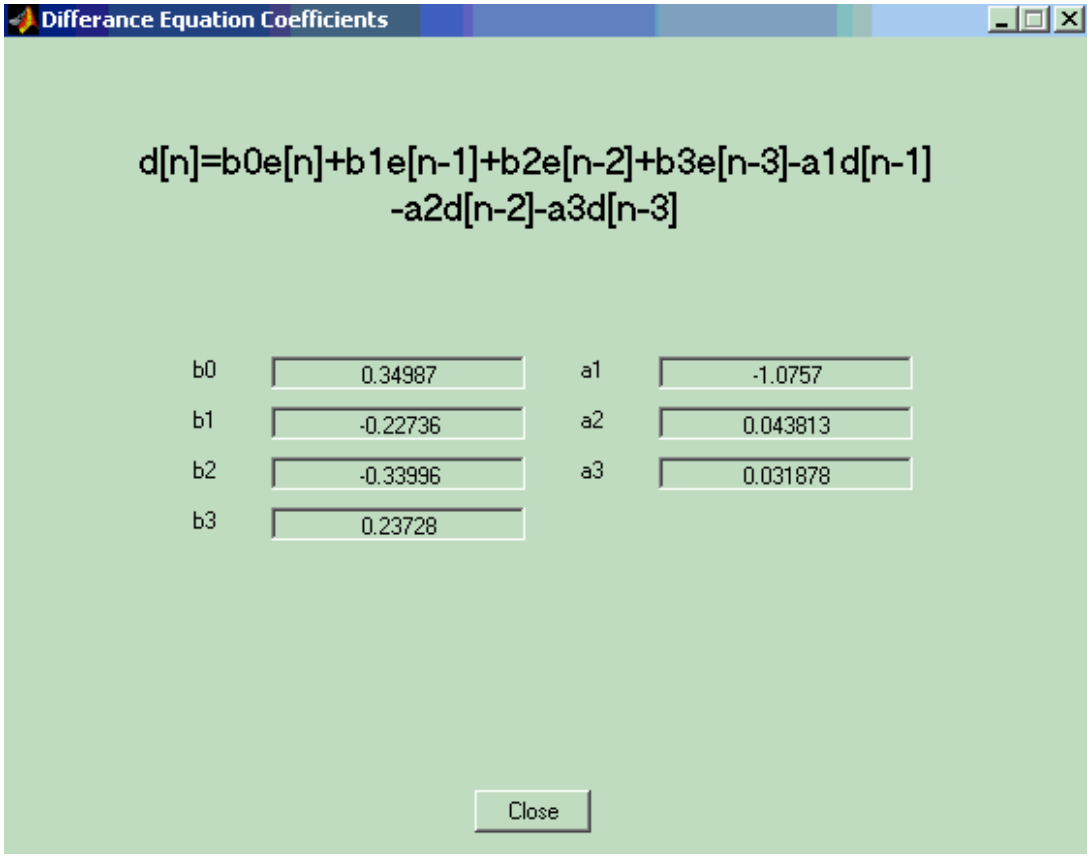

Figure 6-10 : Difference Equation coefficients for Digital Controller realization

CHAPTER 7

CONCLUSION AND FUTURE WORK

7.1 Conclusion

In this Thesis , after a review of the main average modeling techniques for switching DC/DC converters a general small-signal discrete state-space model was developed. The main approximation in deriving this model was representing the duty cycle modulations that control the SMPS switches as weighted impulse functions. To make the model more accurate steady state waveform acquisition was utilized using Fourier analysis.

Then a large signal model was derived which turned out to be a linear function with respect to the converter inputs but nonlinear with respect to the duty cycle modulations as expected. Building upon that model an alternate small signal model was derived. Throughout the derivations certain symmetric properties in the form of the state-space equations were helpful in introducing definitions that simplified the notation to a large extent.

Both the Large and the small signal model were implemented for the case example of the Half-Bridge DC/DC with current doubler topology. All 3 main control schemes of the Half-Bridge (Symmetric , Asymmetric , DCS) were considered and their dynamic properties such as the frequency response and time response were compared. Finally a lab prototype was built with

a compensator and its frequency response was compared with the frequency response obtained from the developed small signal models.

The final chapter of this thesis reviewed an implementation of the derived models in MATLAB as a Design Platform GUI. After the description of the different components of this platform a design example was presented.

7.2 Future Work

Future work will include more verification of the models derived here for both open loop and close loop. The main two expansions on the models will be to generalize them more so that they work for a converter with an arbitrary number of switches , the symmetry inherit in the model equations will enable the induction of this most general model. Then most importantly an extension to the case of DCM will be attempted.

Other ideas in Discrete modeling will be investigated , such as the use input decimation so that it is possible to sample the input at a much higher sampling rate than the switching frequency. The reason this could be interesting is that continuous models in general account for both input and duty cycle as continuous , while discrete models account for both input and duty cycle as discrete , while in reality the input is continuous and the duty cycle is discrete. This idea if successfully implemented can mitigate any inaccuracies that abound when attempting to get an input to output transfer function from a discrete model.

All of this future work will be published in a Ph.D. dissertion and the open literature.

REFERENCES

[1] A general unified approach to modeling switching-converter power stages, R. D. Middlebrook and S. Cuk. ,in 1976 IEEE PESC Rec., pp. 18–34.

[2] Simplified Analysis of PWM Converters using Model of PWM Switch Part I and Part II : Vatche Vorperian , IEEE Transactions on Aerospace and Electronic Systems ,VOL 26, No.3, May 1990

[3] A New Continuous-Time Model for Current-Mode Control , Raymond B. Ridley , IEEE Transactions on Power Electronics Vol 6, No. 2, April 1991.

[4] Study of System instability in Solar Array Based Power Systems , Kasemsan Siri , IEEE Transactions on Aerospace and Electronic Systems Vol 36 , No. 3 , July 2000.

[5] Sampled-Data Modeling of Switching regulators , Arthur R. Brown and R.D. Middlebrook, IEEE Power Electronics Specialists Conference, 1981 record, pp349-369

[6] Discrete Modeling and Analysis of Switching Regulators, Dennis J. Packard , PhD thesis, California institute of technology , May 1976

[7] Zero-Voltage-Switching Half-Bridge DC–DC Converter With Modified PWM Control Method, Hong Mao, Jaber Abu-Qahouq, Shiguo Luo, and Issa Batarseh. IEEE Transactions on Power Electronics, VOL. 19, NO. 4, July 2004

[8] Unified Analog and Digital Models for Half Bridge Converter with Current Doubler Rectifier, Liangbin Yao, Jaber Abu-Qahouq, and Issa Batarseh, IEEE Applied Power Electronics Conference and Exposition, APEC'2005, March 2005

[9] Discrete model of DCS controlled half-bridge with current doubler for digital controller design, Shoubaki, E., Abu-Qahouq, J., Batarseh, I., Applied Power Electronics Conference and Exposition, APEC 2005 , March 2005